Sm-Nd and C-ISOTOPE CHEMOSTRATIGRAPHY OF ORDOVICIAN EPEIRIC SEA CARBONATES, MIDCONTINENT OF NORTH AMERICA

A Thesis Submitted to the College of
Graduate Studies and Research
in Partial Fulfillment of the Requirements
for the Degree of Doctor in Philosophy
in the Department of Geological Sciences
University of Saskatchewan
Saskatoon

By
Kerrie C. Fanton

PERMISSION TO USE

In presenting this thesis in partial fulfillment of the requirements for a Postgraduate degree from the University of Saskatchewan, I agree that the Libraries of the University may make it freely available for inspection. I further agree that permission for copying of this thesis in any manner, in whole or in part, for scholarly purposes may be granted by the professor [or professors] who supervised my thesis work or, in their absence, by the Head of the Department or the Dean of the College in which my thesis work was done. It is understood that any copying or publication or use of this thesis or parts thereof for financial gain shall not be allowed without my written permission. It is also understood that due recognition shall be given to me and to the University of Saskatchewan in any scholarly use which may be made of any material in this thesis.

Requests for permission to copy or to make other use of material in this thesis in whole or in part should be addressed to:

Head of the Department of Geological Sciences
University of Saskatchewan
Saskatoon, Saskatchewan
S7J 5E2

ABSTRACT

Interpreting and correlating epeiric sea sequences is key to understanding ancient marine environments. As a result, ε_{Nd}, $\delta^{13}C$ and Sm/Nd profiles are developed as tools for interpreting epeiric sea carbonates. Previously, ε_{Nd} and $\delta^{13}C$ profiles in epeiric sea carbonates have been used to study changes in the Nd isotope balance and C-cycle of adjacent *ocean water*. Instead, ε_{Nd}, $\delta^{13}C$ and Sm/Nd profiles of Ordovician Midcontinent carbonates of North America demonstrate that fluctuations in sea level and depth are driving local changes in the ε_{Nd}, $\delta^{13}C$ and Sm/Nd composition of epeiric seawater.

Dissolved Nd derived from the Transcontinental Arch, Taconic Highlands and the Iapetus Ocean determine the ε_{Nd} composition of Midcontinent seawater. As sea level fluctuated, submergence of the Arch and an influx of Iapetus ocean waters adjusted the Nd isotope balance of epeiric seawater. As a result, ε_{Nd} profiles can be used to track the submergence history of the Late Ordovician Midcontinent. Comparison of stratigraphic variations in carbonate Sm/Nd ratios with sea level curves, conodont paleoecology, and the ε_{Nd} profiles also suggests that variations in Sm/Nd ratios are related to changes in depth. However, processes effecting Sm/Nd ratios in epeiric seas may be varied and require further investigation.

Sea level fluctuations and the waxing and waning of cool, nutrient rich, oxygen poor Iapetus waters onto the craton adjusted productivity and organic carbon burial rates on the Ordovician Midcontinent. Close to the Transcontinental Arch sea level rise caused an increase in organic carbon burial and productivity, while close to the Sebree Trough, and the influx of Iapetus waters, sea level rise caused a decrease in organic carbon burial and productivity. Differences in local C-cycling across a single epeiric sea encourage caution

when using $\delta^{13}C$ profiles from epeiric sea carbonates to track changes in the C-cycle of adjacent oceans.

Because of their connection to sea level fluctuations, variations in the ε_{Nd}, $\delta^{13}C$ and Sm/Nd profiles can also used to correlate Ordovician Midcontinent carbonates. However, the ability to correlate coeval strata using these profiles is limited by changes in depositional environment across the craton, which cause excursions to be absent, dampened, or magnified.

ACKNOWLEDGEMENTS

I am very grateful to my supervisor Dr. Chris Holmden for his support, input and invaluable discussions. I also wish to thank Fran Haidl, Dr. Godfrey Nowlan, Dr. Brian Witzke and Dr. Dennis Kolata for their help in selecting appropriate samples and for imparting some of their vast knowledge on Ordovician strata of Saskatchewan, Iowa and Illinois. Thank you to The Department of Geology staff, especially D. Fox, D. Cordeiro, N. Choo, T. Prokopiuk, B. Britton and T. Chappell, for their advice and assistance. Thank you to R. Hines, M. Mathe, K. Panchuk and C. Miller for the support and understanding that comes with sharing a similar experience and thank you to my family, the Fantons and the Dalzells, for their unflagging belief in my abilities. Finally, I owe a large debt of gratitude to M. Dalzell for his unending patience, encouragement and understanding.

This study was supported by the Natural Sciences and Engineering Research Council of Canada in the form of an individual research grant to Dr. C. Holmden and a University of Saskatchewan Scholarship to myself.

TABLE OF CONTENTS

LIST OF TABLES

LIST OF FIGURES

CHAPTER 1. BACKGROUND AND MOTIVATION

Much of the ancient marine rock record is comprised of thick carbonate sequences deposited in epeiric or epicontinental seas, which are defined as relatively shallow seas that extended far into the interior of the continents during periods of higher sea level. Epeiric sea strata are especially important to understanding Paleozoic paleoenvironments as these rocks preserve the only record of Paleozoic marine deposition over long periods of time. Preserved in the carbonate or phosphate of epeiric sea strata are the neodymium isotope composition (ε_{Nd}), carbon isotope composition ($\delta^{13}C$) and Sm/Nd (Samarium/Neodymium) ratio of ancient epeiric seawater, three pieces of information that may be used to reconstruct Paleozoic environments. This information is commonly displayed as stratigraphic profiles, which plot the ε_{Nd} or $\delta^{13}C$ composition of the rocks against stratigraphic age, in order to monitor changes in the ε_{Nd} and $\delta^{13}C$ composition of seawater over time. Interpretations of changes in the ε_{Nd} and $\delta^{13}C$ profiles, usually termed excursions, have been primarily shaped by an ocean centered view, which treats the ε_{Nd} and $\delta^{13}C$ composition of epeiric seawater as a proxy for the composition of adjacent ocean water or in some cases for all marine waters.

An ocean centered view of ε_{Nd} and $\delta^{13}C$ profiles from epeiric sea strata have allowed these profiles to be used to track changes in ocean basin configuration, ocean circulation, the global C-cycle, oceanic nutrient levels, oceanic oxygen levels and even faunal extinction (Keto and Jacobsen, 1987; Keto and Jacobsen, 1988; Magaritz and Holser, 1990; Joachimski

and Buggisch, 1993; Bickert et al., 1997; Kaljo et al., 1997; Felitsyn et al., 1998; Veizer et al., 1999; Saltzman, 2002; Saltzman, 2003). In contrast with this ocean centered view are several studies that demonstrate that the ε_{Nd} and $\delta^{13}C$ composition of epeiric seas are not necessarily representative of the adjacent ocean (Patterson and Walter, 1994; Holmden et al., 1998; Panchuk, 2002; Brand and Bruckschen, 2002; Immenhauser et al., 2002; Immenhauser et al., 2003); a view that would require a new perspective on the interpretation and application of ε_{Nd} and $\delta^{13}C$ profiles from epeiric sea strata. Sm/Nd profiles in epeiric sea carbonates may also prove to be reliable indicators of environmental change in epeiric seas. To date, other rare earth elements (REEs) from epeiric sea sediments have been used to infer changes in ocean circulation and paleoenvironment, but few studies have focused on using Sm/Nd ratios to investigate epeiric sea environments (Wright et al., 1984; Grandjean and Alberède, 1989; Bertram et al., 1992; Grandjean-Lécuyer et al., 1993; Girard and Alberède, 1996; Bellanca et al., 1997; Picard et al., 2002).

The ocean centered view used to interpret ε_{Nd} and $\delta^{13}C$ profiles relies primarily on two premises: (1) residence time, which is the length of time an element resides in solution from the time it enters seawater to the time it is removed from seawater; and (2) size of the ocean reservoir in comparison to the epeiric sea. The residence time of Nd and C in seawater, based on modern oceans, is approximately 100 to 1000 years for Nd (Piepgras et al., 1979; Piepgras and Wasserburg, 1980; Elderfield and Greaves, 1982) and 1.8 ka to 55 ka years for C (Holser et al. 1996). In comparison, the time required to mix all the modern oceans is estimated at a few hundred to a thousand years (Holser et al., 1996). As a result, the residence time of C is long enough to ensure that the $\delta^{13}C$ composition of all modern oceans is relatively homogeneous, while the shorter residence time of Nd, close to that of the mixing

time of the oceans, may allow different ε_{Nd} values to develop between modern oceans.

The residence times of Nd and C in ancient epeiric seas is unclear, due in part to a lack of modern analogues. It has been assumed, however, based on modern oceans that the residence times of both Nd and C are greater than the time it takes to thoroughly mix epeiric seawater with neighbouring ocean water (Veizer et al., 1986; Keto and Jacobsen, 1987; Keto and Jacobsen, 1988; Veizer et al., 1999). Hence, the ocean centered view contends that epeiric seas and their neighbouring oceans have the same Nd or C isotope composition (Keto and Jacobsen, 1987; Keto and Jacobsen, 1988; Magaritz and Holser, 1990; Joachimski and Buggisch, 1993; Veizer et al., 1999; Saltzman, 2002; Saltzman, 2003). In the case of C, the longer residence time has been used to assume that the $\delta^{13}C$ composition of an epeiric sea represents the $\delta^{13}C$ composition of all contemporaneous marine waters (Veizer et al., 1980; Veizer et al., 1986; Veizer et al., 1999). Because the reservoir of Nd or C in the oceans is much larger than that of a single epeiric sea, the Nd or C isotope composition of the neighbouring ocean would then dominate the Nd or C isotope composition of the adjacent epeiric sea. Therefore profiles of ε_{Nd} or $\delta^{13}C$ profiles through ancient epeiric sea strata would be interpreted to reflect changes in the Nd isotope balance or C-cycling of the ancient oceans.

Indiscriminately using ε_{Nd} and $\delta^{13}C$ profiles in epeiric sea strata to isolate changes in the Nd isotope balance or C-cycle of the *oceans* has been challenged by a series of studies from both modern oceans and ancient epeiric seas. The large variability in the ε_{Nd} values of modern mixed surface layers, from -1.5 to -11, throughout the eastern Indian Ocean and adjacent seas (Amakawa et al., 2000) implies that Nd in a shallower column of water, possibly analogous to an epeiric sea, may have a very short residence time. This would

suggest that an epeiric sea could easily develop a different ε_{Nd} value compared to an adjacent ocean. Differences of up to 4‰ between the $\delta^{13}C$ composition of modern seawater on the Bahaman Banks and the adjacent deep ocean have also been taken as evidence that a shallower water column, like in an epeiric sea, can have a $\delta^{13}C$ composition that is not determined by the $\delta^{13}C$ value of the adjacent ocean (Patterson and Walter, 1994).

The ε_{Nd} and $\delta^{13}C$ values of ancient seawater cannot be measured directly, but Holmden et al. (1998) used the Ordovician Millbrig and Deicke K-bentonites from North America to define a single time plane of carbonates and phosphates that record coeval ε_{Nd} and $\delta^{13}C$ values of epeiric seawater covering the eastern and central United States. Their time plane revealed that ε_{Nd} and $\delta^{13}C$ values of epeiric seawater differed from projected Iapetus Ocean water values and that ε_{Nd} and $\delta^{13}C$ values could also be used to divide the epeiric sea into isotopically distinct water masses. Holmden et al. (1998) attributed these coeval variations in ε_{Nd} and $\delta^{13}C$ to local controls on the Nd isotope balance and C-cycle of the epeiric sea. Panchuk (2002) corroborated and enhanced the C isotope work by Holmden et al. (1998), defining an even greater variation in $\delta^{13}C$ values across the Midcontinent epeiric sea. Different ε_{Nd} values have also been identified between coeval Cretaceous strata of the Western Interior Seaway and the neighboring Pacific Ocean and Gulf of Mexico (Whittaker and Kyser, 1993) as well as between Cretaceous strata of the West African Platform and the adjacent Atlantic Ocean (Grandjean et al., 1988).

Historically, the interpretation and uses of ε_{Nd} and $\delta^{13}C$ profiles in epeiric sea carbonates have been established from an ocean centered viewpoint, in some cases before more recent work revealing the role of the epeiric sea in determining ε_{Nd} and $\delta^{13}C$ compositions and in other cases in spite of it. Interpretations of ε_{Nd} profiles are predicated

on the behaviour of ε_{Nd} in modern oceans, which dictates that dissolved Nd in seawater is derived from weathering of surrounding continental crust (Goldstein and Jacobsen, 1987; Piepgras et al., 1979; Piepgras and Wasserburg, 1980). The ε_{Nd} value of surrounding continental crust is dependent on age and rock composition. An ocean basin like the Pacific, which is surrounded by overall younger crust with a greater volcanic component, has a different ε_{Nd} value than does the Atlantic, which is surrounded by relatively older continental crust (Piepgras and Wasserburg, 1980). Therefore, it is believed that changes in the ε_{Nd} value of a single ocean over time can be used to identify changes in the average age of surrounding crust to an ocean basin due to plate tectonic events and opening of an ocean basin to circulation with neighbouring oceans (Keto and Jacobsen, 1987; Stille et al., 1996; Vance and Burton, 1999). For example, Stille (1992) identified paleocirculation changes during the opening of the south Atlantic and the Drake Passage by using ε_{Nd} values of Atlantic ocean phosphates that range in age from 80 Ma to Present. Similar studies, seeking to predict changes in ocean basin geometry, have been attempted for the Paleozoic Iapetus and Panthalassa oceans but have relied on the ε_{Nd} values from neighbouring Paleozoic epeiric sea sediments (Keto and Jacobsen, 1987; Keto and Jacobsen, 1988) to monitor changes in oceanic ε_{Nd} values.

Although the inputs and outputs to the ocean carbon reservoir are believed to be varied and complicated, changes in the $\delta^{13}C$ composition of the ocean carbon reservoir are primarily attributed to changes in the rate of oceanic productivity and the rate of organic carbon burial in the oceans (Scholle and Arthur, 1980; Arthur et al., 1987; Brasier, 1992; Holser, 1997; Kump and Arthur, 1999). Increased productivity in the oceans depletes the surrounding water column in ^{12}C relative to ^{13}C because organic matter preferentially

incorporates ^{12}C, thereby leaving the oceans relatively enriched in ^{13}C. Burial of ^{12}C enriched organic carbon instead of oxidation of organic carbon, also removes ^{12}C from the water column, leaving it relatively ^{13}C enriched. Enrichment of the water column in ^{13}C is recorded in carbonates as a positive shift in $\delta^{13}C$ values. Changes in past oceanic productivity and organic carbon burial rates have been successfully identified using $\delta^{13}C$ profiles through ancient ocean sediments (Scholle and Arthur, 1980; Woodruff and Savin, 1995; Baum et al., 1994; Singer and Shemesh, 1995). It is also common practice through much of the Phanerozoic where ocean sediments are not available because of inaccessibility, erosion or subduction, to use $\delta^{13}C$ profiles through epeiric sea strata to monitor changes in the rate of productivity and organic matter burial in neighbouring oceans. In addition, changing rates of oceanic organic matter productivity or burial, predicted with epeiric sea profiles, have been further linked to large scale changes in ocean circulation that result in widespread anoxic conditions or increased upwelling of nutrient rich waters (Magaritz and Stemmerik, 1989; Magaritz et al., 1992; Joachimski and Buggisch, 1993; Brenchley et al., 1994; Wenzel and Joachimski, 1996; Patzkowsky et al., 1997; Pancost et al., 1999; Brenchley et al., 2003; Saltzman, 2003). The long residence time of carbon in the oceans has also been used to infer that $\delta^{13}C$ excursions will be recorded in contemporaneous epeiric sea strata across a craton and between cratons, suggesting that $\delta^{13}C$ excursions in epeiric strata can be used to correlate strata potentially from around the world (Joachimski and Buggisch, 1993; Kimura et al., 1997; Saltzman, 2001; Brenchley et al., 2003).

If changes in the Nd isotope balance or C-cycle of an epeiric sea can be independent from changes in the adjacent ocean, then the traditional ocean centered view used to interpret ε_{Nd} and $\delta^{13}C$ profiles through epeiric sea strata may, in many cases, be inappropriate. An

epeiric sea, in comparison to the surrounding oceans, may posses a shallower water column, different circulation patterns, local sea level changes and a greater proportion of land to surface area of water. All these independent factors require that changes in the ε_{Nd} and $\delta^{13}C$ profiles of epeiric sea strata be re-evaluated in the context of local changes in the C-cycle and Nd isotope balance of the epeiric sea. Despite the body of work highlighting how important the epeiric sea may be in determining the ε_{Nd} and $\delta^{13}C$ composition of epeiric sea strata, there is a dearth of work that explores how the ε_{Nd} and $\delta^{13}C$ compositions of an epeiric sea are established and what drives local changes in the ε_{Nd} and $\delta^{13}C$ composition of an epeiric sea. Without this understanding not only may ε_{Nd} and $\delta^{13}C$ profiles in epeiric sea strata be misinterpreted but the full potential these profiles may have for interpreting and correlating epeiric sea strata may also go unrealized.

The two primary objectives of the following chapters are to use ε_{Nd} and $\delta^{13}C$ profiles through the Ordovician epeiric sea strata of the Midcontinent of North America (Fig. 1.1) (1) as a template for how variations in the Nd isotope balance and C-cycle can be driven by local changes within the epeiric sea and (2) to determine possible applications for correlating and interpreting epeiric sea strata. Chapters 2 and 3 use ε_{Nd} and $\delta^{13}C$ profiles through Ordovician carbonate sections from Iowa and Saskatchewan to establish how sea level fluctuations may be the driving force behind local changes in the Nd isotope balance or C-cycling of epeiric seas. In doing so, these two chapters evaluate the feasibility of using epeiric sea carbonates as a means of tracking changes in the ε_{Nd} and $\delta^{13}C$ composition of seawater and touch on the uses of ε_{Nd} and $\delta^{13}C$ profiles for interpreting and correlating epeiric sea strata. Chapter 4 expands on the conclusions drawn in chapters 2 and 3 by constructing ε_{Nd} and $\delta^{13}C$ profiles through two contemporaneous Ordovician carbonate

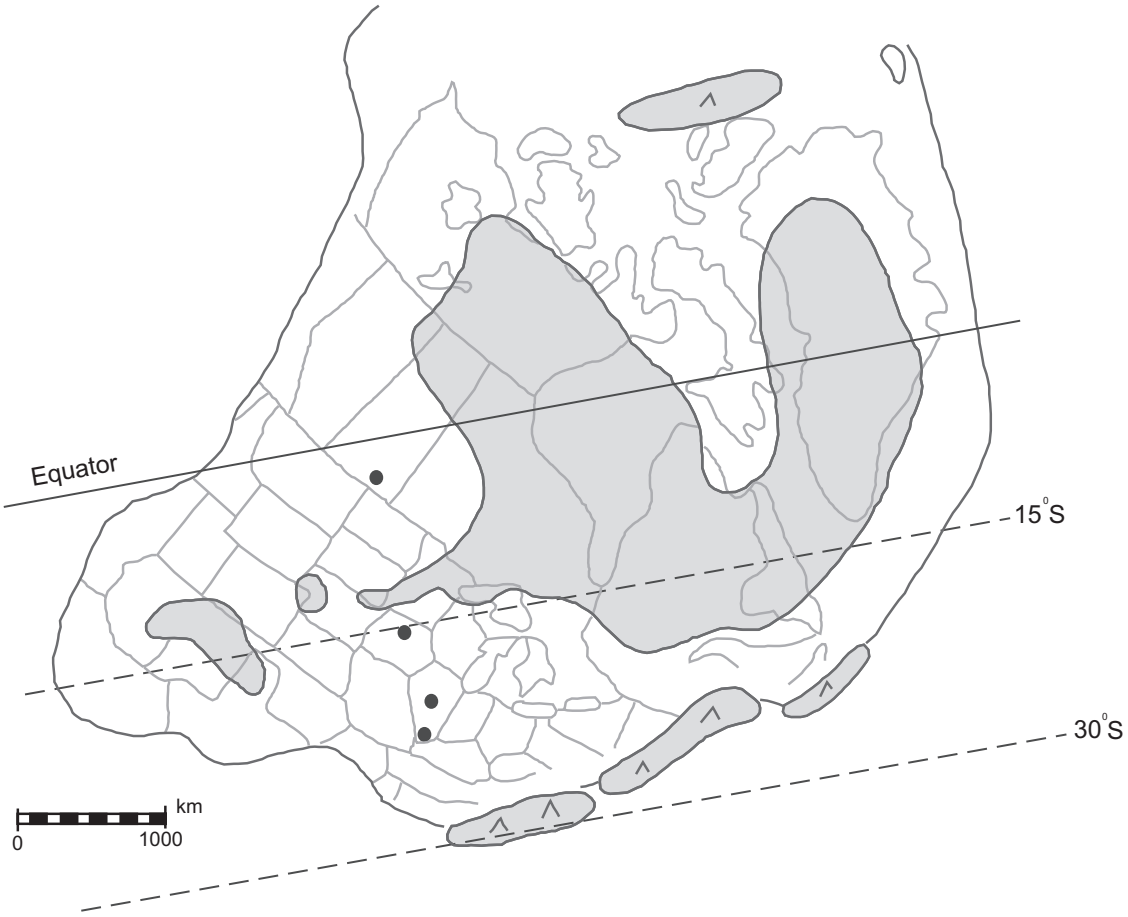

Fig. 1.1 Generalized Middle to Late Ordovician paleogeography of North America modified from Witzke, 1990. Dark lines show continental margins, shaded areas show distribution of land and intervening areas are covered by epeiric seas. Dark circles indicate areas of Midcontinent Ordovician strata sampled for this study.

sections of Illinois. These additional profiles located in the middle of the Midcontinent epeiric sea, further from shore and in a different depositional environment, provide a means of evaluating how sea level fluctuations may cause distinct changes in the Nd isotope balance and C-cycling of different parts of a single epeiric sea. As such, this chapter also attempts to delineate possible advantages and limitations to correlating and interpreting epeiric sea strata with ε_{Nd} and $\delta^{13}C$ profiles.

Another goal threaded through the following chapters is to investigate a possible connection between Sm/Nd ratios in the Midcontinent epeiric sea carbonates and environmental change. Such a correlation would not only add another tool for understanding epeiric seas, but may also contribute to a long standing debate over the use of rare earth elements (REE) preserved in epeiric sea phosphates and carbonates. The REE, which include Sm and Nd, are a set of chemically cohesive elements with a +3 charge that display a decreasing ionic radius with increasing atomic number. This small difference in size may be exploited by environmental processes causing variations in the concentrations of the REE (Hoyle et al., 1984; Elderfield and Pagett, 1986; German and Elderfield, 1990; Sholkovitz and Schneider, 1991; Laenen et al., 1997; Sholkovitz and Szymczak, 2000; Picard et al., 2002). These variations can be determined by measuring REE ratios, such as Sm/Nd, or by plotting REE concentration, normalized to a standard, against atomic number.

Modern ocean waters display a REE pattern that is enriched in the heavy REE, those with high atomic number, relative to the light REE, those with lower atomic number (Palmer, 1985; Elderfield et al., 1990). In contrast, REE patterns of Paleozoic epeiric sea sediments are enriched in middle REE (MREE), those elements with an atomic number in the middle of the group. Some regard these MREE profiles as characteristic of Paleozoic

seawater. They attribute the difference between ancient and modern seawater REE patterns to processes active in shallow epeiric seas that are not observed in modern environments because modern analogs for such extensive shallow inland seas are difficult to find (Wright et al., 1984; Grandjean and Albarède, 1989; Girard and Albarède, 1996). Others hold that exaggerated MREE profiles in epeiric sea sediments are a result of diagenetic alteration (Lécuyer et al., 1998; Reynard et al., 1999). A correlation between fluctuations in Sm/Nd ratios of carbonates, part of the MREE, and environmental change may indicate that changes in the REE patterns of epeiric sea sediments are a result of processes active at the time of deposition rather than diagenesis.

The following chapters of the thesis are presented as journal articles, although only chapter 2 has been published at the time of submission of this thesis. Each chapter contains an introduction, geologic setting, analytical, discussion and conclusion section. Repetition of stratigraphic descriptions and geologic setting may occur between chapters because all samples were collected from the Ordovician strata of Iowa, Illinois and Saskatchewan. For chapter 2 conodont identifications and some stratigraphic description were contributed by G. Nowlan and F. Haidl. Preparation of chapter 3 for submission to a journal will be completed in 2005. Chapter 4 is a preliminary draft of a journal article but does make reference to previous discussions in chapters 2 and 3 of the thesis.

CHAPTER 2. $^{143}Nd/^{144}Nd$ AND Sm/Nd STRATIGRAPHY OF UPPER ORDOVICIAN EPEIRIC SEA CARBONATES

2.1 Introduction

The discovery that ε_{Nd} values of modern seawater differ between oceans led to the idea that variations in ε_{Nd} of past seawater, recorded in marine sediments, can be used to track changes in the configuration of ocean basins and in ocean circulation (Piepgras et al., 1979; Keto and Jacobsen, 1987; Keto and Jacobsen, 1988; Stille et al., 1996; Vance and Burton, 1999). Neodymium can be used in this way because: (1) it has a residence time shorter than the interocean mixing time, and (2) its isotopic composition in seawater is controlled by the weathering flux of Nd from surrounding continental crust and delivered to oceans in the dissolved load of rivers. Because ε_{Nd} of the continental crust is age dependent, differences in the mean age of crust comprising the watershed to each basin ensures that the ε_{Nd} of seawater differs between ocean basins (Piepgras et al. 1979; Piepgras and Wasserburg, 1980; Goldstein and Jacobsen, 1987).

Widespread application of Nd isotopes to the study of Paleozoic oceans has been hampered by a marine sediment record dominated by epeiric sea deposits. Holmden et al. (1998) questioned whether ε_{Nd} values preserved in epeiric sea sediments could be used to represent ε_{Nd} values of adjacent paleoceans, showing that seawater ε_{Nd} values recorded in Upper Ordovician conodonts across the Mohawkian Sea (ε_{Nd} = -6 to -19) are markedly different from those of the adjacent Iapetus Ocean (ε_{Nd} = 0.6 to -5). Additionally, Whittaker

and Kyser (1993) reported stratigraphic variations in the ε_{Nd} values of molluscs from the Cretaceous Western Interior Seaway that are larger than expected for mixing of seawater onlapping the craton from the Pacific Ocean and Gulf of Mexico. Grandjean et al. (1988) showed that ε_{Nd} values in the shallow Cretaceous sea of the West African Platform were variable, and offset from those of the adjoining Atlantic Ocean. Although these studies question the reliability of epeiric sea sediments as a record of ε_{Nd} for bordering paleoceans, the utility of Nd isotopes as a paleogeographic tool can be realized if the scale of inquiry is limited to the epicontinental environment, where Nd isotopes can be used to study the dynamics of epeiric seawater across individual continents.

This thesis focus on the interior epeiric seas of North America during the Middle and Late Ordovician (Fig. 2.1). Specifically, we show that stratigraphic changes in the ε_{Nd} values of Middle and Upper Ordovician carbonates bordering the Transcontinental Arch and Canadian Shield record the submergence history of the North American craton. The premise is that the Nd isotope balance in epeiric seawater across North America was primarily controlled by the relative contributions of Nd weathered from the Taconic Orogen (ε_{Nd} = -6 to -9) and the low relief Precambrian basement of the Transcontinental Arch and Canadian Shield (ε_{Nd} = -22 to –15) (Fig. 2.1). During sea level rise progressive submergence of the Arch and Shield reduced the weathering flux of Precambrian-sourced Nd to surrounding epeiric seas of the Williston Basin in Saskatchewan and the central Midcontinent in Iowa (Fig. 2.1). Therefore, positive shifts in ε_{Nd} values of successively younger epeiric sea carbonates are inferred to record progressive inundation of the Arch and Shield and an adjustment in the Nd isotope balance of seawater towards greater relative contributions of Nd from the Taconic Orogen. Negative shifts in ε_{Nd} indicate increased emergence of the

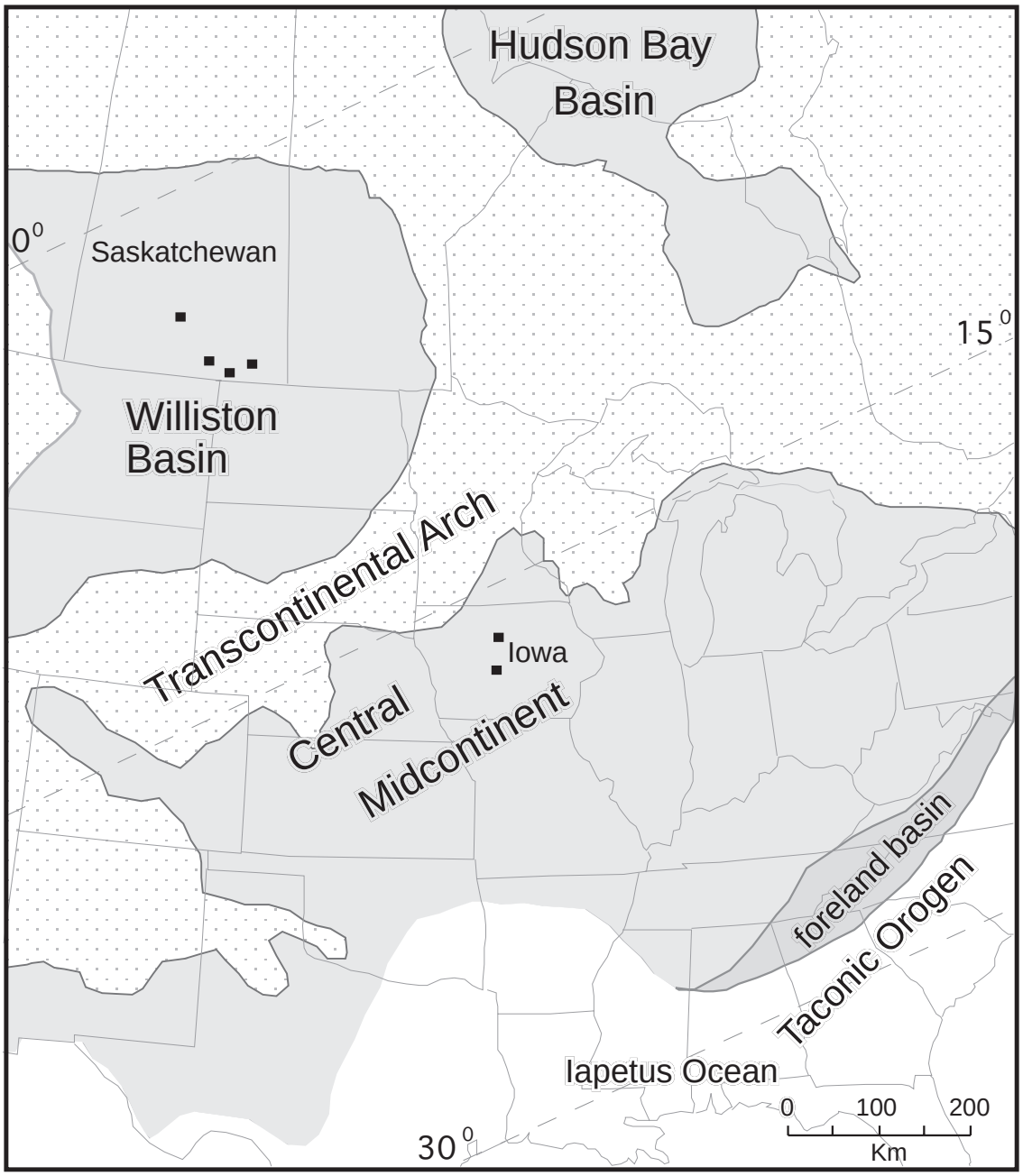

Figure 2.1 Generalized paleogeography of central North America at the beginning of the Late Ordovician. Epeiric seas are grey and exposed Precambrian basement of the Transcontinental Arch and Canadian Shield, including exposed sediment derived from the Arch or Shield are stippled. Exposed basement and basin edges are based on the present day zero edge of Ordovician strata from Cook and Bally (1975). Squares represent location of sampled cores.

Arch and Shield from relative sea level fall. Because sea level changes and the ε_{Nd} profile of carbonates are linked, it is possible to correlate Upper Ordovician marine sediments between intracratonic basins of North America, demonstrating the potential for Nd isotope stratigraphy. We also show that stratigraphic variations in Sm/Nd ratios of carbonates hold potential as a proxy for changing depth in epeiric sea environments.

In this paper we additionally evaluate the potential for whole-rock carbonate to preserve the ε_{Nd} values of ancient epeiric seawater. Traditionally, biogenic apatites, such as conodonts, have been relied upon to record the isotopic composition of Nd in ancient seawater (Wright et al., 1984; Shaw and Wasserburg, 1985; Keto and Jacobsen, 1987; Keto and Jacobsen, 1988; Grandjean et al., 1988; Holmden et al., 1998; Martin and Haley, 2000). Biogenic apatite sequesters Nd from seawater postmortem at the seawater-sediment interface and is relatively unaffected by diagenesis (Bernat, 1975; Wright et al., 1984; Shaw and Wasserburg, 1985; Grandjean et al., 1987; Grandjean and Albarède, 1989; Holmden et al., 1996). Conodonts, however, are extremely small fossils (< 100 μg per element), and even though Nd concentrations may range between 50 and 2100 ppm, low fossil yields from marine carbonates may provide insufficient Nd for routine mass spectrometric analysis of Nd^{+} ions. This dependence on conodont yields can limit the construction of detailed Nd isotopic profiles in marine sediments. By contrast, marine carbonate rocks have high enough Nd concentrations that, at most, only a few grams are necessary for analysis and can, within a carbonate sequence, offer another medium for Nd isotope stratigraphy.

2.2 Stratigraphy

2.2.1 Iowa

Middle through Upper Ordovician strata in Iowa belong to the Decorah, Dunleith, Wise Lake and Dubuque formations of the Galena Group, and to the overlying Maquoketa Formation (Fig. 2.2). The Decorah Formation consists of mixed shale and carbonate. Shales thicken to the northwest towards source areas on the Transcontinental Arch; shale to carbonate transitions within the Decorah signify transgression of these source areas (Witzke, 1980; Witzke and Kolata, 1989; Witzke and Bunker, 1996). The progression from upper shaly units of the Decorah to dominantly carbonates in the lower Dunleith is construed as a depositional deepening. A continued drop in clastic content and expansion of a purer, although still slightly argillaceous, carbonate facies in the mid-Dunleith is interpreted as further drowning of the Transcontinental Arch (Witzke and Kolata, 1989; Witzke and Bunker, 1996). The overlying Wise Lake contains the purest carbonate lithologies in the Galena Group, suggesting deposition was coincident with continued submergence of the Arch. The upward increase in calcareous algae and storm-generated grainstone layers further indicates depositional conditions were shallowing toward the top of the Wise Lake Formation (Witzke and Kolata, 1989). The return of thin shale interbeds in the overlying carbonate strata of the Dubuque are attributed to a new source of detritus from the distant Taconic Orogen (Witzke and Bunker, 1996). Compared to the Wise Lake, the relative absence of calcareous algae and the increase in lime mud suggests that middle and upper Dubuque deposition occurred in deeper, quieter waters (Witzke and Kolata, 1989; Witzke and Bunker, 1996).

The Dubuque and Maquoketa are separated by a prominent hardground surface

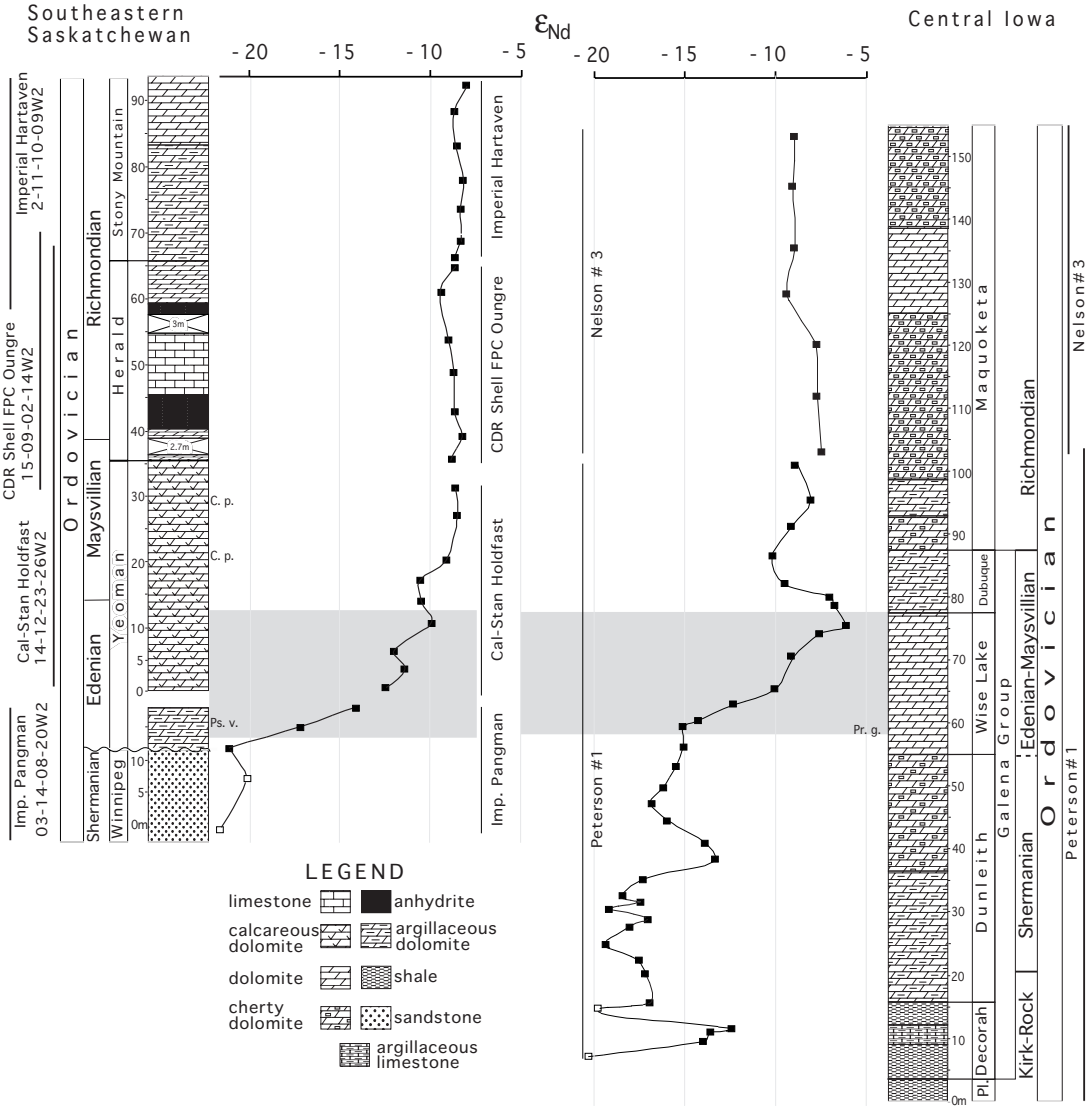

Figure 2.2 ε_{Nd} profiles of Ordovician strata from Saskatchewan and Iowa. The shaded boxes indicate correlation of the Yeoman Formation of the Williston Basin and the Wise Lake Formation of the central Midcontinent, across the Transcontinental Arch. Closed squares are data from the acid soluble fraction of carbonates, and open squares are data from shale or sandstone. Rock types are generalized. Placement of Iowa stage boundaries are from Witzke and Bunker (1996). Saskatchewan stage boundaries are based on conodonts from this study and Norford et al. (1994). Core identifications and the extent of stratigraphic overlap between cores is shown next to the stratigraphic sections. Actual sampled core intervals are shown next to the ε_{Nd} profiles. Lettering along both sections designates conodonts recovered from that interval. Pr.g. = *Periodon grandis*. C.p. = *Columbodina penna*. Ps.v. = *Pseudobelodina vulgaris vulgaris*. Pl = Platteville Formation and Kirk-Rock represents the undifferentiated Kirkfieldian through Rocklandian stages.

that is capped by the basal phosphorite unit of the Maquoketa. This interval represents an episode of transgressive deepening and related sediment starvation, and is overlain by organic rich brown shale, which marks the deepest depositional facies within the Upper Ordovician strata of Iowa (Witzke and Bunker, 1996). The brown shales grade laterally to argillaceous carbonate in northern and western Iowa, a common pattern throughout the Maquoketa, where shales represent the distal margin of an extensive clastic wedge derived from eastern Taconic sources (Witzke, 1987a). Although several other transgressive-regressive cycles occur through the rest of Maquoketa deposition, only this basal maximum transgression is of concern to this study.

2.2.2 Saskatchewan

The sampled interval of Upper Ordovician strata in Saskatchewan includes the upper portion of the Winnipeg Formation, composed of green-grey and black shales, and the Yeoman, Herald, and Stony Mountain formations which are characterized by a repetition of carbonate and evaporite intervals (Fig. 2.2). The change from a clastic to a carbonate-dominated environment at the base of the section marks a deepening event and drowning of the siliclastic source terranes of the Transcontinental Arch and Precambrian Shield (Kendall, 1976; Witzke, 1980). A disconformity separates the Yeoman from the underlying Winnipeg in this area. The carbonate and evaporite strata have been interpreted as brining upward cycles which, where complete, are composed of lower burrow-mottled carbonate, a middle laminated carbonate, and an upper sub-aqueous evaporite unit (Kendall, 1976; Longman et al., 1983).

Recent work, utilizing new core data from the upper Yeoman and lower Herald,

documents a shallowing-upward sequence (Pratt et al., 1996; Haidl et al., 1997; Canter, 1998; Kreis and Kent, 2000). Fossiliferous rudstones, boundstones, and coated grain facies above burrow mottled carbonates, together with evidence for localized subaerial exposure in the lower portion of the laminated unit, suggest that a sequence boundary is present between the lower laminated unit and the overlying laterally extensive laminated carbonates and basin-centered subaqueously deposited anhydrites. Further work is required to establish the detailed sequence stratigraphic framework of these and overlying carbonate and evaporite strata in the Herald and Stony Mountain formations.

In southeastern Saskatchewan, the basal unit of the Stony Mountain consists of fossiliferous, argillaceous to slightly argillaceous carbonates, which indicate a return to open marine conditions (Kendall, 1976). Overlying carbonates have a higher content of terrigenous clay and silt (Fuller, 1961; Kendall, 1976). The source of clastic detritus is to the southeast, either from the Transcontinental Arch and Shield (Witzke, 1980) or the Taconic Orogen (Osadetz and Haidl, 1989). The remainder of the Stony Mountain is composed of nodular, slightly argillaceous carbonates overlain by laminated dolostones capped by a thin anhydrite bed (Kendall, 1976).

2.3 Conodont biofacies

Nd isotopic profiles have been compared with biofacies represented by conodonts in core samples. The relative abundance of conodont genera believed to have lived at or near the sediment-water interface (benthic or nektobenthic life habitat) has been computed for each sample and compared with the patterns in Nd isotopes and Sm/Nd ratios.

Seddon and Sweet (1971) first recognized that the distribution of Ordovician

conodont genera and species are affected by facies; they attributed this to a pelagic habitat for conodonts. Instead, Barnes and Fåhraeus (1975) suggested that most Ordovician conodont genera were benthic or nektobenthic. A study specific to Upper Ordovician biofacies by Sweet and Bergström (1984) recognized six conodont biofacies for the Edenian-Maysvillian of North America.

The biofacies recognized by Sweet and Bergström (1984) are modified herein to reflect local faunas and comparative work by Nowlan and Barnes (1981). The biofacies for the Late Ordovician in order from shallowest to deepest are based on conodont genera believed to be of benthic or nektobenthic habit: 1. *Rhipidognathus* biofacies; 2. *Oulodus-Aphelognathus* biofacies; 3. *Plectodina* biofacies; 4. *Phragmodus* biofacies; 5. *Amorphognathus* biofacies. The genera *Panderodus* and *Drepanoistodus* and many of the other simple cone genera, such as *Belodina* and *Pseudobelodina,* are believed to be pelagic conodonts.

2.4 Sampling

Four cores from southern and central Saskatchewan, separated by up to 100 km, and two cores from central Iowa were sampled in order to construct continuous, or nearly continuous, Middle and Late Ordovician ε_{Nd} profiles on either side of the Transcontinental Arch (Fig. 2.2). Lithologic descriptions and formation boundary picks on cores from Saskatchewan are by Kendall (1976), and F.H. and G.N. (this study). For the Iowa cores (Peterson #1 T90N R27W Sec. 10 NE NE NE NW and Nelson #3 T79N R29W Sec. 12 SE NW SE) lithofacies and formation boundaries are by B.J. Witzke (unpublished data). Three of the four Saskatchewan cores overlap stratigraphically (Fig. 2.2) and are correlated using

formation boundaries as the datum. However, the Imperial Pangman 3-14-8-20 and Cal-Stan Holdfast 14-12-23-26 cores, which comprise the upper Winnipeg and basal Yeoman formations, do not overlap, leaving what is considered to be a small gap in the sampled section (Fig. 2.2). Although the Iowa cores are believed to overlap stratigraphically, the Nelson #3 core contains the upper Dubuque Formation and the majority of the Maquoketa Formation and the Peterson #1 core includes the entire Galena Group and the basal Maquoketa Formation, the exact correlation is uncertain. Since the ε_{Nd} profiles of the cores do not overlap, we chose to place the Nelson #3 ε_{Nd} profile stratigraphically above that of the Peterson #1 core (Fig. 2.2).

Subsurface depths varied widely between overlapping cores (Table 2.1, Table 2.2). Therefore, to simplify presentation of the ε_{Nd} data, overlapping cores were combined and depicted as a single measured stratigraphic section. The zero meter mark is placed arbitrarily at the base of the sampled section, regardless of the subsurface depth, and stratigraphic position between subsequent younger samples is displayed in meters, rather than in declining depth from the surface (Fig. 2.2).

In total, 41 carbonate samples from Iowa and 26 carbonate samples from Saskatchewan were collected for Sm-Nd isotopic analysis. In addition, two shale samples were analyzed from the Decorah Formation, and two sandstone samples were analyzed from the Winnipeg Formation. Twenty-eight samples in Iowa and 26 samples in Saskatchewan were processed for conodonts.

2.5 Analytical techniques

A homogeneous powder was created for each carbonate hand sample from 100 g of

Table 2.1. Sm and Nd isotope and concentration data from Saskatchewan core samples

Subsurface depth (m)	Compiled section (m)	Fm.[a]	Nd (ppm)	Sm (ppm)	Sm/Nd (atom)	$^{147}Sm/^{144}Nd$	$^{143}Nd/^{144}Nd$	$\varepsilon_{Nd}(450)$[b]
Acid soluble fraction of carbonates and whole rock sandstone[c] samples								
Hartaven 2-11-10-9W2								
2254.9	92.4	St	0.43	0.077	0.173	0.1095	0.511980	-7.8
2259.5	88.5	St	0.58	0.10	0.168	0.1068	0.511933	-8.6
2264.8	83.2	St	2.62	0.51	0.185	0.1171	0.511967	-8.5
2270.0	78.0	St	5.30	1.05	0.188	0.1195	0.511997	-8.1
2274.5	73.5	St	4.24	0.88	0.196	0.1246	0.512004	-8.2
2279.3	68.7	St	3.09	0.67	0.206	0.1308	0.512026	-8.2
2283.4	64.8	St	0.43	0.089	0.198	0.1257	0.511991	-8.5
Oungre 15-9-2-14W2								
3024.8	64.5	H	0.68	0.13	0.178	0.1127	0.511954	-8.5
3029.7	60.9	H	1.36	0.29	0.202	0.1282	0.511956	-9.4
3036.1	53.4	H	0.25	0.057	0.217	0.1378	0.512009	-8.9
3042.2	48.4	H	0.52	0.098	0.178	0.1130	0.511952	-8.6
3048.2	42.4	H	1.00	0.20	0.188	0.1194	0.511970	-8.6
3051.9	38.8	H	0.34	0.071	0.201	0.1277	0.512020	-8.1
3055.6	35.0	H	0.33	0.067	0.194	0.1228	0.511970	-8.8
Holdfast 14-12-23-26W2								
1739.5	30.8	Y	0.59	0.15	0.236	0.1494	0.512063	-8.5
1743.7	26.6	Y	0.3	0.062	0.199	0.1261	0.511999	-8.4
1750.7	19.8	Y	0.45	0.11	0.226	0.1432	0.512017	-9.1
1753.5	16.8	Y	0.54	0.13	0.229	0.1450	0.511949	-10.5
1756.8	13.7	Y	0.48	0.11	0.211	0.1342	0.511921	-10.4
1760.4	10.1	Y	0.38	0.084	0.211	0.1341	0.511947	-9.9
1764.2	6.1	Y	0.56	0.13	0.221	0.1400	0.511860	-11.9
1767.3	3.0	Y	0.5	0.11	0.214	0.1358	0.511878	-11.3
1770.2	0.3	Y	0.5	0.11	0.206	0.1308	0.511811	-12.4
Pangman 3-14-8-20W2								
2576.6	18.8	Y	2.25	0.38	0.161	0.1024	0.511643	-14.0
2579.6	15.9	Y	7.40	1.17	0.151	0.0957	0.511466	-17.1
2582.9	12.5	Y	31.0	6.72	0.206	0.1310	0.511363	-21.1
2587.7[c]	7.9	W	130	24.6	0.180	0.1142	0.511348	-20.4
2595.4[c]	0	W	40.5	8.28	0.195	0.1238	0.511294	-22.0
Conodont Data								
Hartaven 2-11-10-9W2								
2265.1	83.5	St	189	34.5	0.174	0.1105	0.51193	-8.9
2273.3	72.3	St	115	23.2	0.192	0.1216	0.511954	-9.0
2282.6	64.0	St	100	19.9	0.189	0.1201	0.512021	-7.6

[a] Name of the formation samples were collected from. St = Stony Mountain. H= Herald. Y= Yeoman; W=Winnipeg

[b] ε_{Nd} values calculated at 450Ma. $\varepsilon_{Nd}(450) = \{((^{143}Nd/^{144}Nd_{sample(0)} - (^{147}Sm/^{144}Nd_{sample(0)} (e^{\lambda(450Ma)}-1)))/ (^{143}Nd/^{144}Nd_{CHUR(0)} - (^{147}Sm/^{144}Nd_{CHUR(0)} (e^{\lambda(450Ma)} - 1))))-1\} \times 10^4$. present day = (0).

[c] Denotes whole rock sandstone samples

Table 2.2. Sm and Nd isotope and concentration data for Iowa core samples.

subsurface depth (m)	compiled section (m)	Fm.[a]	Nd (ppm)	Sm (ppm)	Sm/Nd	$^{147}Sm/^{144}Nd$	$^{143}Nd/^{144}Nd$	$\varepsilon_{Nd}(450)$[b]
Acid soluble fraction of carbonates and whole rock shale[c] samples								
Nelson #3								
428.5	154.0	Mq	4.44	0.98	0.211	0.1337	0.512007	-8.7
436.5	146.1	Mq	5.32	1.17	0.210	0.1332	0.511995	-8.9
446.5	136.0	Mq	5.97	1.30	0.207	0.1311	0.511999	-8.8
454.2	128.4	Mq	4.16	0.92	0.212	0.1344	0.511982	-9.2
462.7	119.9	Mq	4.19	0.83	0.188	0.1194	0.512011	-7.8
470.9	111.6	Mq	3.57	0.71	0.189	0.1200	0.512017	-7.7
480.1	102.5	Mq	4.38	0.83	0.181	0.1151	0.512015	-7.5
Peterson #1								
265.8	101.8	Mq	1.51	0.33	0.206	0.1308	0.511991	-8.8
271.8	96.0	Mq	4.89	1.25	0.245	0.1552	0.512100	-8.1
275.6	92.0	Mq	6.22	1.59	0.244	0.1549	0.512050	-9.1
280.6	87.2	Db	6.88	2.00	0.277	0.1755	0.512054	-10.2
285.0	82.6	Db	6.67	1.73	0.248	0.1572	0.512033	-9.5
286.9	80.8	Db	6.77	1.62	0.228	0.1450	0.512122	-7.1
288.3	79.2	Db	7.08	1.63	0.220	0.1395	0.512120	-6.8
291.7	75.9	WL	5.53	1.02	0.177	0.1121	0.512070	-6.2
293.0	74.7	WL	9.72	1.87	0.183	0.1163	0.512010	-7.6
296.8	71.0	WL	3.11	0.63	0.193	0.1222	0.511959	-9.0
301.9	65.8	WL	1.55	0.33	0.204	0.1294	0.511930	-10.0
304.3	63.4	WL	6.52	1.37	0.200	0.1268	0.511810	-12.2
306.9	60.7	WL	1.91	0.42	0.210	0.1333	0.511716	-14.3
308.0	59.7	WL	2.55	0.57	0.213	0.1354	0.511690	-15.0
311.0	56.7	WL	3.41	0.76	0.213	0.1354	0.511691	-15.0
314.4	53.3	Dl	2.41	0.55	0.218	0.1381	0.511675	-15.4
317.6	50.0	Dl	4.72	1.11	0.224	0.1422	0.511653	-16.1
320.0	47.5	Dl	5.13	1.14	0.212	0.1348	0.511596	-16.8
322.8	44.8	Dl	2.12	0.50	0.226	0.1436	0.511672	-15.8
326.4	41.1	Dl	3.76	0.87	0.222	0.1405	0.511766	-13.8
329.6	37.9	Dl	2.42	0.49	0.192	0.1218	0.511725	-13.5
332.2	35.4	Dl	10.4	2.29	0.211	0.1337	0.511570	-17.2
334.3	32.3	Dl	7.78	1.55	0.190	0.1205	0.511466	-18.5
335.7	31.9	Dl	6.04	1.15	0.181	0.1149	0.511510	-17.3
337.3	30.5	Dl	13.8	3.03	0.210	0.1331	0.511476	-19.0
338.4	29.2	Dl	22.8	4.61	0.193	0.1222	0.511549	-17.0
339.9	27.7	Dl	15.6	3.00	0.184	0.1167	0.511484	-17.9
342.6	25.0	Dl	9.87	2.05	0.198	0.1256	0.511446	-19.2
345.2	22.4	Dl	2.77	0.51	0.174	0.1104	0.511493	-17.4

(continued)

Table 2.2 (Continued)

subsurface depth (m)	compiled section (m)	Fm.[a]	Nd (ppm)	Sm (ppm)	Sm/Nd	$^{147}Sm/^{144}Nd$	$^{143}Nd/^{144}Nd$	$\varepsilon_{Nd}(450)$[b]
347.7	20.1	Dl	1.03	0.18	0.168	0.1065	0.511501	-17.0
352.2	15.4	Dl	20.4	3.98	0.186	0.1180	0.511544	-16.8
353.7[c]	14.0	Dc	14.6	2.10	0.140	0.0886	0.511320	-19.5
356.1	11.6	Dc	5.04	0.89	0.169	0.1073	0.511740	-12.4
356.8	11.0	Dc	2.68	0.49	0.174	0.1106	0.511694	-13.5
358.3	9.4	Dc	4.90	0.95	0.183	0.1160	0.511688	-13.9
360.6[c]	7.0	Dc	47.0	8.10	0.165	0.1046	0.511330	-20.2
Insoluble residue of carbonates								
Peterson #1								
271.8	96.0	Mq	26.4	3.13	0.113	0.0716	0.511837	-8.5
285.0	82.6	Db	23.2	2.75	0.113	0.0717	0.511825	-8.7
288.3	79.2	Db	23.2	2.82	0.116	0.0733	0.511903	-7.2
293.0	74.7	WL	14.2	1.98	0.133	0.0841	0.511788	-10.1
304.3	63.4	WL	4.67	0.67	0.137	0.0870	0.511754	-10.9
311.0	56.7	WL	10.9	1.18	0.102	0.0649	0.511689	-10.9
320.0	47.5	Dl	6.26	0.78	0.119	0.0754	0.511618	-12.9
332.2	35.4	Dl	6.59	1.02	0.147	0.0931	0.511597	-14.4
342.6	25.0	Dl	8.59	1.27	0.141	0.0893	0.511379	-18.4
356.1	11.6	Dc	7.4	1.11	0.143	0.0905	0.511410	-17.9
356.8	11.0	Dc	11.7	1.71	0.140	0.0887	0.511367	-18.6
Calculated carbonate whole rock data[d]								
Peterson #1								
271.8	96.0	Mq	7.91	1.51	0.183	0.1164	0.511977	-8.3
285.0	82.6	Db	9.52	1.90	0.192	0.1218	0.512059	-9.2
288.3	79.2	Db	8.79	1.75	0.191	0.1215	0.511946	-7.0
293.0	74.7	WL	10.3	1.88	0.175	0.1111	0.511969	-8.2
304.3	63.4	WL	6.42	1.33	0.199	0.1263	0.511808	-12.1
311.0	56.7	WL	3.89	0.78	0.194	0.1230	0.511691	-14.3
320.0	47.5	Dl	5.35	1.07	0.192	0.1215	0.511601	-15.9
332.2	35.4	Dl	9.06	1.85	0.196	0.1242	0.511577	-16.5
342.6	25.0	Dl	9.50	1.82	0.184	0.1168	0.511428	-19.0
356.1	11.6	Dc	5.20	0.91	0.167	0.1058	0.511707	-12.9
356.8	11.0	Dc	3.13	0.55	0.169	0.1071	0.511633	-14.5
Conodont data								
Peterson #1								
291.7	75.9	WL	294	56.7	0.184	0.1164	0.512027	-7.3
299.5	68.1	WL	267	54.4	0.194	0.1230	0.511872	-10.7
317.6	50.0	Dl	173	44.5	0.244	0.1551	0.511600	-16.7

[a] Name of the formation samples were collected from: Mq = Maquoketa; Db = Dubuque; WL = Wise Lake; Dl = Dunleith; Dc = Decorah.

[b] ε_{Nd} values calculated at 450Ma. $\varepsilon_{Nd}(450) = \{((^{143}Nd/^{144}Nd_{sample(0)} - (^{147}Sm/^{144}Nd_{sample(0)}(e^{\lambda(450Ma)}-1)))/(^{143}Nd/^{144}Nd_{CHUR(0)} - ^{147}Sm/^{144}Nd_{CHUR(0)}(e^{\lambda(450Ma)}-1))))-1\} \times 10^4$. Present day = (0)

[c] Denotes whole-rock shale samples. [d] Whole-rock carbonate values are based on material balance calculations that use measured values from the insoluble-residue and acid-soluble fractions

rock. Two grams of powder were weighed into a 50 ml centrifuge tube. The carbonate was then dissolved by adding 0.5 ml increments of 6.0 N HCl dropwise, waiting until each increment had completely reacted before adding the next. When dissolution was completed the solution was centrifuged to separate the acid soluble fraction from the acid insoluble fraction. The supernate was passed through a syringe filter with a 0.2 μm teflon PTFE membrane to ensure removal of any fine HCl-insoluble particles. The resulting clear solution was then spiked with a ^{149}Sm-^{150}Nd tracer, gently agitated, and left overnight to ensure sample-spike equilibration.

The rare earth elements (REEs) were stripped from this high Ca^{+2} and Mg^{+2} solution using a Fe-hydroxide co-precipitation technique modified from Edwards et al. (1987). Nine mg of Fe^{+3}, as $FeCl_3$ in HCl, were added to the solution. Dropwise addition of concentrated ammonium hydroxide caused the iron to flocculate and the solution to turn from yellow to clear. The Fe-hydroxide floccules and the adsorbed REEs were centrifuged, the supernate was discarded, and the precipitate rinsed three times in ultrapure water. Nd yields from the Fe-coprecipitation technique were 100%.

Eleven samples of the HCl-insoluble residues (IR) were further treated by soaking them in 1 to 2 ml of 6.0 N HCl for two hours to ensure complete removal of any remaining biogenic apatite. The residues were then rinsed with ultrapure water, dried and weighed; 30 to 90 mg were removed, spiked with the ^{149}Sm-^{150}Nd tracer and dissolved in an HF/ HNO_3 solution.

Conodonts were separated from 200 to 650 g of carbonate using 10% acetic acid, then concentrated by sieving and heavy liquid separation, and brushed in ultrapure water to remove adhering material. Conodonts were weighed, spiked with a ^{149}Sm-^{150}Nd tracer

solution, and dissolved in 2.0 N HNO_3.

Sm and Nd were separated with standard chromatography methods using HDEHP coated teflon powder. Purified Sm and Nd were loaded onto side Re filaments of a double filament assembly and analyzed on a Finnigan MAT 261 instrument as Sm^+ and Nd^+ ions using a static multi-collection routine. Totally spiked isotope abundance measurements were unmixed for tracer isotopes and corrected for instrumental mass fractionation using an iterative procedure described by Eugster et al. (1969). $^{143}Nd/^{144}Nd$ ratios were normalized to $^{146}Nd/^{144}Nd$ of 0.7219 and Sm isotope ratios were normalized to $^{148}Sm/^{154}Sm$ of 0.494190. External reproducibility of $^{143}Nd/^{144}Nd$ is ± 0.000017 (2σ), based on replicate analyses of our internal Nd Ames standard. Over the course of this work the La Jolla standard yielded $^{143}Nd/^{144}Nd = 0.511841$.

Epsilon Nd values presented in the text are back-corrected using the measured $^{147}Sm/^{144}Nd$ ratios to the time of deposition at 450 Ma and can be written:

$$\varepsilon_{Nd}(450) = \{((^{143}Nd/^{144}Nd_{sample(0)} - (^{147}Sm/^{144}Nd_{sample(0)}(e^{\lambda(450Ma)}-1)))/(^{143}Nd/^{144}Nd_{CHUR(0)} - ^{147}Sm/^{144}Nd_{CHUR(0)}(e^{\lambda(450Ma)}-1))))-1\} \times 10^4 \quad \text{Equation 3.1}$$

where $\lambda = 6.54 \times 10^{-12}\ y^{-1}$, (0) = present day and CHUR is defined as the chondritic uniform reservoir. Although the stratigraphic age of the sampled section spans approximately 13 Ma, the maximum error introduced by using a single age for all samples is less than 0.2 epsilon units. Excursions in the ε_{Nd} profiles through the Ordovician Iowa and Saskatchewan carbonates are defined as having an initial steady increase in values followed by a steady

decrease in values. The magnitude of this change must be greater than 2.5 epsilon units to clearly distinguish the excursion from analytical error and to be judged to have represented a significant change in the Nd isotope balance of the Midcontinent epeiric sea. A shift in ε_{Nd} values is defined by a positive increase or decrease in values that is not followed by the opposing trend and may occur over a greater stratigraphic interval than an excursion.

2.6 Carbonates as a medium for Nd isotope stratigraphy

The molar Nd/Ca ratio of modern seawater is about $2x10^{-9}$ (Shaw and Wasserburg, 1985). Assuming there is no fractionation of Nd from Ca during calcification by marine organisms, biogenic carbonates should contain approximately 3 ppb of Nd, but such low concentrations are observed only in the detritus-free carbonate of some living organisms (Shaw and Wasserburg, 1985). Recently deposited, detritus-free limestones and dolostones have concentrations that are higher by several orders of magnitude, indicating that lattice-bound Nd accounts for only a small portion of the bulk Nd in carbonate material (Shaw and Wasserburg, 1985). Consequently, it has been suggested that the majority of Nd in recent marine carbonates is acquired by incorporation of a REE-rich, Fe-Mn phase on growing crystal surfaces (Turekian et al., 1973) or as a REE-rich Fe-Mn surficial coating acquired after death of the organism (Palmer, 1985; Shaw and Wasserburg, 1985). Because Fe-Mn floccules scavenge REEs from seawater, metalliferous coatings have ε_{Nd} values identical to seawater (Palmer, 1985; Palmer and Elderfield, 1985).

Ancient epeiric sea carbonates have widely varying Nd concentrations (0.1 to 20 ppm) (Banner et al., 1988; Bellanca et al., 1997). Differences in depositional settings between modern oceans and ancient epeiric seas, such as depth, salinity and particulate flux, may

account for some of the increase in concentration. However, a potentially important source of Nd in epeiric sea carbonates is the non-carbonate fraction composed of detrital and authigenic silicates, oxides, and biogenic apatite grains. Dissolution of a whole rock carbonate results in two fractions, an acid soluble (AS) fraction encompassing all carbonate and non-carbonate components that are HCl-soluble, and the remaining HCl-insoluble residue (IR).

Whole rock carbonates in this study show a positive correlation between the Nd concentration in the AS fraction and weight percent IR (Fig. 2.3a). This correlation suggests Nd and Sm in the AS fraction are not just derived from the carbonate but are being leached from the non-carbonate component, which is represented by the weight percent of IR in each sample, thereby influencing the Nd concentration of the AS fraction. However this correlation does not clarify what fraction of the non-carbonate component was mobilized. Igneous silicate and oxide minerals will be relatively unaffected by the HCl digestion and can be ruled out as significant sources of REE to the AS fraction. Cation exchange sites in clay minerals may contribute some REE, but Awwiller (1994) found that Eocene shales from south central Texas contained only 30 ppb of Nd in exchangeable sites. This is expected given the low concentrations of trivalent REEs in aqueous fluids relative to the more concentrated monovalent and divalent ions, such as Ca^{+2} and Na^{+1}, which compete with the REEs for positions in exchangeable sites. Accordingly, exchangeable Nd in clays cannot account for the 1-10 ppm of HCl-soluble Nd leached from Eocene shales (Awwiller, 1994).

Assuming that the HCl digestion does not further disturb the clay mineral lattice, the mobile Nd in the non-carbonate fraction likely originates from soluble REE-rich accessory phases, like apatite, or Fe-Mn coatings on detrital grains. Fragments of biogenic

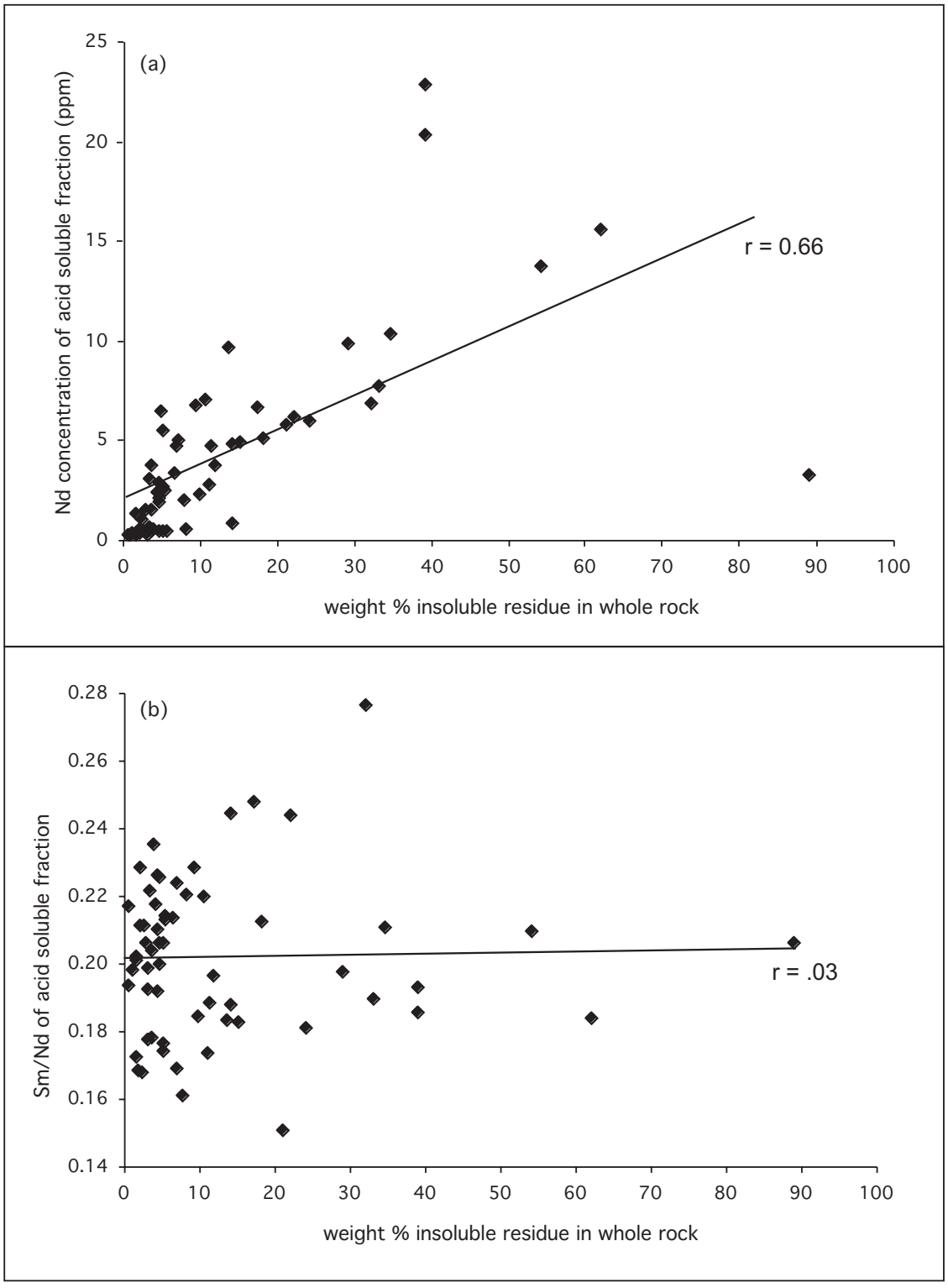

Figure 2.3 The weight percent insoluble residue versus (a) the Nd concentration and (b) the Sm/Nd ratios of the acid soluble fraction of Iowa and Saskatchewan carbonates. Plots display linear regression lines with determined correlation coefficients, r.

apatite have been observed in the < 0.2 μm fraction of shales (Ohr et al., 1991), and are likely a ubiquitous REE-rich phase in many marine sediments. Even marine carbonates with low yields of phosphatic fossils may contain finely dispersed apatite mineral debris. The concentration of Nd in biogenic apatite (100-2000 ppm) and Fe-Mn coatings (150-600 ppm) are very high (Wright et al., 1984; Shaw and Wasserburg, 1985; Staudigel et al., 1985; Palmer, 1985; Palmer and Elderfield, 1985; Palmer and Elderfield, 1986) and can account for the majority of mobile Nd in our non-carbonate fraction. In fact biogenic apatite and Fe-Mn coatings have also been found to contribute the majority of Nd to the leachate of shales (Schaltegger et al., 1994; Awwiller, 1994).

Regardless of the source, the similarity in ε_{Nd} values between the apatite of six conodont samples and the AS fraction of their enclosing whole rock carbonate (Table 2.2) indicates that the bulk of the Nd in the AS fraction is derived from seawater overlying the depositional site, or from early diagenetic pore waters. There is also a close correspondence between Sm/Nd ratios of the AS fractions of carbonates and coexisting conodonts (mostly within 0.01 units; Table 2.2), indicating that the Sm/Nd ratios of the AS fractions are not changed by carbonate dissolution in the laboratory. Sm/Nd ratios of the AS fractions are also comparable to those determined by Holmden et al. (1998) for late Middle Ordovician biogenic apatite sampled across a single K-bentonite defined time slice extending between the Transcontinental Arch and Taconic Orogen.

Even though the Sm/Nd ratios of the AS fraction appear to remain unchanged during acid digestion, this observation must be reconciled with the low Sm/Nd ratios (0.10-0.14) of the IR (Table 2.2). Similarly low Sm/Nd ratios have also been documented for the residues resulting from acid leaching of shales, and of marlstone (Awwiller, 1994; Ohr et al., 1994;

Bellanca et al., 1997). One explanation for our low Sm/Nd ratios is that the non-carbonate fraction consists of a mixture of HCl-insoluble phases with relatively low Sm/Nd ratios (the IR), and acid soluble phases, like biogenic apatite and Fe-Mn coatings on detrital grains, with relatively high Sm/Nd ratios. HCl dissolution preferentially removes the apatite and coatings, leaving low Sm/Nd ratios in the remaining IR. Alternatively, we cannot rule out the possibility that the Sm/Nd ratios of the IR are altered as a direct consequence of acid digestion in the laboratory and preferentially leaching of Sm over Nd from the IR, but the close correspondence between Sm/Nd ratios of conodonts and the AS fractions would suggest that this is not the case.

Since almost all samples have experienced some degree of dolomitization, we must consider the effect of diagenesis on the ε_{Nd} values and Sm/Nd ratios of the carbonates. Banner et al. (1988) found that the ε_{Nd} values of marine limestones remained unchanged during two major episodes of extensive dolomitization. Marine and non-marine diagenetic fluids have such low Nd concentrations that fluid:rock ratios on the order of 10^3 or higher are necessary to alter the ε_{Nd} values of the original limestone (Banner et al., 1988), including the Fe-Mn coatings and biogenic apatite (Palmer and Elderfield, 1986; Grandjean and Albarède, 1989; Holmden et al., 1996). Even though Fe-Mn coatings and floccules may be susceptible to dissolution and reprecipitation during diagenesis in response to changing oxidation states in pore waters, the Nd isotopic composition should remain unaffected because the main source of Nd to pore waters is most likely from the dissolution of the floccules or coatings (Palmer and Elderfield, 1985).

Although REE profiles, and therefore Sm/Nd ratios, are more susceptible to diagenetic effects than ε_{Nd} values, Palmer and Elderfield (1986) showed that REE profiles

of Atlantic foraminifera of Recent and Cenozoic age had Sm/Nd ratios that differed by only 0.02 units. Such a small change in Sm/Nd would have little effect on the overall shape of our ε_{Nd} profile, where variations are on the order of 3 to 10 epsilon units.

We conclude that the AS fraction appears to record the ε_{Nd} values of contemporaneous seawater. Dissolvable phases in the non-carbonate component will elevate Nd concentrations in the AS fraction but the majority of this excess Nd is likely provided by biogenic apatite and Fe-Mn coatings. These two phases scavenge Nd from seawater, and therefore contribute Nd with an isotopic composition equivalent to that preserved within the carbonate lattice. Finally, even if clay interlayer sights are disturbed during carbonate dissolution, this may not effect preservation of seawater ε_{Nd} values because pelagic clays and overlying ocean water can have similar Nd isotopic compositions (Goldstein and O'Nions, 1981) as can the dissolved and detrital fractions of rivers (Goldstein and Jacobsen, 1987).

2.7 Nd isotopic profile-Iowa

Nd from the AS fraction in Iowa carbonates exhibits four major oscillations in ε_{Nd} (Fig. 2.4) that are interpreted to reflect fluctuations in sea level. The excursions in the mid-Decorah (I-1), basal Dunleith (I-2), and mid-Dunleith (I-3) display a pattern of initially increasing, then decreasing ε_{Nd} values (Fig. 2.4, Table 2.2). Increasing ε_{Nd} values of the I-1, I-2 and I-3 excursions are interpreted as mixtures of Precambrian and Taconic-derived Nd that resulted from sea level rise, partial submergence of the Transcontinental Arch and Canadian Shield, and westward expansion of water masses carrying Taconic-derived Nd (Fig. 2.4, Table 2.2). Decreasing ε_{Nd} values reflect sea level fall and re-establishment of the Precambrian Arch and Shield signatures. In comparison to I-1 and I-3, the smaller magnitude

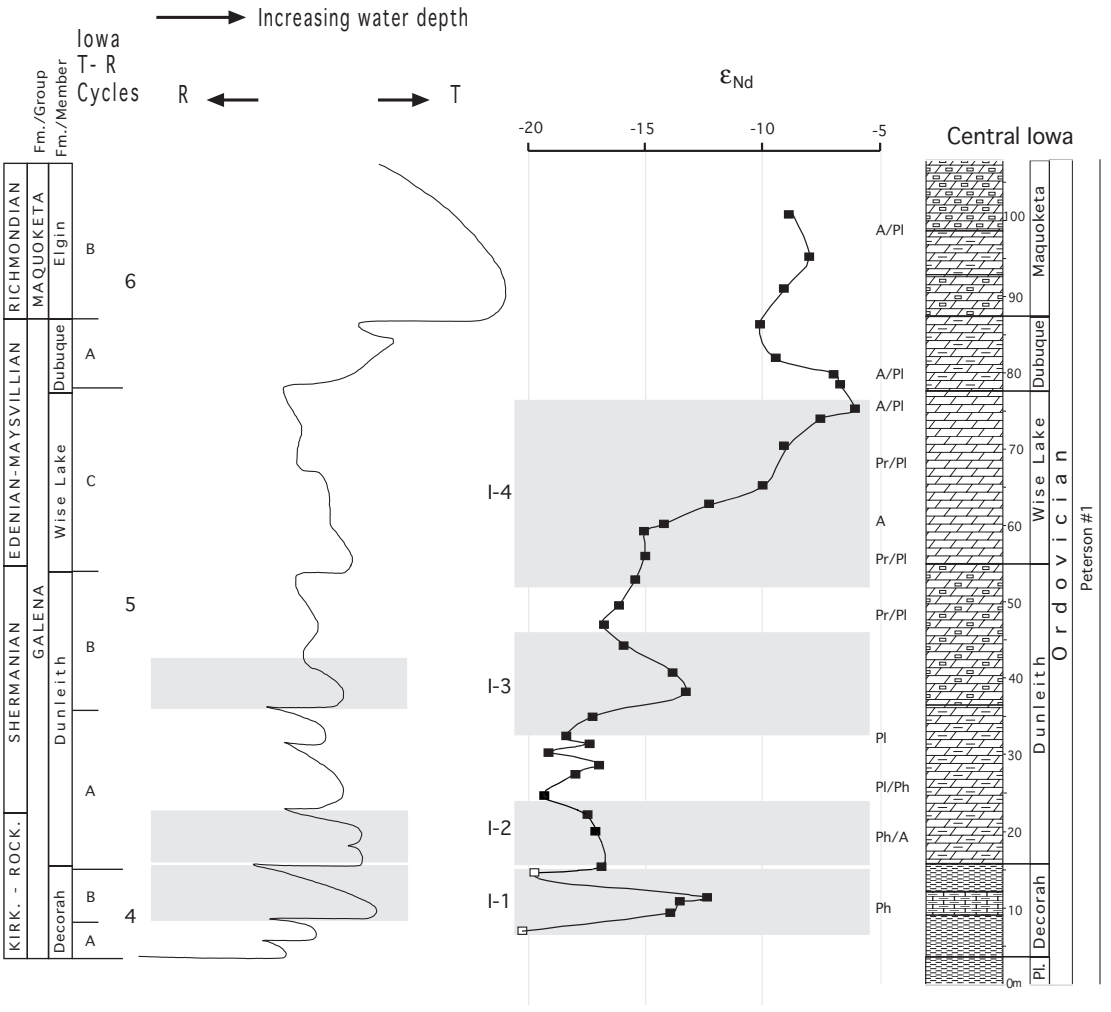

Figure 2.4 Comparison of the ε_{Nd} curve from Iowa, the sea level curve of Witzke and Bunker (1996) and conodont paleoecology from this study, which is denoted by lettering next to the Iowa section. Conodont abbreviations are listed by decreasing depth: A. = *Amophognathus*. Ph. = *Phragmodus*. Pr. = *Periodon*. Pl. = *Plectodina*. Other abbreviations are as in Fig. 2.2.

I-2 excursion from ε_{Nd} = -19 to -17 suggests a smaller contribution of Taconic-derived Nd. Alternatively, the I-2 excursion could reflect local changes in the weighted, average flux of Nd from basement terranes of the Arch and Shield.

The fourth excursion (I-4) is characterized by a steady increase in ε_{Nd} through the Wise Lake, from -15 to -6.2, with no corresponding return to pre-shift values (Fig. 2.4, Table 2.2). The I-4 shift reflects complete submergence of the Arch and Shield, leaving the Taconic Orogen as the sole provider of dissolved Nd to the central Midcontinent epeiric sea. Epsilon Nd values indicative of Taconic-derived Nd persist for the remainder of the sampled section.

Important similarities and differences are evident between the ε_{Nd} record of Late Ordovician sea level change and conventional sea level curves for the Iowa area that may record either eustatic or local changes in sea level (Fig. 2.4) (Witzke and Kolata, 1989 and Witzke and Bunker, 1996). The I-1, I-2 and I-3 isotopic excursions all mirror predicted transgressive-regressive events (T-R cycles, 4B, 5A and 5B respectively) (Fig. 2.4), and small ε_{Nd} excursions between I-2 and I-3 correspond to T-R subcycles within the 5A T-R event. As expected, the positive isotopic shifts denote transgressions marked by decreases in clastic content, expansion of carbonate facies, and drowning of siliclastic source terranes. The negative isotopic shifts signify regressions marked by shale progradation or general increase in the clastic content of the carbonates. A transgressive event should ostensibly correspond with the I-4 ε_{Nd} shift, but an upward increase in calcareous algae and storm-generated grainstone layers through this interval (T-R cycle 5C) indicates a regressive event, culminating in maximum regression at the top of the Wise Lake (Fig. 2.4) (Witzke and Kolata, 1989; Witzke and Bunker, 1996).

The I-4 isotopic excursion highlights an important distinction between sea level curves and the Nd isotope profile. The ε_{Nd} profile preserves sea level changes relative to the height of the Arch and Shield, much like preserving a watermark on the side of the emergent Precambrian basement. Therefore, the ε_{Nd} profile cannot distinguish between eustatic sea level change and relative sea level change resulting from uplift or subsidence of the Arch and Shield. The sea level curve of Witzke and Bunker (1996) is, instead, a reflection of changing depth of the water column. Therefore we suggest that during the I-4 interval, sea level rose relative to the Arch while water depth shallowed due to a carbonate production rate that exceeded the rate of sea level rise.

The sea level interpretation of the Nd isotopic profile is also compatible with paleoecologic interpretations based on conodonts collected from the cored section. Although sparse, specimens of *Phragmodus undatus* recovered from samples at the peak of the positive excursions of I-1 and I-2 are consistent with a relatively deeper water facies (Fig. 2.4). Specimens of *Plectodina*, a genus indicating intermediate depth, appear in the conodont assemblages between the I-2 and I-3 transgressions, coinciding with the return of more negative ε_{Nd} values (ε_{Nd} = -19) (Fig. 2.4). Species of *Amorphognathus* and *Periodon* appear throughout the I-4 interval (Fig. 2.4). These genera are immigrants from the cold water Atlantic faunal region on the continental margin and are generally deeper, cooler water forms. However they also occur with significant quantities of the intermediate depth *Plectodina* from the Midcontinent faunal region. Although a mixed conodont fauna through the I-4 interval is ambiguous regarding depth, the presence of the immigrant eastern fauna coincides with the increasing contribution of dissolved Nd from the Taconic Orogen, as recorded in Iowa carbonates.

The persistence of purely Taconic-derived Nd from the top of the Wise Lake into the lower Maquoketa (Fig. 2.2, Table 2.2) indicates that the Precambrian basement remained covered by seawater, or carbonate sediment following the I-4 shift. In either case, the flux of Nd weathered from the Precambrian basement of the Arch and Shield is shut-off, and until the Precambrian basement is re-exposed ε_{Nd} values of neighboring carbonates can no longer resolve changes in sea level. For example, the ε_{Nd} profile cannot resolve the large transgression at the base of the Maquoketa (Fig. 2.4).

An interesting question concerns the timing of the re-exposure of Precambrian basement and re-establishment of Precambrian derived Nd in Iowa carbonates. Thus far, ε_{Nd} data for Phanerozoic clastic successions of the southeastern United States and the Arctic show that after the Late Ordovician the Precambrian source signature is not observed again in the Paleozoic (Patchett et al., 1999a; Gleason et al., 1995). Patchett et al. (1999a) propose that cannibalistic recycling of the large volume of sediment derived from the Taconic and the Caledonian Orogenies dominated the sedimentary budget until the rise of the Cordillera began to shed new sediment. The ε_{Nd} values of carbonates in the continental interior may be more sensitive to changes in the age make-up of surrounding exposed crust and re-exposure of Precambrian basement.

Correlated changes in ε_{Nd}, sea level, and conodont paleoecology provide strong evidence linking submergence of the Arch and Shield with changes in the Nd isotope balance in neighboring epeiric seas. However, the net flux of Nd into Midcontinent seas is also influenced by changes in source area weathering rates. For example, uplift of the Taconic Orogen may accelerate weathering, delivering more Nd to Midcontinent seas and shifting the isotope balance towards the Taconic signature. Likewise, temporal variations in climate

(aridity/humidity) over the Arch and Shield may also influence weathering rates, shifting the isotope balance towards the Precambrian basement signature. Although changes in weathering rates should influence the Nd isotope balance in epeiric seas, it is difficult to isolate this control from changes in the total area of exposed crust. For example, Taconic uplift has been associated with subsidence and sea level rise as a result of flexural warping of the eastern margin of North America (Holland and Patzkowsky, 1996). Therefore, uplift and increased weathering of the Taconic Orogen will be associated with a relative sea level rise and submergence of the Arch and Shield. Our interpretation that the ε_{Nd} profile predominantly records the Late Ordovician submergence history of the Arch and Shield is the simplest explanation of a potentially complex system.

The question of whether ε_{Nd} values of carbonates could be affected by windborn detritus or volcanic ash must be addressed. Nd is particle reactive and is likely to remain sequestered to particles during sedimentation. Jones et al. (1994) showed that modern ash from Pacific rim volcanic arcs contributed minimal REE to North Pacific deep water. Holmden et al. (1996) showed that conodonts from within 10 cm of the Millbrig K-bentonite had ε_{Nd} values that appeared to be unaffected by Nd derived from the altered volcanic ash. Ash falls may influence the ε_{Nd} values of epeiric seawater during ash fall, but the duration of such an event is short in comparison to our ε_{Nd} excursions, which likely span hundreds of thousands of years.

2.8 Nd isotope stratigraphy

In Saskatchewan, Upper Ordovician carbonates of the Yeoman exhibit a single, large positive isotope shift (ε_{Nd} = -21 to -9) that can be correlated with the I-4 shift in Iowa

(Fig. 2.2). Assuming that these isotope excursions are synchronous, the lower part of the Yeoman is correlated with the entire Wise Lake of Iowa. Both shifts in ε_{Nd} value are of similar magnitude and are followed by an uninterrupted succession of carbonates with ε_{Nd} values of approximately -6 to -9 (Fig. 2.2), supporting the interpretation that the I-4 and Yeoman excursions are recording the same sea level rise. Although the magnitudes of the I-4 and Yeoman isotopic shifts are approximately 10 epsilon units, the Yeoman isotope excursion is offset towards more negative values (Fig. 2.2, Tables 2.1 and 2.2), suggesting that the Williston Basin may have continued to receive minor amounts of Nd from small islands of exposed Canadian Shield to the north or east. An extension of the carbonate ε_{Nd} profile into strata older than the Yeoman is prevented by the underlying clastics of the Winnipeg.

It is possible that there is an additional northern source of Nd to the Williston Basin that has been linked by Patchett et al. (1999b) to the early phase of the Caledonian Orogen. An ε_{Nd} shift in clastics of the Arctic Islands occurs between 460 to 440 Ma, and falls within the time frame of our stratigraphic sections (Patchett et al., 1999b). However, because the ε_{Nd} signature of this northern source is indistinguishable from that of the Taconic, the impact of this northern source on the Nd isotope balance of the Williston Basin, or other Midcontinent epeiric seas, will be similar to that described for the Taconic.

The Nd isotope stratigraphy can refine previous correlations between Upper Ordovician marine carbonates across the Transcontinental Arch. In general, recognition of the time equivalency of Galena Group through lower Maquoketa strata with that of the Yeoman and Herald has long been accepted (Sweet and Bergström, 1976; Sweet, 1979; Witzke, 1980). Biostratigraphic and lithostratigraphic refinement of this generalization

has placed the base of the Yeoman equivalent to either the base (Sweet, 1979; Witzke, 1980) or middle (Sloan, 1987) of the Dunleith. Using Nd isotope stratigraphy, we instead correlate the base of the Yeoman with the base of the Wise Lake. The Edenian to Maysvillian age assigned to the Yeoman by Norford et al. (1994) and the conodont faunas recovered from this study, which include *Culombodina penna*, support this conclusion, since the Dunleith is generally considered to be Shermanian in age, whereas the Wise Lake is considered to be Edenian to Maysvillian in age (Fig. 2.2) (Witzke, 1980; Sloan, 1987).

Placement of the Edenian-Shermanian boundary in Iowa is uncertain, however, and has only been provisionally placed at the base of the Wise Lake (Fig. 2.2) (Witzke, 1987a; Witzke and Bunker, 1996). The occurrence of *Periodon grandis*, 5 meters above the base of the Wise Lake in the Peterson #1 core, (Fig. 2.2) constrains the basal portion of the Wise Lake to be no younger than Edenian to earliest Maysvillian. In the Saskatchewan section, the presence of *Pseudobelodina vulgaris vulgaris* at the base of the Yeoman (Fig. 2.2) in the Pangman well indicates an age no older than mid-Edenian. In addition, the presence of specimens of *C. penna* within the Yeoman in the Holdfast core (Fig. 2.2) indicates a mid-Edenian to mid-Maysvillian age. Since the isotope stratigraphy indicates that the base of the Yeoman is equivalent to the base of the Wise Lake, we can combine the biostratigraphic data from Iowa and Saskatchewan to conclude that in our cores the base of the Yeoman and Wise Lake must be mid-Edenian to earliest Maysvillian in age.

One further paleogeographic clarification within the Williston Basin can be made using the ε_{Nd} value of the clastics that comprise the argillaceous interval of the Stony Mountain. These argillaceous carbonates and shale interbeds thicken toward the eastern margins of the basin, which are delineated by the Arch and Shield. Witzke (1980) suggested

these shales were derived from the Arch. Osadetz and Haidl (1989) argued for a source of clastics beyond the Arch and Shield from the Taconic Orogen. The ε_{Nd} value for the clastics in this interval yielded -8, a clear Taconic source signature. Knowing that clastics in Saskatchewan have a Taconic source indicates that the Arch was once again submerged and that a seaway connected the central Midcontinent and the Williston Basin.

2.9 Sm/Nd profiles and depth

Sm/Nd ratios of the AS fractions display large variations throughout both the Iowa and Saskatchewan sections. Such large variations warrant further investigation into the possible mechanisms controlling fractionation of Sm from Nd and the potential paleoenvironmental implications. Holmden et al. (1998) found that across the 454 Ma Millbrig-Deicke K-bentonite time slice, Sm/Nd ratios of conodonts bordering the Arch ranged from 0.17-0.21, while those bordering the Taconic Highlands ranged from 0.20-0.26. These findings initially suggest that the stratigraphic variations in Sm/Nd ratios of this study, from 0.15 to 0.27 (Table 2.1, Table 2.2), may be related to changes in REE provenance. However, both Iowa and Saskatchewan carbonates with ε_{Nd} values indicative of Taconic-derived Nd have corresponding Sm/Nd ratios that span the entire range of observed values, from 0.17 to 0.27 (Fig. 2.5).

Fractionation of Sm/Nd during acid digestion of the carbonates is also ruled out because Sm/Nd ratios of the AS fraction of carbonates are similar to conodonts. Furthermore, the post shift ε_{Nd} values in the Saskatchewan section are nearly constant for 70 meters of stratigraphic section despite large variations in Sm/Nd ratios (Table 2.1, Fig. 2.5). This suggests that fractionation of Sm from Nd was established at the time of deposition, or

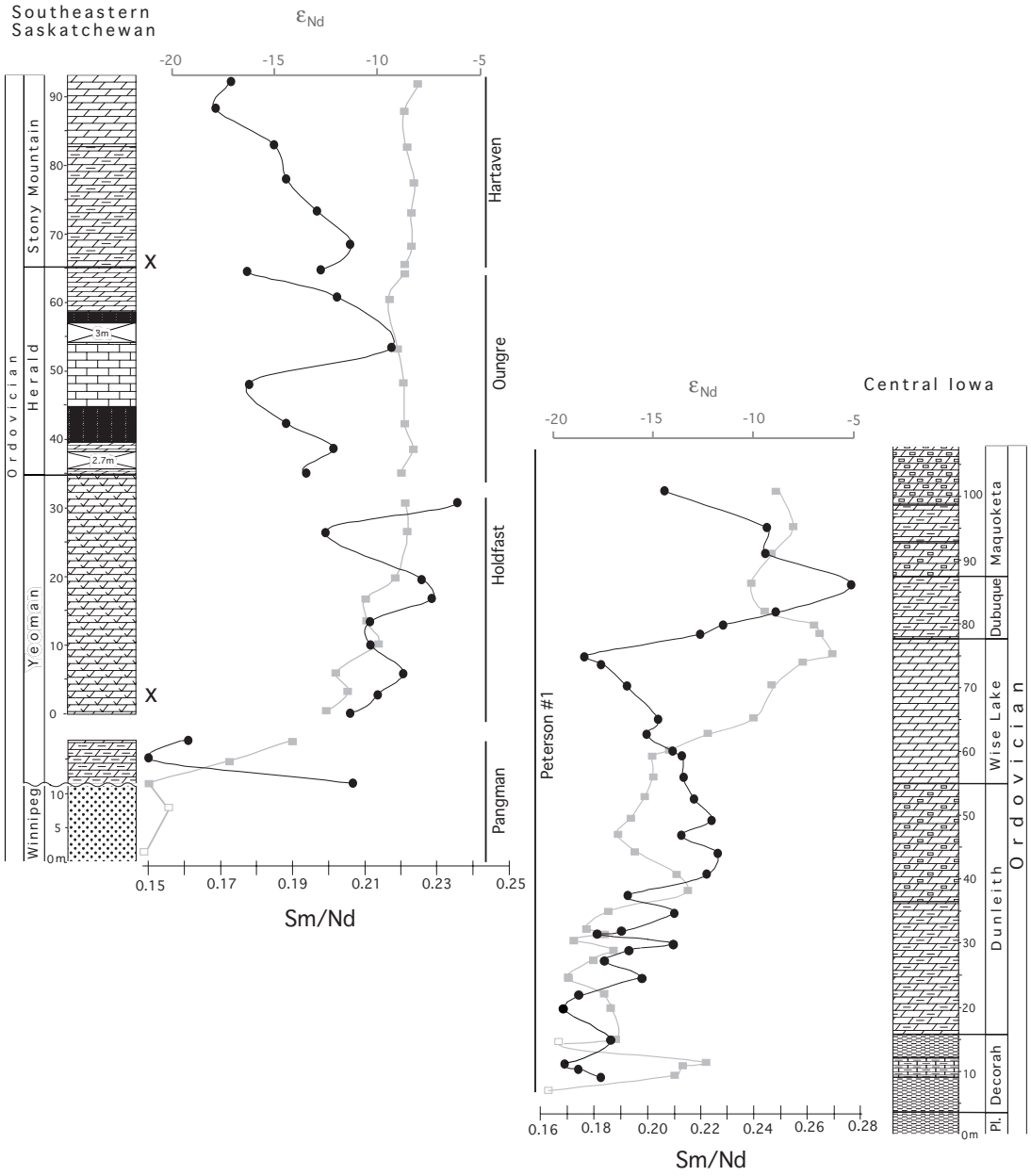

Figure 2.5 Statigraphic variations in Sm/Nd ratios of the acid soluble fraction of carbonates from Iowa and Saskatchewan are shown in black circles and compared to the complimentary ε_{Nd} curve shown in grey squares. An X denotes transgressive events in Saskatchewan based on the sedimentology. Open squares indicate data from shale or sandstone.

shortly thereafter. The low clastic content throughout the Saskatchewan section minimizes the impact of potential leaching of the non-carbonate fraction during carbonate dissolution, and no correlations exist between Sm/Nd ratios and weight percent IR in either the Saskatchewan or Iowa sections (Fig. 2.3b). Therefore, we conclude that Sm/Nd ratios, and more generally REE fractionation, are responding to locally changing conditions in the epeiric sea.

Fractionation of REEs in global surface waters is well known (Hoyle et al., 1984; Elderfield et al., 1990; German and Elderfield 1990; Piepgras and Jacobsen, 1992). For example, comparing REE profiles of rivers, estuaries, coastal seas and deep oceans has revealed that surface waters become progressively enriched in HREE as they move toward the deep ocean (Elderfield et al., 1990). This has been attributed, in part, to preferential adsorption of LREE onto authigenic particulates, which are then transported to the sediments leaving the water column of each successive environment (from rivers to deep oceans) enriched in the more soluble HREE (Elderfield et al., 1990; Byrne and Kim, 1990). Fractionation of REEs may also occur in pore waters as a result of adsorption and desorption from these particulates (Elderfield and Sholkovitz, 1987; Elderfield et al, 1990).

An evaluation of stratigraphic changes in Sm/Nd from the Iowa section yields some clues about the paleoenvironmental factor(s) influencing the fractionation of Sm/Nd in the epeiric sea environment. A comparison of variations in Sm/Nd ratios with the sea level curve shows a close correspondence between increasing Sm/Nd ratios and increasing water depth (Fig. 2.6). The most striking example is the agreement between the dramatic increase in Sm/Nd ratios from the base of the Dubuque to the base of the Maquoketa, and the transgressive phases of cycles 6A and 6B (Fig. 2.6), which culminate in the deepest

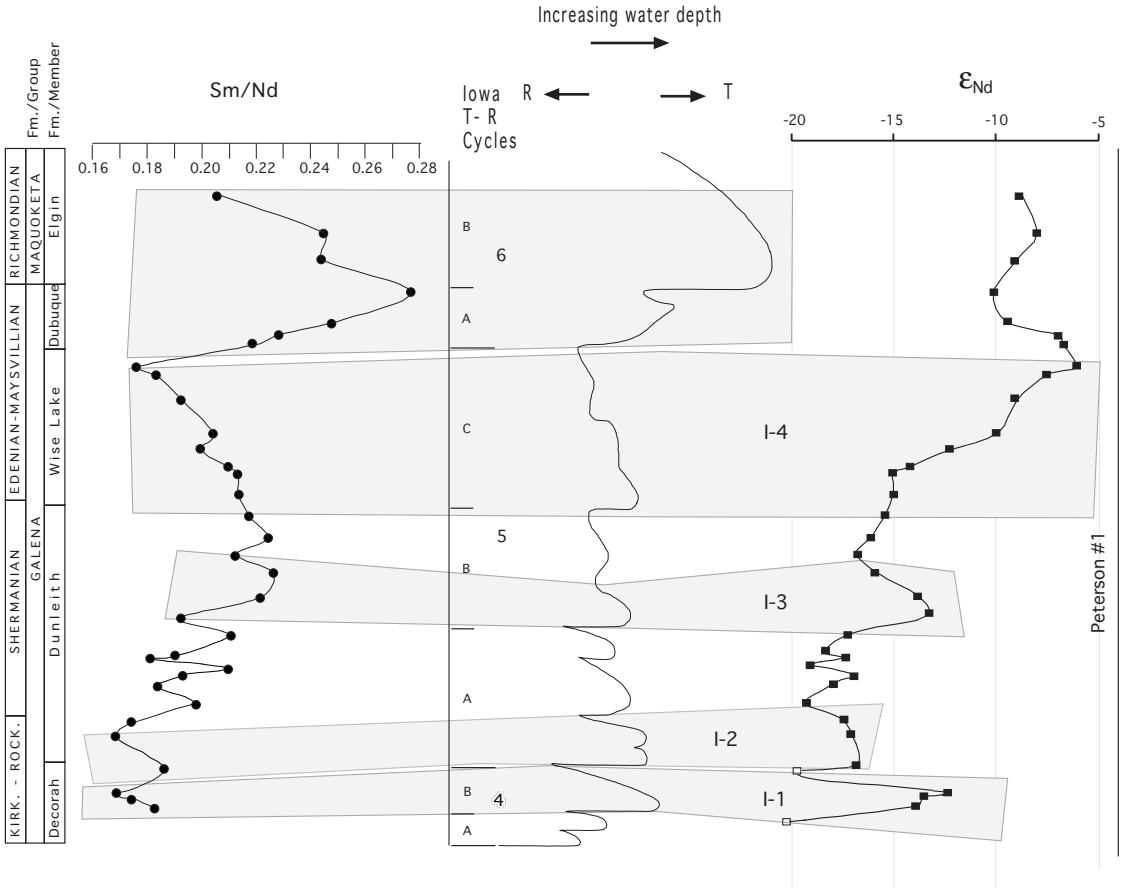

Figure 2.6 Comparison of the Sm/Nd and ε_{Nd} profiles of Iowa carbonates with the sea level curve of Witzke and Bunker (1996), showing a relatively close correspondence between increasing Sm/Nd and increasing depth and vice versa. Shaded regions represent correlative sea level events predicted by the profiles. Open square symbols indicate shale samples. Other abbreviations are as in Fig. 2.2.

depositional environment in the Late Ordovician of Iowa. The ε_{Nd} profile is unable to resolve this transgression because the Arch and Shield are submerged during this interval, further emphasizing our contention that variations of Sm/Nd ratios are independent of changes in the weathering source of REEs.

The 5C regression (Fig. 2.6) provides another example that stratigraphic changes in Sm/Nd are a proxy for changing depth. A steady decrease in Sm/Nd through the Wise Lake is coincident with a steady decrease in water depth based on the sea level curve (Fig. 2.6). In contrast the ε_{Nd} I-4 shift indicates that simultaneously the Arch and Shield were being submerged. Together, the ε_{Nd} and Sm/Nd curves reveal the dual nature of this sea level event, where depth is shallowing as a result of decreasing accommodation space even though sea level is rising relative to the Arch and Shield.

Positive excursions in Sm/Nd ratios are also identified with transgressive-regressive cycles 4B, 5A and 5B, and the I-1, I-2 and I-3 excursions in the ε_{Nd} curve (Fig. 2.6). A close comparison of Sm/Nd and ε_{Nd} variations in these three intervals demonstrates that the two curves are not entirely coincident (Fig. 2.5). The offset may reflect the fact that changes in sea level relative to the Arch and Shield are not necessarily synchronous with changes in depth, as seen in the example of the 5C regression. Additional variations in Sm/Nd ratios between the I-1 and I-2 intervals may correspond to the small variations in ε_{Nd} values and the smaller T-R cycles within the 5A interval.

Facies variations in parts of the Saskatchewan section are cryptic or absent, making it difficult to construct a detailed sea level curve that can be compared to the profile of Sm/Nd ratios. However, Sm/Nd ratios do increase coincident with the ε_{Nd} excursion at the base of the Yeoman and with one other well known transgressive event at the base of the Stony

Mountain (Fig.2.5). It would appear that the profile of Sm/Nd ratios in Saskatchewan is also responding to changing depth, but aside from the large transgressions identified, a more detailed facies investigation is required to verify this interpretation.

Our analysis indicates that Sm/Nd variations in carbonate sediment are responding to changes in depth, but the specific mechanism of REE fractionation is unresolved. We speculate that fractionation of Sm/Nd may be related to lateral offshore transport of REEs towards deeper environments since stratigraphic changes in water depth are related to distance from the paleoshoreline. Additionally, REE profiles in conodonts of Paleozoic age exhibit pronounced MREE enriched patterns rather than the HREE enriched pattern of modern seawater. Although many regard this pattern as characteristic of Paleozoic seawater (Wright et al., 1984; Grandjean and Albarède, 1989; Girard and Albarède, 1996) the origin is poorly understood, with some studies attributing MREE enrichment to early diagenesis of the REE in phosphates (Lécuyer et al., 1998; Reynard et al., 1999). Bearing in mind that the apex of the REE profile is at Gd (Gadolinium), the stratigraphic changes in Sm/Nd ratios observed in this study may reflect differing degrees of MREE enrichment, rather than the HREE enrichment seen in modern environments.

2.10 Conclusions

Late Ordovician epeiric seas of North America had Nd isotopic compositions established by the relative contributions of Nd derived from weathering of the Precambrian basement of the Transcontinental Arch and Canadian Shield and relatively younger crust of the Taconic Orogen. Seawater ε_{Nd} values are preserved in the acid soluble (AS) fraction of carbonates and are similar to the ε_{Nd} values of coexisting conodonts. This implies that

Nd in the AS fraction is primarily derived from biogenic apatite and Fe-Mn coatings, two phases that are known to record ε_{Nd} of past seawater.

The profiles of ε_{Nd} values of Late Ordovician carbonates from the Midcontinent of North America show four major excursions in ε_{Nd}, that closely track sea level fluctuations. Changing sea level influenced the weathering flux of Nd from Precambrian and Taconic crustal sources by submerging or exposing large expanses of the low-relief Arch and Shield, which caused a shift in the Nd isotope balance of neighboring epeiric seas. Transgressions are recorded as shifts towards more positive ε_{Nd} values, reflecting a proportionally greater influx from the Taconic Orogen. Regressions are recorded as negative isotope shifts if the Precambrian basement was once again exposed to weathering. In this way the ε_{Nd} profile is actually a sea level curve that reflects the submergence history of the Transcontinental Arch and Canadian Shield.

Because Late Ordovician sea level fluctuations change the isotope balance of Nd in North American epeiric seas, interbasinal correlation is possible using Nd isotope stratigraphy. This is demonstrated by our correlation between the Yeoman Formation in the Williston Basin of Saskatchewan and the Wise Lake Formation in the central Midcontinent of Iowa, across the Transcontinental Arch. Nd isotope stratigraphy has potential application wherever the mean age of emergent crust surrounding intracratonic basins changes dramatically over time. Cratonic environments in the initial stages of active orogenesis are potential candidates because of the addition of juvenile crust with relatively positive ε_{Nd} values, the impact of orogeny on sediment dispersal networks, and tectonically driven sea level changes.

The same carbonates used to construct ε_{Nd} profiles also displayed smooth variations

in the Sm/Nd ratios of their AS fractions. Comparison of these Sm/Nd variations with the sea level curve, conodont paleoecology, and the ε_{Nd} profile are consistent with the interpretation that stratigraphic variations in Sm/Nd ratios reflect changes in depth of epeiric seas. Stratigraphic increases in Sm/Nd ratios of carbonates record increasing depth, whereas stratigraphic decreases in Sm/Nd ratios record decreasing depth. A mechanism explaining the observed depth related fractionation of Sm from Nd in epeiric sea environments is unresolved and requires further study. However, we have determined that in contrast to ε_{Nd}, variations in Sm/Nd ratios are independent of changes in REE provenance. As a depth recorder, stratigraphic variations in Sm/Nd ratios have a potentially wide range of applications in studies relating to the paleoceanography of ancient epeiric seas.

CHAPTER 3. $\delta^{13}C$ EXCURSIONS IN THE ORDOVICIAN GALENA GROUP OF LAURENTIA, EXPRESSIONS OF SEA LEVEL DRIVEN CHANGES IN LOCAL CARBON CYCLING

3.1 Introduction

The record of sea level changes in the past are constructed from stratigraphic successions deposited in epeiric seas, including continental margin facies, and also when available from ocean sediments. Preserved in the same epeiric sea strata and ocean sediments are $\delta^{13}C$ excursions that are thought to record changes in the carbon isotope composition of the ocean carbon reservoir (Arthur et al., 1988; Magaritz and Holser, 1990; Magaritz et al., 1992; Brenchley et al., 1994; Holser, 1997; Veizer et al., 1999). Recurrent correlations between sea level fluctuations and $\delta^{13}C$ excursions have led to the conclusion that sea level fluctuations are driving changes in the ocean carbon reservoir (Arthur et al., 1987; Joachimski and Buggisch, 1993; Wenzel and Joachimski, 1996; Glumac and Walker, 1998; Azmy et al., 1998; Perfetta et al., 1999). Primarily, sea level fluctuations are believed to drive changes in organic matter productivity, rates of organic matter burial, and the carbon isotope composition of terrestrial runoff to the oceans (Scholle and Arthur, 1980; Magaritz and Stemmerik, 1989; Baum et al., 1994; Jenkyns, 1996; Kaljo et al., 1997; Kump et al., 1999). Sea level fluctuations and changes in the ocean carbon reservoir are also flags for other large scale environmental changes in circulation, climate, and biological diversification and extinction. Therefore, $\delta^{13}C$ excursions in epeiric sea strata and ocean sediments are

often used to identify these environmental changes (Ripperdan et al., 1992; Saltzman et al., 1995; Patzkowsky et al., 1997; Saltzman et al., 1998; Saltzman, 2003). However, no single explanation exists to connect sea level, $\delta^{13}C$ excursions and individual environmental changes because positive $\delta^{13}C$ excursions have been correlated to both sea level rise and sea level fall (Arthur et al., 1987; Magaritz and Stemmerik, 1989; Wenzel and Joachimski, 1996; Glumac and Walker, 1998; Perfetta et al., 1999).

The correlation between sea level fluctuations and $\delta^{13}C$ excursions in ocean sediments strongly suggests a relationship between sea level and the ocean carbon reservoir. However, it may not always be correct to assume that $\delta^{13}C$ excursions in epeiric sea strata reflect changes in the carbon isotope composition of the ocean carbon reservoir and that these epeiric sea $\delta^{13}C$ excursions can be used to identify global environmental changes. The residence time of carbon in ancient epeiric seas may be greatly reduced, in comparison to modern oceans, due to smaller size and shallower depth of the epeiric reservoir and restricted circulation between epeiric seas and the surface ocean. This could lead to spatial variations in $\delta^{13}C$ values between temporally equivalent strata within an epeiric sea, between epeiric sea strata and adjacent ocean sediments, and between epeiric sea strata from different cratons (Holmden et al., 1998; Brand and Bruckschen, 2002; Immenhauser et al., 2002).

As an example, Patterson and Walter (1994) showed that differences in $\delta^{13}C$ values of up to 4‰ can develop between the dissolved inorganic carbon (DIC) of modern seawater on carbonate platforms and neighboring deep oceans. They suggested that a similar process might occur between epeiric seas and adjacent oceans. Holmden et al. (1998) and Panchuk (2002) then observed a similar variation to that of Patterson et al. (1994) in $\delta^{13}C$ values across a single North American Ordovician epeiric sea, recorded in spatial variations in

$\delta^{13}C_{carb}$ and $\delta^{13}C_{org}$ values of time equivalent strata. Following up on these ideas, Immenhauser et al. (2003) concluded that a $\delta^{13}C$ excursion from the Late Carboniferous (middle Atokan) strata of the Cantabrian Mountains of northern Spain could be attributed to locally driven changes in C-cycling as a result of changing epeiric seawater circulation. Immenhauser et al. (2003) noted that the difficulty in distinguishing between local and global controls of C-cycling results in a poor understanding of ancient $\delta^{13}C$ records from shallow marine seas.

The possibilities for sea level driven changes in local C-cycling within an epeiric sea are largely unexplored despite evidence that C-cycling in epeiric seas may have been dominated by local rather than global controls. This thesis provides one example of sea level driven changes in local C-cycling within an epeiric sea using a $\delta^{13}C$ profile exhibiting five positive excursions recorded in Upper Ordovician epeiric sea strata from the Midcontinent of North America. A sea level curve based on lithology and fauna, plus new geochemical proxies for sea level (ε_{Nd}) and water depth (Sm/Nd) (Fanton et al., 2003) allow us to determine that sea level rise drove all five positive $\delta^{13}C$ excursions, providing one of the most well-defined and repetitive correlations of sea level change and $\delta^{13}C$ excursions through one section. This correlation allows us to present an example of how sea level drives changes in local or regional C-cycling in epeiric seas by using paleocirculation patterns for the Midcontinent of North America, rather than sea level driven changes in global C-cycling. The Ordovician Midcontinent example suggests that regional controls on local C-cycling need to be considered whenever $\delta^{13}C$ profiles from epeiric sea strata correlate with sea level change. Evaluating such regional controls on C-cycling has important implications when gauging the extent or significance of environmental change

by the relative magnitude of a $\delta^{13}C$ excursion preserved in epeiric sea carbonates. In addition, the continuing development of $\delta^{13}C$ profiles through Middle and Upper Ordovician carbonates of the North American Midcontinent and their application to interpreting possible global environmental changes, including their relationship to end Ordovician glaciation, (Patzkowsky et al., 1997; Ludvigson et al., 1996; Pancost et al., 1999; Simo et al., 2003; Ludvigson et al., 2004) makes it imperative that we understand and identify the impact of local C-cycling within the Ordovician Midcontinent.

3.2 Geology and Paleocirculation

Middle through Upper Ordovician strata (Turinian to Richmondian age) in Iowa belong to the Decorah, Dunleith, Wise Lake and Dubuque formations of the Galena Group, and to the overlying Maquoketa Formation. The Decorah Formation is further divided into the Spechts Ferry and overlying Guttenberg members (Fig. 3.1). Galena Group strata, the primary focus of this study, comprise part of a mixed siliclastic/carbonate platform that extended eastward from the Transcontinental Arch across the Midcontinent of North America (Fig. 3.1). The Galena Group is underlain by the Platteville Group and is equivalent to the Black River Limestone, a term defined by the type section of carbonate rocks in New York and used to denote carbonates of the Turinian Stage across the eastern United States (Fig. 3.1) (Kolata et al., 2001).

Paleoceanographic reconstructions of North America indicate that the late Middle and Late Ordovician epeiric sea of the Midcontinent region underwent a major reorganization in circulation that began during deposition of the upper Platteville Group (Wilde, 1991; Kolata et al., 2001; Pope and Steffen, 2003). The lower Platteville Group and related

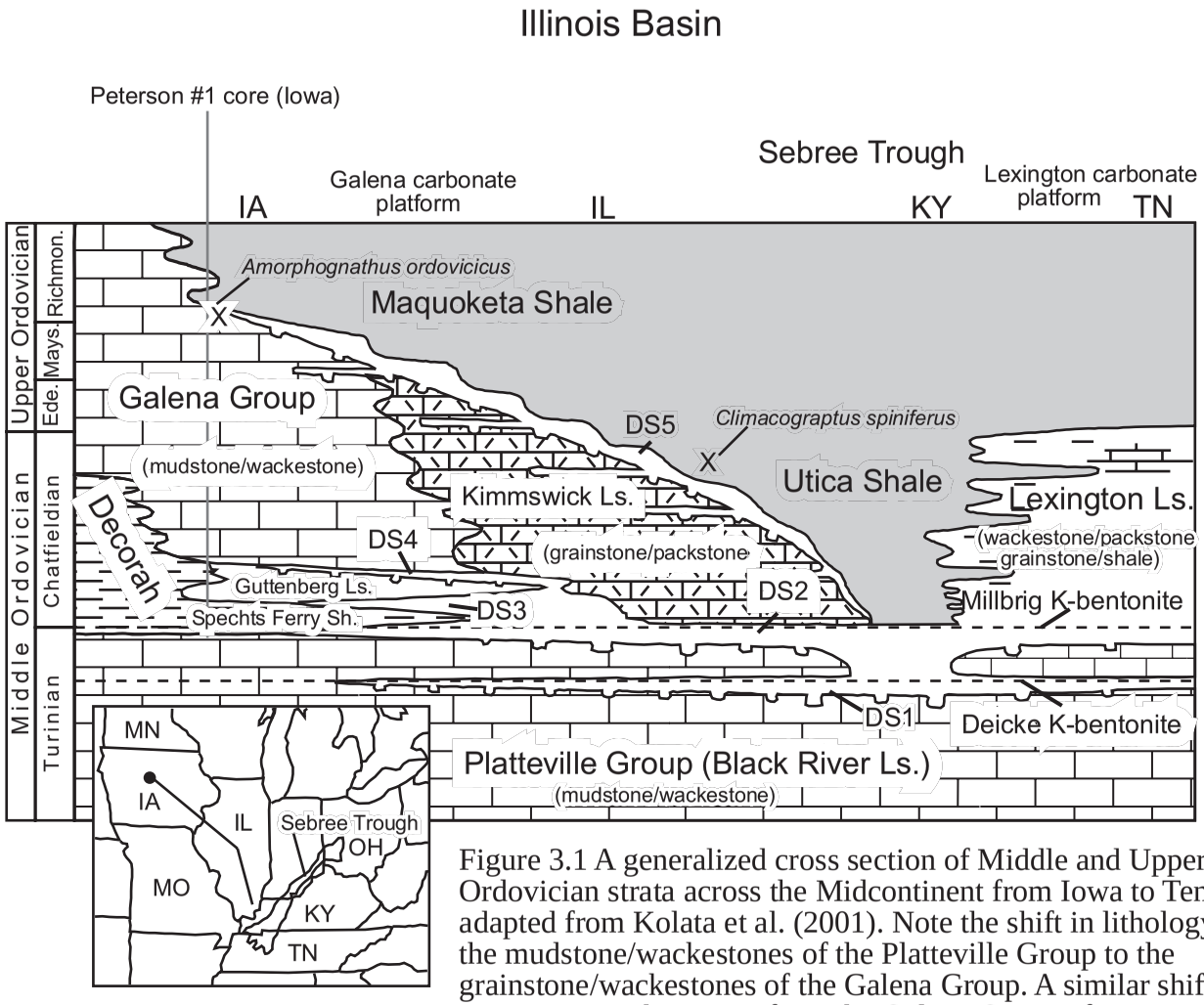

Figure 3.1 A generalized cross section of Middle and Upper Ordovician strata across the Midcontinent from Iowa to Tenessee, adapted from Kolata et al. (2001). Note the shift in lithology from the mudstone/wackestones of the Platteville Group to the grainstone/wackestones of the Galena Group. A similar shift in lithology occurs across the craton from the Galena Group of Iowa to the Galena Group of Illinois. DS1 through DS5 mark phosphatic hardgrounds and X indicates important conodont and graptolite fauna.

Black River Limestone are characterized by mudstones, wackestones, coated grains, ooids and associated evaporites (Fig. 3.1). Depositional waters were thought to be warm and restricted with a lagoonal-type circulation characterized by a net outflow of bottom waters towards the continental margin (Kolata et al, 2001). Seawater exchange between the surface ocean and epeiric sea was restricted at this time. By contrast, the upper Platteville Group and Galena Group are increasingly dominated by prominent phosphatic hardgrounds, grainstones, packstones and shales (Fig. 3.1), which are interpreted to reflect a shift to cooler water, quasi-estuarine circulation across the Galena Platform (Witzke, 1987b; Raatz and Ludvigson, 1996; Kolata et al., 2001).

Quasi-estuarine circulation is characterized by a net outflow of warm, low salinity, surface waters from the epeiric sea to the surface ocean, driven by increased freshwater runoff from the Taconic Highlands coupled with warm, southwestward sweeping, wind driven surface currents (Witzke, 1987b; Raatz and Ludvigson, 1996) (Fig. 3.2a). A subtropical convergence zone developed along the southern edge of the Midcontinent as these warmer surface currents converged with northward moving cool subpolar currents (Wilde, 1991; Kolata et al., 2001). An overall sea level rise in the Ordovician and net outflow of surface currents, allowed these cool, phosphate rich, oxygen poor waters to be brought on to the craton at depth (Witzke, 1987b). Kolata et al. (2001) identified the Sebree Trough, a shale filled bathymetric low developed over the failed Reelfoot rift (Kolata and Nelson, 1991), as the likely conduit for funneling these deeper waters onto the craton (Fig. 3.2a). A stratified water column developed across much of the epeiric sea with warm, low salinity, oxygenated surface waters separated by a pycnocline from cool, oxygen poor, phosphate rich bottom waters (Witzke, 1987b, Raatz and Ludvigson, 1996; Kolata et al.,

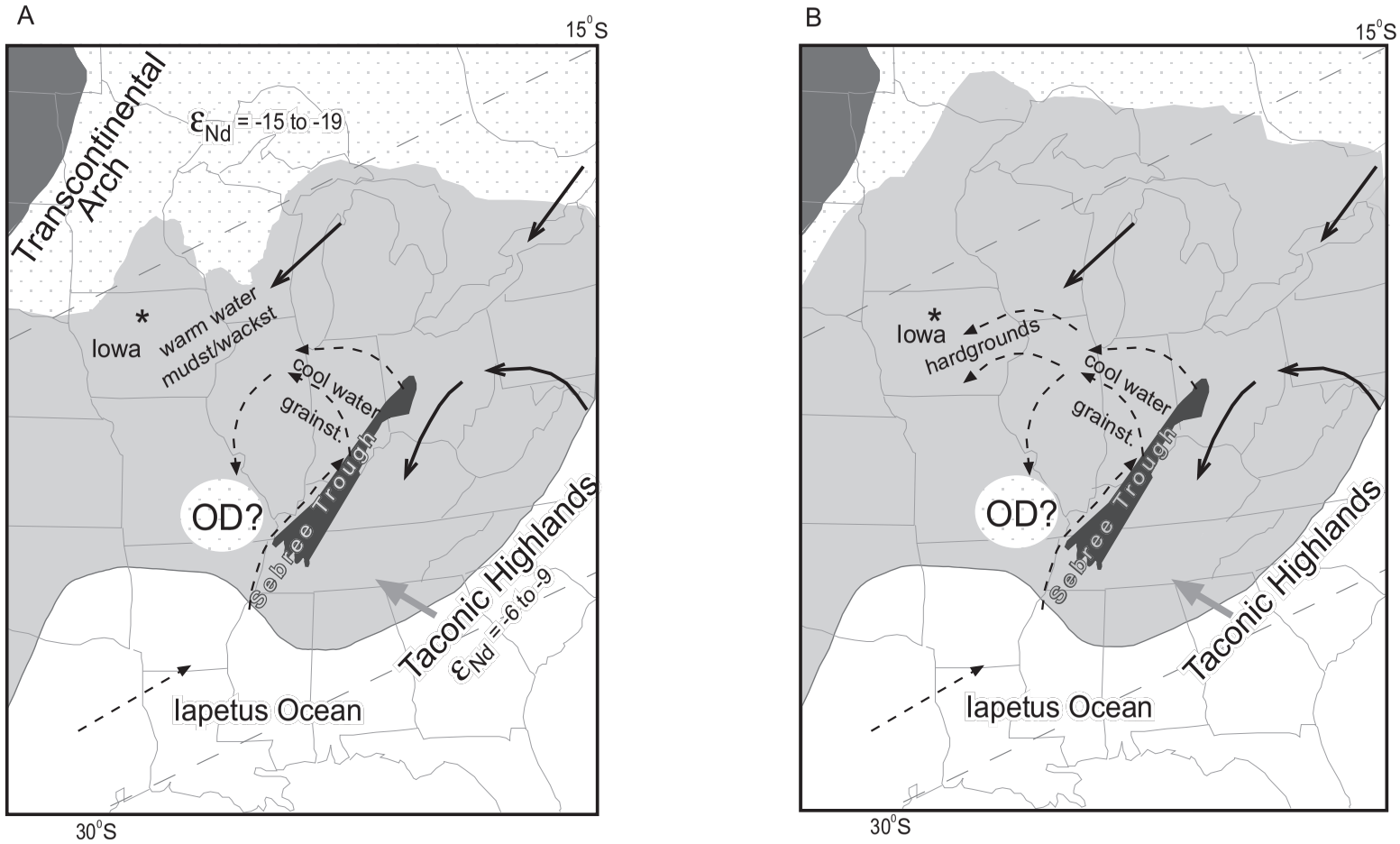

Figure 3.2 Maps of the latest Turinian and Chatfieldian of the Midcontinent region of North America. Stippled areas denote exposed Precambrian basement. Black solid arrows indicate circulation of surface waters and black dashed arrows indicate circulation of cool, oxygen poor, phosphate rich bottom waters. The grey arrows indicate prevailing wind direction. The * locates the Iowa sampling location. (A) Displays quasi-estuarine circulation during the latest Turinian. (B) Displays subsequent sea level rise and the expansion of quasi-estuarine circulation and cool, oxygen poor, phosphate rich bottom waters into the Iowa area. O.D. = Ozark Dome.

2001). Closer to the Transcontinental Arch, salinity stratification was enhanced due to freshwater runoff from the Arch, which further decreased salinity of the surface layer (Ludvigson et al., 1996).

The central Iowa carbonates do not display the facies transition from mudstones to grainstones and packstones that marks the shift from lagoonal to quasi-estuarine circulation that occurs further east, closer to the Sebree Trough (Kolata et al., 2001). Instead, the Galena Group of central Iowa is comprised of mudstones, argillaceous wackestones and packstones, punctuated by intervals of shale and grainstones (Fig. 3.1) (Witzke and Bunker, 1996). Phosphatic hardgrounds occur but may not be as thick or as easily traceable as those closer to the Sebree Trough. Kolata et al. (2001) interpreted this higher occurrence of mudstones and wackestones as continued deposition under relatively warm water conditions, an indication that the Iowa area was not as strongly influenced by the cooler, oxygen poor, phosphate rich bottom waters spilling out of the Sebree Trough to the east.

3.3 Methods

Whole rock, partially dolomitized, limestones were collected from the Ordovician Galena Group of central Iowa (Peterson #1 core T90N R27W Sec. 10 NE NE NE NW) (Fig. 1). Powdered samples, for analysis of the $\delta^{13}C$ value of carbonates ($\delta^{13}C_{carb}$), were processed following McCrea (1950) and analyzed using a Finnigan MAT Delta E dual inlet GIRMS. Bulk organic matter was analyzed for the $\delta^{13}C$ value of organic carbon ($\delta^{13}C_{org}$) using a combustion furnace (ANCA-GSL) attached to a Europa Scientific 20-20 continuous flow isotope ratio mass spectrometer. The residue remaining after HCl digestion of the whole rock carbonate was combusted in the ANCA-GSL to determine the fractional weight

of total organic carbon (TOC). External precision of $\delta^{13}C_{carb}$ is better than ± 0.2‰ using NBS19, which yielded 1.95 ± 0.10‰ (2σ). External precision for $\delta^{13}C_{org}$ is better than ±0.3‰ based on an internal Chickpea standard calibrated against NBS1575.

3.4 Results

Five positive $\delta^{13}C$ excursions, and corresponding increases in TOC, can be identified in the Galena Group (Fig 3.3, Table 3.1). The term excursion is here used loosely to describe any change greater than 0.5‰ that can usually be observed in both the $\delta^{13}C_{carb}$ and $\delta^{13}C_{org}$ profiles, for simplicity this definition may encompass what might otherwise be considered a trend or shift in $\delta^{13}C$ values (e.g. the C4 or C5 excursions). Only excursion C1 (Fig. 3.3), equivalent to the Guttenberg $\delta^{13}C$ excursion in the Decorah Formation, has previously been reported, first in eastern Iowa (Hatch et al., 1987; Jacobson et al., 1995; Ludvigson et al., 1996; Simo et al., 2003) and then in Pennsylvania (Patzkowsky et al., 1997) and Baltica (Ainsaar et al., 1999). Further work has indicated that this excursion may be even more widespread across the North American Midcontinent (Bergström et al., 2001; Saltzman et al., 2001). Additional $\delta^{13}C$ excursions have also been reported from the Spechts Ferry Member of the Decorah Formation and in the underlying Platteville Group (Ludvigson et al., 2000; Ludvigson et al., 2001; Ludvigson et al., 2004)

Corresponding trends in the $\delta^{13}C_{carb}$ profile and organic $\delta^{13}C_{org}$ profile indicate that these curves preserve changes in the $\delta^{13}C_{DIC}$ of seawater despite having been partially dolomitized (Fig. 3.3, Table 3.1). Since diagenetic processes affecting carbonate and organic matter are different, diagenesis generates differences between $\delta^{13}C_{carb}$ and $\delta^{13}C_{org}$ profiles (Magaritz et al., 1992). Differences, however, are observed in only two instances: (1) there

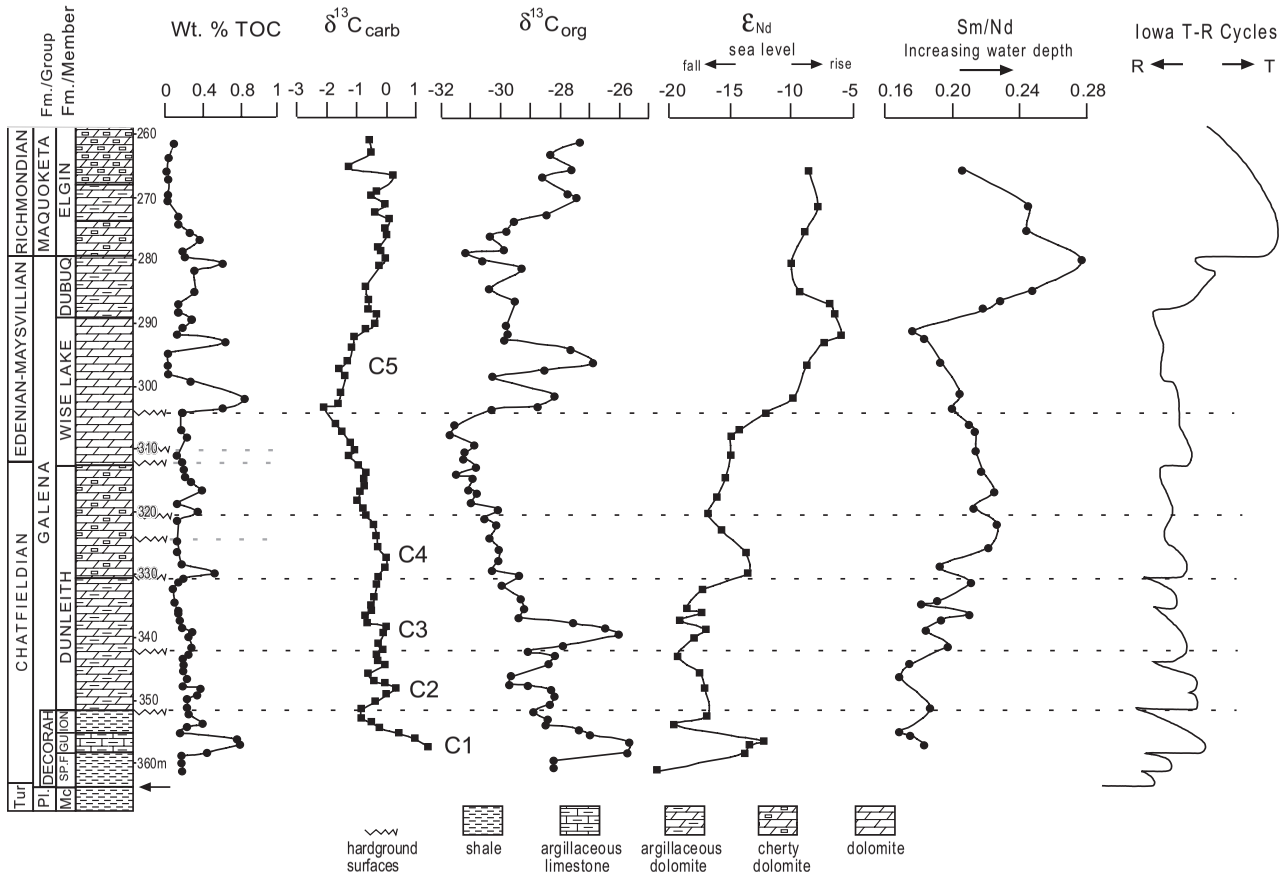

Figure 3.3 $\delta^{13}C_{carb}$, $\delta^{13}C_{org}$ and TOC curves compared to the chemostratigraphic sea level proxies of ε_{Nd} and Sm/Nd from Fanton et al. (2002) and a sea level curve from Witzke and Bunker (1996). C1 through C5 denote the five $\delta^{13}C$ excursions in the section. Black dashed lines mark hardground surfaces that are associated with $\delta^{13}C$ excursions, and grey dashed lines mark hardground surfaces not associated with $\delta^{13}C$ excursions . The black arrow marks the approximate stratigraphic position of the time-slice from Holmden et al. (1998). DUBUQ=Dubuque Fm.; Pl=Platteville Grp..; Mc=McGregor Mbr.; Tur.=Turinian; SP.F.=Specht's Ferry Mbr.; GU=Guttenberg Mbr.

Table 3.1 Data collected from the Peterson #1 core, central Iowa

subsurface depth meters (feet)	$\delta^{13}C_{carb}$	$\delta^{13}C_{org}$	%TOC[#]
261.5 (858)	-0.6	-27.3	0.10
263.7 (865)	-0.5	-28.3	0.04
265.8 (872)	-1.3	-27.6	0.02
267.1 (876.2)	0.2	-28.6	0.04
269.7 (884.7)	-0.3	-27.7	0.04
270.5 (887.4)	-0.5	-27.4	0.02
271.8 (891.8)	-0.1	N.D.	N.D.
272.9 (895.5)	-0.4	-28.4	0.14
274.1 (899.4)	0.1	-29.5	0.15
275.6 (904.3)	0.0	-29.8	0.26
276.6 (907.6)	0.0	-30.3	0.37
278.7 (914.3)	-0.3	-29.8	0.19
279.4 (916.6)	-0.2	-31.1	0.21
280.4 (920)	0.0	-30.6	0.61
281.6 (924)	-0.2	-29.2	0.32
285.0 (935)	-0.7	-30.3	0.31
286.9 (941.2)	-0.6	-29.5	0.15
288.3 (946)	-0.6	N.D.	0.15
289.3 (949.3)	-0.3	N.D.	0.29
290.7 (953.8)	-0.4	-29.8	0.19
291.7 (957)	-0.7	-29.7	0.13
293.0 (961.3)	-1.1	-29.9	0.63
294.8 (967.1)	-1.2	-27.6	0.04
296.8 (973.8)	-1.3	-26.9	0.04
298.0 (977.6)	-1.6	-28.5	0.04
299.2 (981.7)	-1.4	-30.2	0.27
301.9 (990.4)	-1.5	-28.2	0.84
303.4 (995.4)	-1.6	-28.7	0.61
304.3 (998.3)	-2.1	-30.3	0.19
306.9 (1007)	-1.7	-31.5	0.17
308.0 (1010.5)	-1.5	-31.7	0.23
309.8 (1016.5)	-1.2	-30.9	N.D.
311.0 (1020.4)	-1.1	-31.1	0.14
312.0 (1023.5)	-1.3	-31.2	0.17
313.2 (1027.5)	-0.9	-30.8	0.20
314.4 (1031.5)	-0.7	-31.4	0.22
315.2 (1034.2)	-0.8	-30.9	0.27
316.5 (1038.5)	-0.7	-31.1	0.40
317.6 (1042)	-0.9	-30.8	N.D.

Table 3.1 (continued)

subsurface depth meters (feet)	$\delta^{13}C_{carb}$	$\delta^{13}C_{org}$	%TOC[#]
318.8 (1046)	-1.0	-30.9	0.13
320 (1050)	-0.8	-30.0	0.34
321.3 (1054)	-0.7	-30.5	0.14
322.8 (1059)	-0.4	-30.1	N.D.*
324.6 (1065)	-0.3	-30.3	0.13
326.4 (1071)	-0.3	-30.0	0.15
328.3 (1077)	0.0	-30.1	0.19
329.6 (1081.5)	0.0	-30.3	0.52
330.4 (1084)	N.D.	-29.4	0.19
331.2 (1086.5)	-0.3	N.D.	0.15
332.2 (1090)	-0.3	-29.9	0.09
334.3 (1096.9)	-0.4	-29.3	0.11
335.7 (1101.5)	-0.5	-29.2	0.12
336.5 (1104)	-0.5	N.D.	0.14
337.3 (1106.5)	-0.7	-29.3	0.14
338.4 (1110.1)	-0.7	-27.6	0.17
339.2 (1112.7)	0.0	-26.5	0.28
339.9 (1115.2)	-0.1	-26.0	0.26
341.7 (1121)	-0.3	-27.9	0.27
342.6 (1124)	-0.1	-29.1	0.25
343.5 (1127.1)	-0.3	-28.4	0.18
344.3 (1129.7)	-0.3	-28.2	0.19
345.2 (1132.5)	0.0	N.D.	0.19
346.6 (1137)	-0.6	-29.6	0.24
347.7 (1140.8)	-0.4	-29.7	0.19
348.1 (1142)	0.0	-29.0	0.37
349.0 (1145)	0.3	-28.3	0.34
349.9 (1148)	0.0	-28.2	0.24
351.1 (1151.8)	-0.4	-28.3	0.26
352.2(1155.5)	-0.8	-28.9	0.26
353.7(1160.5)	-0.8	-28.4	0.39
354.2(1162.2)	-0.5	-28.5	0.24
355.1 (1165.1)	-0.2	-27.3	0.15
356.1 (1168.4)	0.5	-26.9	0.74
356.8 (1170.6)	1.0	-25.6	0.79
358.3 (1175.6)	1.4	-25.7	0.45
359.1 (1178.0)	N.D.	-28.3	0.18
360.2 (1181.6)	N.D.	-28.2	0.18
361.3 (1185.3)	N.D.	-28.4	0.19

N.D. = not determined, [#]fractional weight of total organic carbon in each whole rock sample. Isotope data measured in per mil

is no C4 $\delta^{13}C_{org}$ excursion to match the observed $\delta^{13}C_{carb}$ excursion; and (2) the magnitude of the excursions differ between the $\delta^{13}C_{org}$ and $\delta^{13}C_{carb}$ profiles (Fig. 3.3).

Magnitude differences between Guttenberg (C1) $\delta^{13}C_{org}$ and $\delta^{13}C_{carb}$ excursions have been reported by Hatch et al. (1987) and Ludvigson et al. (1996). Applying compound specific isotope ratio analysis of organic matter, Pancost et al. (1999) concluded that this 5‰ difference in magnitude between Guttenberg $\delta^{13}C_{carb}$ and $\delta^{13}C_{org}$ values was due to the presence of ^{13}C-enriched organic compounds belonging to a single organism, the organic walled microfossil *Gloeocapsomorpha prisca*. Increased concentrations of *G. prisca* over the excursion interval amplified the $\delta^{13}C$ excursion recorded in bulk organic matter from 3.5‰ to 8‰. By analogy, we suggest that increased abundances of *G. prisca* may be responsible for enhanced $\delta^{13}C_{org}$ values in the C1, C2, C3 and C5 excursions in central Iowa (Fig. 3.3). The absence of a well defined $\delta^{13}C_{org}$ shift over the C4 interval (Fig. 3.3) may be due to the absence of *G. prisca* over this interval. If the presence of *G. prisca* magnifies the $\delta^{13}C_{org}$ excursions, thus making them easier to identify, then the lack of *G. prisca* over the C4 interval may make it difficult to resolve the expected 1‰ excursion from the $\delta^{13}C_{org}$ profile, which contains a high degree of small rapid fluctuations in values over this interval. Because the abundance of *G. prisca* organic matter in our samples is unknown, the magnitude of the $\delta^{13}C_{org}$ profiles cannot be corrected. Thus, we consider the $\delta^{13}C_{carb}$ profile to be a better proxy for magnitude changes in the carbon isotope balance of the epeiric sea. These $\delta^{13}C_{carb}$ excursions are well defined in a profile that lacks small rapid, fluctuations or "background noise" to obscure the excursions, which yield magnitudes of 2.2, 1.2, 0.7, 1.0 and 1.7‰, for excursions C1 through C5 respectively (Fig. 3.3, Table 3.1). Of all these excursions, only C5 is characterized by a positive shift in $\delta^{13}C_{carb}$, with no

return to initial pre-excursion values. The C5 $\delta^{13}C_{org}$ excursion is bifurcated, possibly as a result of fluctuating *G. prisca* abundances. However, the baseline shift in $\delta^{13}C_{org}$ from -31.6‰ to -29.9‰ matches the magnitude of the shift in $\delta^{13}C_{carb}$ and like the $\delta^{13}C_{carb}$ profile there is no return to initial pre-excursion values (Fig. 3.3, Table 3.1).

3.5 Association of sea level and $\delta^{13}C$

Comparison of the $\delta^{13}C$ profiles to both a sea level curve constructed from lithology and fauna, which may record either local or eustatic changes and sea level, and from chemostratigraphic sea level curves reveals a close association between sea level fluctuations and the C1-C5 $\delta^{13}C$ excursions (Fig. 3.3). Sea level curves record relative changes in water depth based on variations in grain size, lithology, sedimentary structures and bathymetric evidence from fossils. In the Iowa area the sea level curve constructed by Witzke and Bunker (1996) is based primarily on clastic content and shale progradation from the Transcontinental Arch source areas, on the increasing frequency of storm generated grainstone beds, abundance of calcareous algae, hardground surfaces and thin condensed intervals. Fanton et al. (2002) used ε_{Nd} profiles in Galena Group carbonates to construct a chemostratigraphic sea level curve that records the submergence history of the Transcontinental Arch and Canadian Shield in the Middle and Late Ordovician. The ε_{Nd} sea level curve is based on the premise that the isotope balance of Nd in epeiric seawater across North America was controlled by inputs of Nd weathered from: (1) low relief islands of the Precambrian basement of the Arch and Shield (ε_{Nd} = -22 to -15) and (2) from the relatively younger highlands of the Taconic Orogen (ε_{Nd} = -6 to -9) on the eastern margin of the continent (Fig. 3.2a, Fig. 3.4). During sea level rise, progressive inundation of the

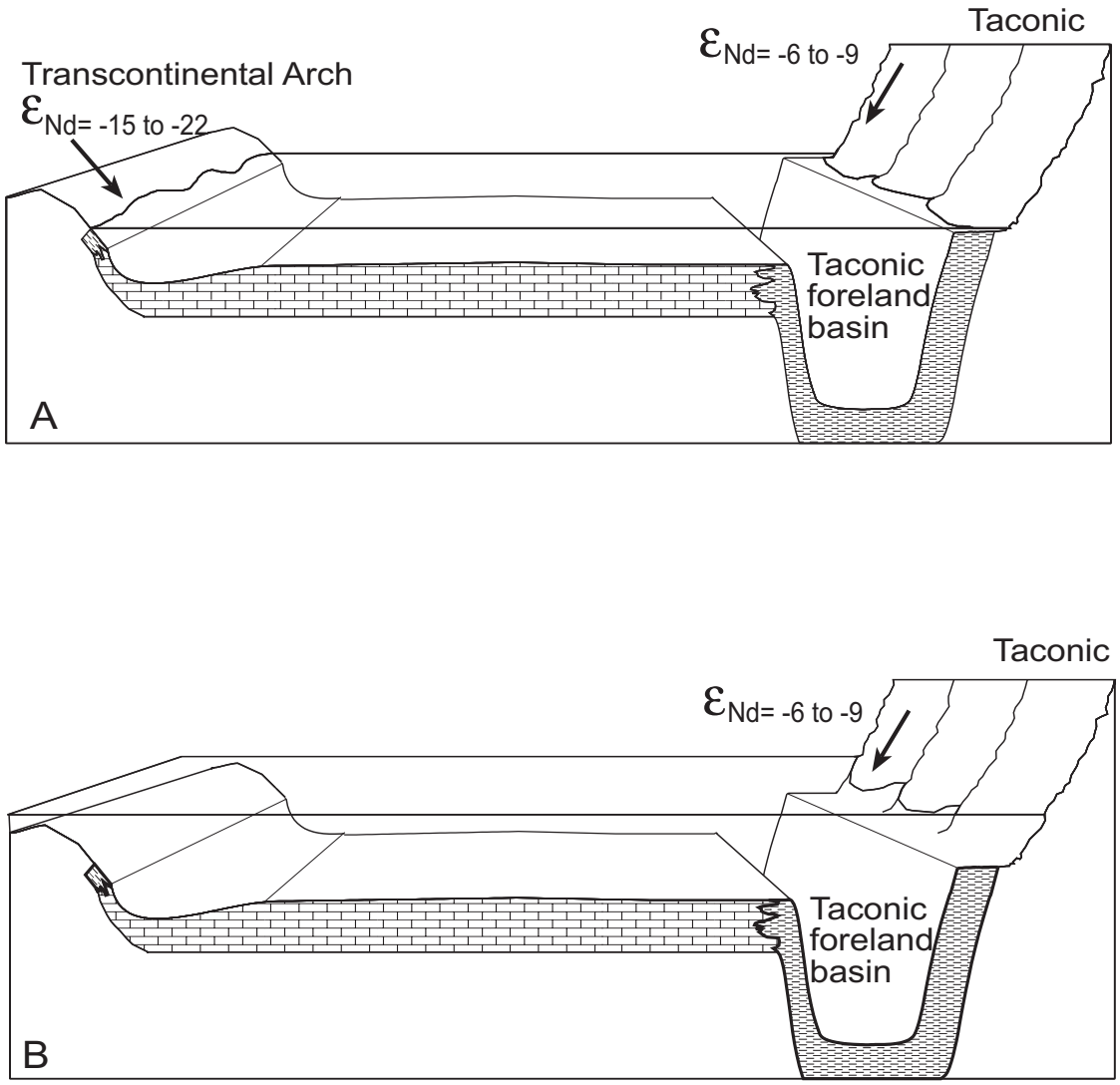

Figure 3.4 General cross-section across the Midcontinent from the Iowa area to the Taconic Highlands. The Sebree Trough is not included in this section. (A) Displays the input of dissolved Nd from the Precambrian basement of the Transcontinental Arch and from the Taconic Highlands. (B) Displays sea level rise and submergence of the relatively low lying Arch, resulting in an overall positive shift in the ε_{Nd} value of Midcontinent seawater.

Arch and Shield reduced the weathering flux of older Precambrian-derived Nd to surrounding epeiric seas, causing the ε_{Nd} value to shift towards the more positive Taconic signature (Fig. 3.4). Since the isotope balance of Nd in paleoseawater is recorded in carbonates, positive stratigraphic shifts in the ε_{Nd} of Galena Group carbonates reflect sea level rise and increased submergence of the Arch and Shield, whereas negative shifts in ε_{Nd} reflect periods of emergence of the Arch and Shield and relative sea level fall (Fanton et al., 2002) (Fig. 3.3).

Fanton et al. (2002) also reported that stratigraphic variations in rare earth element (REE) concentrations, specifically carbonate Sm/Nd ratios, seem to correlate with changing water depth inferred from ε_{Nd} profiles and conventional sea level curves. Increases in Sm/Nd ratios correspond with increasing water depth, while decreasing Sm/Nd ratios correspond with decreasing water depth (Fig. 3.3). Modern studies of aqueous environments demonstrate that REE are removed from the water column through adsorption to biogenic and detrital particulates and Fe-Mn flocculates (Byrne and Kim, 1990; Elderfield et al., 1990). This process is more effective at removing light REE (LREE) than heavy REE (HREE) because of the increasing ionic potential of REE across the group from light to heavy. As a result, HREE form stronger ligand-REE complexes in solution, which increases their solubility and decreases their chances of adsorbing to particulates in the water column. As modern surface waters progress from rivers to estuaries to open oceans there is an overall decrease in REE concentrations in solution, and the remaining REE become more enriched in HREE relative to the light (Elderfield et al., 1990). Fanton et al. (2002) hypothesized that in ancient epeiric seas a similar enrichment in HREE would occur from nearshore to offshore environments. Therefore, sea level rise, paleoshoreline retreat and deepening of the water

column would cause a shift to a heavier REE-enriched signature in dissolved REE. This would explain the increased Sm/Nd ratios with depth, as Sm is a heavier REE with a higher ionic potential than is Nd.

Comparison of the conventional sea level curve, ε_{Nd} profile and Sm/Nd profile to our $\delta^{13}C$ profiles reveal that, with one exception, the $\delta^{13}C$ excursions correspond with sea level rise (Fig. 3.3). The one discrepancy is the $\delta^{13}C$ excursion over the C5 interval, where the ε_{Nd} profile indicates sea level rise relative to the exposed Precambrian basement, while the Sm/Nd profile and conventional sea level curve indicate a decrease in paleodepth. This apparent contradiction can be explained if the rate of carbonate accumulation on the platform exceeded the rate of sea level rise relative to exposed land. Eventhough sea level was rising relative to the Precambrian shield, the depth of the water column would shallow as the carbonate began to accumulate. This means that all of the $\delta^{13}C$ excursions, including C5, can be related to a sea level rise and fall relative to the exposed Precambrian basement of the Arch and Shield. The positive limb of each excursion corresponds to sea level rise and the negative limb to sea level fall.

3.6 Sea level forcing of $\delta^{13}C$ excursions

The correlation between sea level rise and fall and the $\delta^{13}C$ excursions is strong evidence that sea level change was the principle environmental factor driving changes in C-cycling across the Midcontinent epeiric sea. The question, then, is whether the $\delta^{13}C$ excursions reflect sea level generated changes in local C-cycling on the Galena platform, or was the ocean carbon reservoir also affected? We propose that the corresponding changes in sea level rise, $\delta^{13}C$ excursions and increasing TOC reflect sea level driven changes in

local carbon burial at the scale of a single epeiric sea or water mass.

Holmden et al. (1998) have already demonstrated that in the late Turinian, just prior to the C1 excursion, the carbon isotope composition of the Midcontinent epeiric sea was controlled by local C-cycling (Fig. 3.3, Fig. 3.5). Using carbonates correlated by the Millbrig and Deicke K-bentonites, Holmden et al. (1998) and Panchuk (2002) developed a thin time-slice of $\delta^{13}C_{carb}$ and $\delta^{13}C_{org}$ values that span the carbonate platforms of the Midcontinent. $\delta^{13}C$ variations observed across this time-slice show that the latest Turinian Midcontinent was characterized by a central water mass with low $\delta^{13}C$ values overlying a clean carbonate facies, and peripheral water masses with high $\delta^{13}C$ values overlying an argillaceous carbonate facies (Holmden et al., 1998; Panchuk, 2002) (Fig. 3.5). Holmden et al. (1998) concluded that the distinct $\delta^{13}C$ signatures of the waters reflected local controls on C-cycling that developed as a result of restricted circulation between the shallow waters of the central Midcontinent and deeper surrounding water masses, including the Iapetus Ocean (Fig. 3.5).

A strong case can be made that sea level fluctuations, and related changes in Midcontinent circulation patterns, will over time drive changes in the local or regional C-cycling observed by Holmden et al. (1998). Under quasi-estuarine circulation, deep, cool phosphate rich, oxygen poor waters from the oxygen minimum zone of the Iapetus ocean were drawn onto the craton through the Sebree Trough (Witzke, 1987b; Raatz and Ludvigson, 1996; Kolata et al., 2001). A stratified water column was established with these deeper cool waters being separated by a pycnocline from warm, oxygenated, low salinity surface waters (Witzke, 1987b, Raatz and Ludvigson, 1996; Kolata et al., 2001). Sea level rise caused cool, oxygen poor, phosphate rich bottom waters from the Iapetus

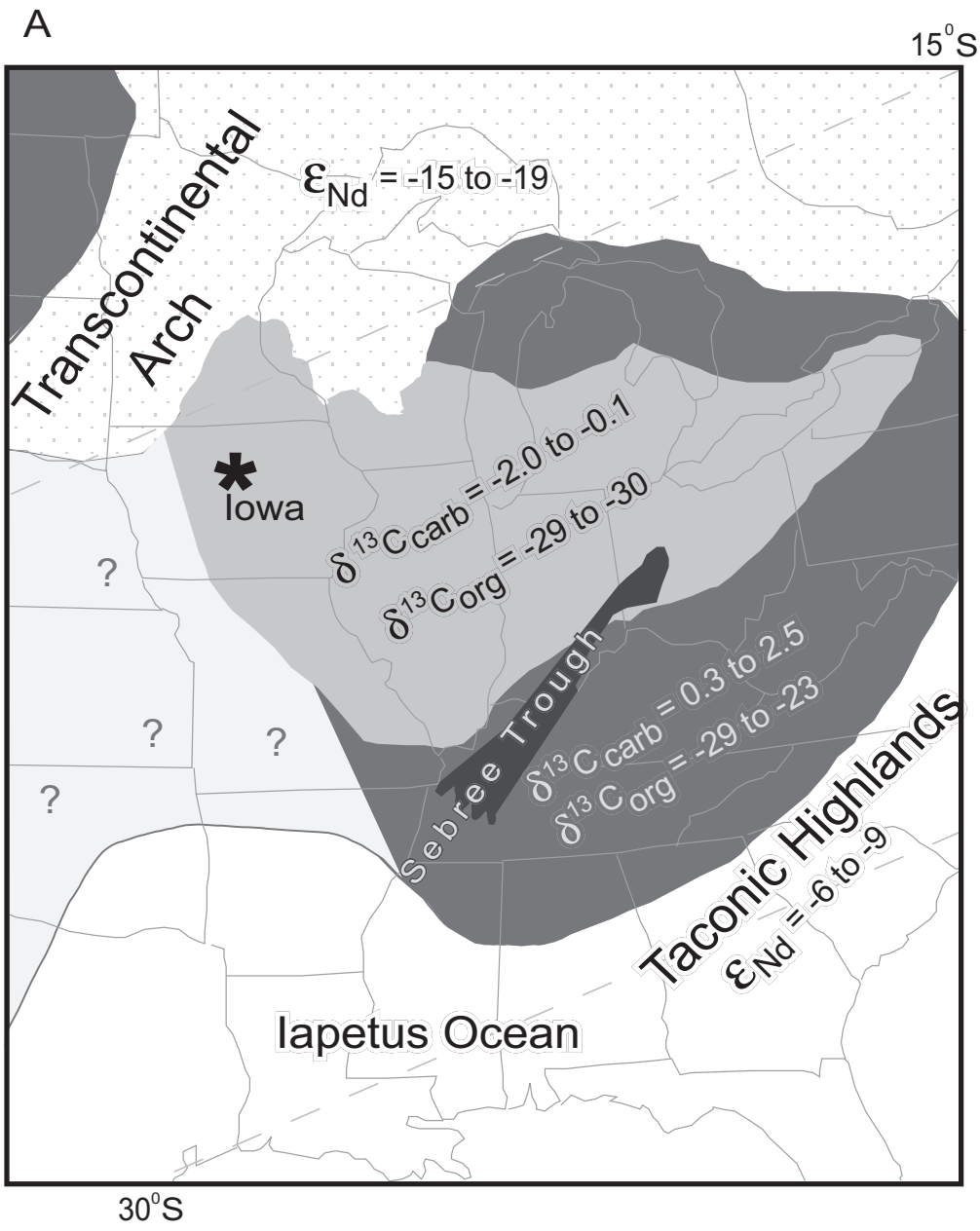

Figure 3.5 Generalized map of the paleogeogaphy of the latest Turinian of the Midcontinent region of North America. Stippled areas denote exposed Precambrian basement. Grey areas are epeiric seawater. The lightest grey area with question marks indicates the area not included in the study of Holmden et al. (1998). The darkest grey area defines the limits of the Sebree Trough. The two intermediate grey areas with $\delta^{13}C$ values define the central Midcontinent water mass with relatively low $\delta^{13}C$ values and the surrounding darker grey marginal water mass with higher $\delta^{13}C$ values. Both the areal extent of the water masses and the $\delta^{13}C$ values are taken from Holmden et al. (1998) and Panchuk (2002).

oxygen minimum zone to spread out of the Sebree Trough and further onto the craton (Fig. 3.6b, Fig. 3.2b) (Witzke, 1987b; Raatz and Ludvigson, 1996; Ludvigson et al., 1996; Kolata et al., 2001). As a result, increased nutrient supply and a decrease in bottom water oxygen levels would increase carbon burial in the interior Midcontinent through increased productivity and preservation of organic matter. Increased burial of carbon would enrich the DIC of Midcontinent waters in ^{13}C, thereby accounting for the initiation of the C1 to C5 excursions. Just as importantly, sea level fall and contraction of nutrient rich and possibly low oxygen bottom waters from the interior Midcontinent would reduce the rate of organic carbon burial as the nutrient supply decreased and productivity declined. The relative increase in freshwater and clastic input from the Arch with sea level fall would also inhibit productivity and burial of carbon (Simo et al., 2003) (Fig. 3.6). Local C-cycling would adjust towards initial conditions, accounting for the negative limb of the C1-C4 $\delta^{13}C$ excursions. We would expect that if sea level remained high, $\delta^{13}C$ values would also remain high rather than be driven back towards initial, pre-excursion conditions by sea level fall. This scenario is exhibited at the base of the Maquoketa Formation, where maximum transgression in the Late Ordovician Midcontinent follows the C5, positive shift in $\delta^{13}C$ (Fig. 3.3). It is believed that a deep, density stratified water column became widespread across the craton at this time (Witzke and Bunker, 1996). Both ε_{Nd} values and eastward thickening shales indicate a complete submergence of the Precambrian basement, leaving only detrital and dissolved source areas from the east. The elevated $\delta^{13}C$ values recorded under these new conditions (Fig. 3.3) would indicate that in response, a new elevated steady-state in C-cycling was established in the Midcontinent epeiric sea.

A relationship between the C1-C5 $\delta^{13}C$ excursions, sea level rise and the spread of

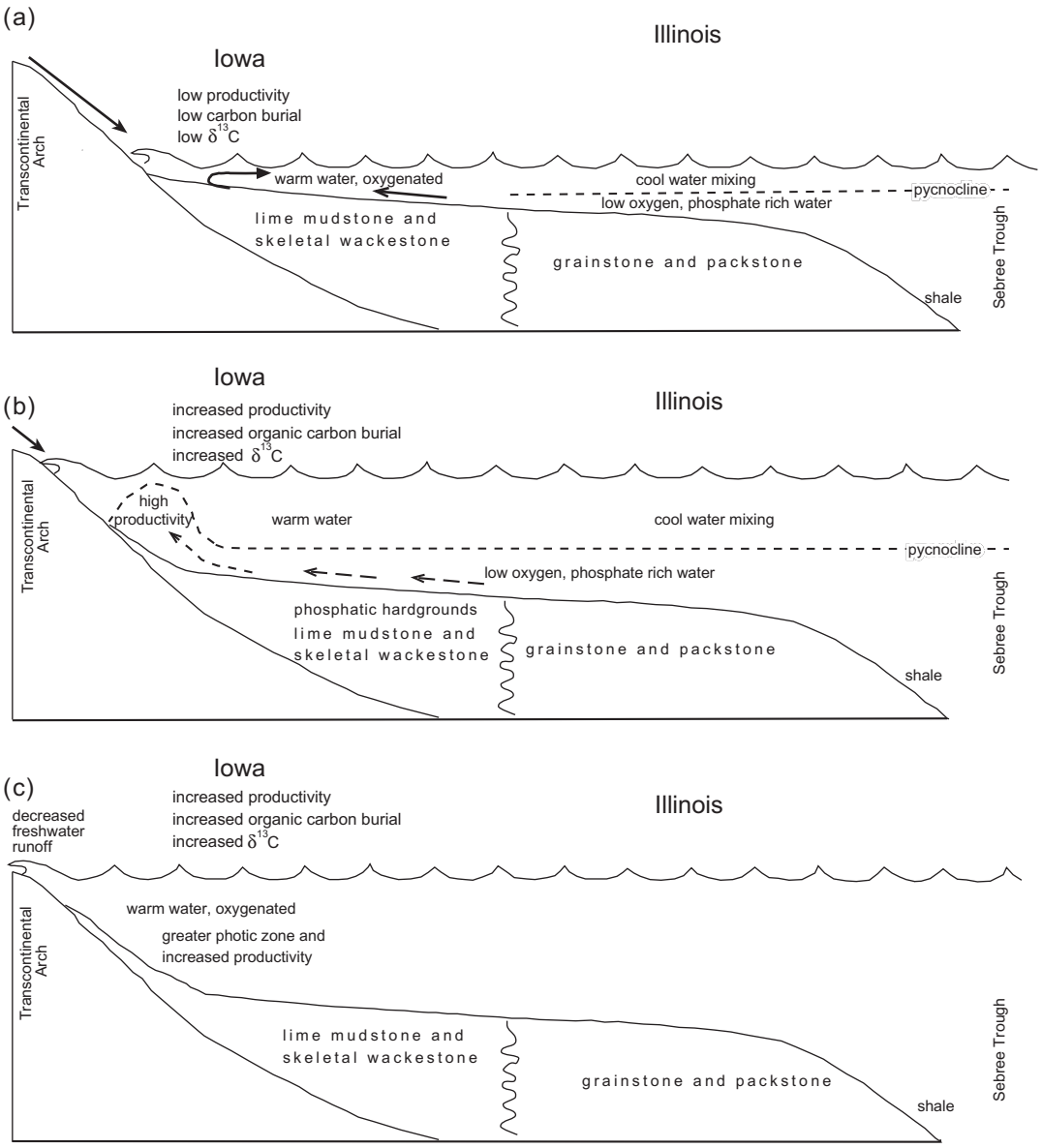

Figure 3.6 A series of cross sections from Iowa to Illinois showing the impact of sea level rise on the $\delta^{13}C$ composition of epeiric seawater in the Iowa area. (a) Exhibits low sea level which results in high freshwater runoff, warm, oxygenated seawater conditions and low $\delta^{13}C$ values in the Iowa area. (b) During sea level rise the oxygen minimum zone from the Iapetus ocean is expanded further onto the craton through the Sebree Trough. As a result cool, phosphate rich, oxygen poor waters are brought into the Iowa area causing upwelling of nutrient rich waters along the Arch. High nutrient levels result in elevated productivity levels and in increased organic carbon burial, which cause an increase in the $\delta^{13}C$ value of epeiric seawater. This example of how sea level can drive local changes in the $\delta^{13}C$ value of epeiric seawater agrees with Ludvigson et al. (1996). Alternatively (c) illustrates conditions predicted by Simo et al. (2003) as a result of sea level rise. In this case sea level rise reduces freshwater runoff from the Arch, which disrupts salinity stratification between surface and bottom waters. The photic zone is expanded as freshwater runoff and clastic input declines, causing an increase in productivity and therefore an increase in the $\delta^{13}C$ value of epeiric seawater in the Iowa area. In either instance (a) or (b) changes in local C-cycling are driven by fluctuations in sea level.

deep, oxygen poor, eutrophic waters is consistent with a model established by Ludvigson et al. (1996) for the Guttenberg (C1) excursion in eastern Iowa. They proposed that expansion of an oxygen minimum zone onto the craton, coupled with freshwater runoff from the Arch would establish a density stratified water column with oxygen poor bottom waters. Increased surface water productivity and the resulting $\delta^{13}C$ excursion would occur due to upwelling of nutrient rich bottom waters as they impinged upon the Transcontinental Arch.

In the Iowa area intermittent incursions of these deep, oxygen poor, eutrophic waters are identified by the occurrence of phosphatic hardground surfaces, interpreted as drowning unconformities (Holland and Patzkowsky, 1996; Raatz and Ludvigson, 1996; Ludvigson et al., 1996; Kolata et al., 2001) and rare grainstone beds within an otherwise warm water mudstone-packstone facies (Kolata et al., 2001). The reoccurrence of $\delta^{13}C$ excursions in units bounded by phosphatic hardgrounds in the upper Platteville Group, as well as the Spechts Ferry and Guttenberg Members of the Decorah Formation, supports a relationship between changes in C-cycling and the spread of deep, oxygen poor, eutrophic waters (Ludvigson et al., 2004). Hardgrounds are well defined in Illinois near the Sebree Trough but are not as prominent in the Galena Group strata of central Iowa (Fig. 3.1) (Kolata et al., 2001). However, smaller hardground surfaces can be found throughout the sampled core section in proximity to the C1-C5 $\delta^{13}C$ excursions (Fig. 3.3). Hardground surfaces occur at the base of the C2, C3 and C5 excursions and near the point of maximum excursion in the C4 excursion. The relationship of hardground surfaces and $\delta^{13}C$ excursions suggests that the C1 to C5 Galena Group excursions are related to, or distal expressions of, drowning unconformities, and the spread of deep, oxygen poor, eutrophic waters during sea level rise. Other hardground surfaces may occur in the section because of local drowning of the

carbonate platform as a result of high or low salinity, temperature change or influx of clastic sediments (Kolata et al., 2001) and therefore may not be associated with a $\delta^{13}C$ excursion.

An alternative model for local circulation patterns and related productivity levels in the Iowa area during Decorah deposition suggests an additional mechanism for driving the C1 to C5 $\delta^{13}C$ excursions. Simo et al. (2003) proposed that during deposition of the Decorah Formation, freshwater runoff from the Transcontinental Arch resulted in a salinity stratified water column with possible intermittent oxygen poor bottom waters. Suspended clastic content eroded from the Arch is suggested to have caused a shallow photic zone with restricted organic productivity (Simo et al., 2003). In this interpretation, sea level rise and submergence of the Arch caused a reduction in freshwater runoff and clastic content, which disrupted salinity stratification, oxygenated the sea floor and expanded the photic zone (Simo et al., 2003). Increased water column clarity and the expanded photic zone is suggested to have increased productivity, which may have led to increased organic carbon burial and an increase in $\delta^{13}C$ values (Fig. 3.6c) (Simo et al., 2003). Increased organic matter productivity in the Guttenberg member is recorded by increasing *G. prisca* abundances and TOC contents (Simo et al., 2003). Therefore, the relationship between increasing TOC contents and the positive C1-C5 excursions in the central Iowa section could also be explained by sea level rise, submergence of the Arch, destratification of the water column and an increase in organic matter productivity and burial. Sea level fall, stratification of the water column and a reduction in the depth of the photic zone would then reduce organic matter productivity and burial, driving the negative limb of the C1-C5 $\delta^{13}C$ excursions.

The correlation of the C1 to C5 $\delta^{13}C$ excursions and TOC with sea level change recorded by the ε_{Nd} curve and the sea level curve from Witzke and Bunker (1996) indicates that sea level fluctuations are driving changes in C-cycling. At least two models have been proposed that would demonstrate how sea level fluctuations can drive local rather than global changes in the C-cycling of the Ordovician Midcontinent epeiric sea. Although these two models use sea level driven changes in local carbon burial as an illustration of how sea level may drive changes in local C-cycling within the epeiric sea, there are several other local C-fluxes that may be adjusted during sea level rise and fall. For example, sea level rise and decreased weathering of the exposed Precambrian basement, may have contributed to the ^{13}C enrichment of Midcontinent waters. Yapp and Poths (1993) used $\delta^{13}C$ values from $Fe(CO_3)OH$ components found in goethites of the Late Ordovician Neda Formation of the Midcontinent, to suggest that there was "substantial biological activity on continental land surfaces prior to widespread colonization of vascular plants." They concluded that this terrestrial organic matter had a $\delta^{13}C_{org}$ value of -27‰. When weathered off the Transcontinental Arch, organic matter would be a source of very depleted DIC relative to neighboring seawater. Therefore, during sea level rise a decrease in weathering and runoff from the Precambrian basement, and a decreased input of the relatively ^{12}C enriched weathering flux, could have caused or added to a positive adjustment in the carbon isotope balance of the adjacent epeiric sea.

Finally, studies of modern day carbonate platforms of Florida Bay and the Bahamas have highlighted the importance of pore water respiration of marine organic matter on the C-cycling of shallow restricted water masses. Patterson and Walter (1994) demonstrated that in comparison to the neighboring ocean, a 4‰ depletion in $\delta^{13}C_{DIC}$ was generated on

the carbonate platforms by the addition of isotopically light carbon through porewater respiration. During sea level fall on the Galena platform, the contribution of isotopically light carbon through pore water respiration may have comprised a significant contribution to the local C-cycle. During episodes of sea level rise that same contribution of isotopically light carbon from pore waters to the local C-cycle would be reduced in significance when compared to the expanded volume of the carbon reservoir of the overlying, deeper water column. This could result in a relative ^{13}C enrichment of Midcontinent waters.

3.7 Implications

The five $\delta^{13}C$ excursions identified in the Galena Group can be explained by sea level forced changes in local C-cycling in the Midcontinent epeiric sea. This explanation is consistent with interpretations of the previously identified Guttenberg excursion (C1) being a regional phenomenon caused by upwelling of nutrient rich waters along the Transcontinental Arch (Hatch et al., 1987; Jacobson et al., 1995; Ludvigson et al., 1996). More recently, the Guttenberg excursion has been reported in Baltica, which led to suggestions that it represents a global shift in ocean C-cycling and, thus, a shift in the $\delta^{13}C$ value of the ocean-atmosphere system (Ainsaar et al. 1999; Meidla et al., 1999). Since we have demonstrated that sea level change can force changes in local C-cycling, we caution against interpreting even globally correlated $\delta^{13}C$ excursions as evidence of ocean-centered changes in the global C-cycle. For example, global sea level change could produce synchronous changes in C-cycling in shallow epeiric seas around the world without producing effects of similar magnitude in the intervening oceans, or ocean sediments. In such an event, we would not expect to see similar magnitudes of $\delta^{13}C$ excursions recorded

on different cratons, or even across the same craton, because the isotope balance of each epeiric sea would be characterized by local C-fluxes of differing magnitudes and isotope compositions. The extent that sea level change can adjust the relative magnitudes of these fluxes would depend on factors such as bathymetry, epeiric sea circulation and degree of restriction of water masses in epeiric seas.

The majority of the $\delta^{13}C$ excursions in epeiric sea environments probably represent superpositions of both local and global changes in C-cycling, and the challenge is to determine which control is dominant, a conclusion also advocated by Immenhauser et al. (2003) based on their Late Carboniferous $\delta^{13}C$ data. Superpositions of local and global $\delta^{13}C$ signals will cause magnitude differences, and even differences in depletion or enrichments in ^{13}C (i.e. positive or negative), in correlative $\delta^{13}C$ excursions from different epeiric sea settings around the world. It is important to bear this in mind when gauging the magnitude or significance of a past environmental perturbation by the magnitude of the $\delta^{13}C$ excursion. Carbon excursions may be amplified in some epeiric sea settings, and dampened in others, thus the true ocean response may be difficult to gauge.

3.8 Conclusions

Ordovician Galena Group carbonates record five positive $\delta^{13}C$ excursions. Correlation of the $\delta^{13}C$ excursions with both conventional and chemostratigraphic sea level proxies suggests that sea level change was the primary force driving changes in C-cycling in the Midcontinent epeiric sea. Sea level rise is thought to have allowed cool, phosphate rich and oxygen poor waters to spread across the Galena carbonate platform (Kolata et al., 2001). Increased productivity, from nutrient upwelling along the Arch, and low oxygen

conditions in bottom waters enhanced carbon burial (as evidenced by increased TOC during sea level rise). Increased carbon burial led to elevated $\delta^{13}C_{DIC}$ values in Midcontinent epeiric seawater, which account for the positive limb of each $\delta^{13}C$ excursion. Sea level rise may have also caused positive $\delta^{13}C$ excursions through submergence of the Arch and a decrease in freshwater runoff and clastic supply to the adjacent epeiric sea. Disruption of salinity stratification, and expansion of the photic zone in a clearer water column would have stimulated productivity and therefore supplemented carbon burial. Sea level fall, and retreat of eutrophic bottom waters, or exposure of the Arch and increased clastic input caused a return to initial $\delta^{13}C$ conditions, as recorded by the negative limb of each of the $\delta^{13}C$ excursions.

The correlation of the sea level and $\delta^{13}C$ curves combined with the circulation models from Kolata et al. (2001), Ludvigson et al. (1996) and Simo et al. (2003) make a strong case for sea level driven changes in local C-cycling, rather than the epeiric sea inheriting changes in the $\delta^{13}C$ signal imparted from the ocean. Global changes in sea level could act synchronously on epeiric sea C-cycles worldwide to create correlative $\delta^{13}C$ excursions in the epeiric setting that may only weakly register in the ocean C-system. Therefore while we do not rule out that $\delta^{13}C$ excursions preserved in epeiric sea carbonates may still be heralds of global environmental change, new models advocating changes in local C-cycling within the epeiric sea need to be factored into interpretations of $\delta^{13}C$ excursions preserved in shallow marine carbonates. Sea level rise and fall may prove in many cases to be the main mechanism driving these local changes in epeiric sea C-cycling.

CHAPTER 4. TESTING ε_{Nd}, $\delta^{13}C$, AND Sm/Nd PROFILES AS CHEMOSTRATIGRAPHIC TOOLS IN EPEIRIC SEAS – A CASE STUDY USING ORDOVICIAN CARBONATES OF ILLINOIS

4.1 Introduction

The ε_{Nd}, $\delta^{13}C$, and Sm/Nd profiles from the Midcontinent Ordovician carbonates of Iowa and Saskatchewan are shown, in the previous chapters of this thesis, to provide an excellent basis for understanding local, sea level driven or sea level related changes in the ε_{Nd}, $\delta^{13}C$ and Sm/Nd composition of an epeiric sea. Therefore, it can be postulated that a contemporaneous sea level change across an epeiric sea should generate coeval, correlative ε_{Nd}, $\delta^{13}C$ and Sm/Nd excursions in carbonates across the craton. In fact, ε_{Nd} excursions were used to correlate Ordovician carbonates of Iowa and Saskatchewan in chapter 2 and multiple studies have relied on $\delta^{13}C$ excursions to correlate strata across cratons, eventhough these excursions have not always been associated with changes in sea level (Saltzman et al., 1995; Patzkowsky et al., 1997; Perfetta et al., 1999; Ludvigson et al., 2004) However, widespread correlations of sea level driven ε_{Nd}, $\delta^{13}C$ and Sm/Nd excursions across a craton are predicated on the assumptions that (1) all ε_{Nd}, $\delta^{13}C$ and Sm/Nd excursions across a single epeiric sea are driven by sea level and (2) that the shape and magnitude of coeval sea level driven excursions do not significantly vary across a single epeiric sea with changes in facies or depositional environment. For example, in the Midcontinent epeiric sea the Nd isotope balance, C-cycling and Sm/Nd ratio of seawater in the Iowa area are greatly

influenced by proximity to the Transcontinental Arch. The Arch acts as a source area for dissolved Nd and influences circulation patterns that promote organic carbon burial and thereby changes in the $\delta^{13}C$ composition of seawater. Further from the Arch, where a different depositional environment or facies may be indicative of differences in circulation patterns and freshwater runoff, changes in the ε_{Nd}, $\delta^{13}C$ and Sm/Nd composition of the Midcontinent epeiric sea may respond differently to sea level fluctuations and resulting excursions may be amplified, dampened or non-existent when compared to the Iowa profiles. Therefore, it is imperative to gauge the influence that depositional environment, which includes such factors as circulation, proximity to major geographic features, depth of the water column and turbidity, may have on sea level driven changes in the ε_{Nd}, $\delta^{13}C$ and Sm/Nd composition of an epeiric sea before these tools can be used to correlate epeiric sea carbonates.

The influence of depositional environment on sea level induced changes in the ε_{Nd}, $\delta^{13}C$ and Sm/Nd composition of an epeiric sea can be most thoroughly investigated using Ordovician Midcontinent carbonates. This is, in part, because the Iowa profiles, discussed in previous chapters, offer a pre-existing example of how sea level drives changes in the ε_{Nd} values, $\delta^{13}C$ values and Sm/Nd ratios of seawater in the depositional environment close to the Transcontinental Arch. In addition, changes in depositional environment across the Ordovician Midcontinent epeiric sea are readily apparent in lateral variations in carbonate lithology and fauna (Keith, 1988; Leslie and Bergström, 1997; Kolata et al., 2001). These variations in lithology and fauna have also been shown to correspond with coeval variations in the ε_{Nd} and $\delta^{13}C$ composition of the rocks, strongly alluding to a connection between depositional environment and the Nd isotope balance and C-cycling of epeiric seawater (Holmden et al., 1998; Panchuk, 2002). Finally, the Ordovician Midcontinent offers several

major geographic features, such as the Transcontinental Arch, Sebree Trough and Taconic Highlands, which have clearly influenced facies distributions (Witzke, 1980; Witzke and Kolata, 1989; Patzkowsky and Holland, 1993; Holland and Patzkowsky, 1997; Kolata et al., 2001) and may also have substantially impacted the ε_{Nd}, $\delta^{13}C$ and Sm/Nd composition of seawater.

To elucidate how a change in depositional environment may influence the isotopic and elemental ratios of epeiric seawater, additional ε_{Nd}, $\delta^{13}C$ and Sm/Nd profiles were constructed through the Middle and Upper Ordovician Galena and Platteville groups of central and southern Illinois. These new sections are within approximately 500 km of the Iowa carbonates but have lithologies and faunas that place them firmly in a different facies (Kolata et al., 2001). The Illinois carbonates are further from the Transcontinental Arch but closer to the Sebree Trough and Taconic Highlands. Therefore, by comparing the Illinois ε_{Nd}, $\delta^{13}C$ and Sm/Nd profiles to known changes in sea level it will be possible to determine if sea level still clearly drives changes in the ε_{Nd}, $\delta^{13}C$ and Sm/Nd composition of seawater in a different depositional environment that is not separated by a large geographic distance from Iowa. These new profiles will also clarify the role that features such as the Arch, the Sebree Trough and the Taconic Highlands may have on influencing the shape and nature of sea level driven changes in the ε_{Nd}, $\delta^{13}C$ and Sm/Nd composition of Midcontinent epeiric seawater.

Finally, comparison of the profiles from Iowa to Illinois will demonstrate whether or not changes in depositional environment, even over short distances, will diminish the ability to correlate these carbonate sequences with the ε_{Nd}, $\delta^{13}C$ and Sm/Nd profiles. To date, establishing a chronostratigraphic framework across the Midcontinent from Iowa to

Illinois has proven difficult (Kolata et al., 2001; Ludvigson et al., 2004). Two prominent K-bentonites in the upper Platteville Group provide the best tie points for correlating coeval strata (Kolata et al., 1987; Leslie and Bergstrom, 1997; Kolata et al., 1998). Otherwise biostratigraphy and lithostratigraphy indicate a sequence of events throughout the Platteville and Galena Groups, including sea level fluctuations and changes in paleocirculation that occur diachronously across the Midcontinent (Sweet, 1984; Bergström and Mitchell, 1992; Kolata et al., 2001).

4.2 Geologic Setting

The upper Platteville Group, Galena Group and Utica shale, alternatively the Maquoketa shale in Iowa, comprise the Upper Ordovician, Turinian to Richmondian, strata of central and southern Illinois (Fig. 4.1) (Witzke and Kolata, 1989; Bergström and Mitchell, 1992; Kolata et al, 2001). Both the Platteville and Galena Groups were part of extensive carbonate platforms that covered the Ordovician Midcontinent of North America between 15°S and 30°S latitude (Scotese and McKerrow, 1990). Despite this similarity each Group represents markedly different depositional environments (Witzke and Kolata, 1989; Keith, 1988; Patzkowsky and Holland, 1993; Holland and Patzkowsky, 1997; Kolata et al., 2001).

The upper Platteville Group is dominated by tropical-like lime mudstones punctuated by the Deicke K-bentonite and a prominent phosphatic hardground surface that is located just below the Deicke K-bentonite (DS1 of Kolata et al., 2001). The boundary of the Platteville and Galena Groups is marked by the Millbrig K-bentonite and a second phosphatic hardground surface (Fig. 4.1) (DS2 of Kolata et al., 2001) (Witzke and Kolata, 1989; Witzke and Bunker, 1996). Features of the upper Platteville Group, including local coralline and

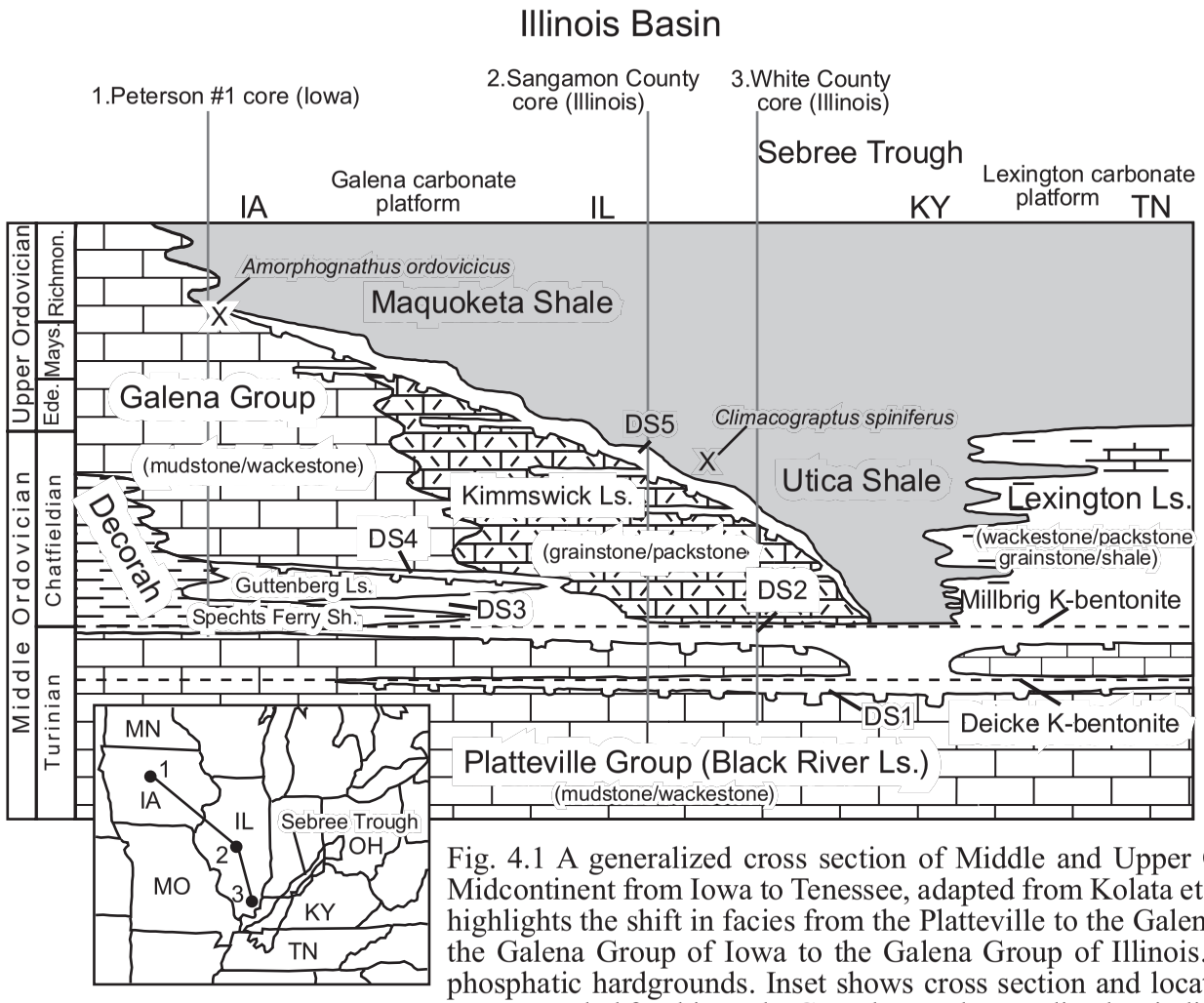

Fig. 4.1 A generalized cross section of Middle and Upper Ordovician strata across the Midcontinent from Iowa to Tenessee, adapted from Kolata et al. (2001). The cross section highlights the shift in facies from the Platteville to the Galena Group in Illinois and from the Galena Group of Iowa to the Galena Group of Illinois. DS1 through DS5 indicate phosphatic hardgrounds. Inset shows cross section and location of the Iowa and Illinois cores sampled for this study. Conodont and graptolite data indicating the diachronous nature of the DS5 surface are marked with an X

peritidal facies in northern Illinois, are suggestive of an overall shallowing upward sedimentary sequence that terminates at the DS2 phosphatic hardground surface (Witzke and Kolata, 1989; Witzke and Bunker, 1996). Deposition of much of the Platteville Group was characterized by relatively warm waters and lagoonal type circulation, which is defined by a net outflow of deep platform waters off the Midcontinent (Fig. 4.2a). Circulation between the Midcontinent epeiric sea and the ocean was restricted (Holmden et al., 1998; Kolata et al., 2001) (Fig 4.2a).

Thickening of Platteville strata eastward across Iowa and southward through Illinois is ascribed to the influence that the failed Late Precambrian-Early Cambrian Reelfoot Rift (Fig. 4.2a) and Rough Creek Graben had on sedimentation rates (Witzke and Kolata, 1989; Kolata and Nelson, 1991; Kolata and Nelson, 1997; Kolata et al., 2001). By the late Turinian, sedimentation rates of the upper Platteville Group were unable to keep up with rapid subsidence rates along the failed Reelfoot Rift. As a result, within this bathymetric low sedimentation stopped, drowning of the carbonate platform began and facies changed from limestone to predominantly shale (Fig. 4.1) (Kolata et al., 2001). This transition was the start of the Sebree Trough, a linear bathymetric depression situated over the failed Rift that extended from central Arkansas northeastward across southern Illinois, Indiana and into Ohio (Fig. 4.2b) (Kolata and Nelson, 1991). Relatively slow deposition of shale in the trough compared to faster depositional rates of the surrounding carbonate platforms perpetuated formation of the Trough (Keith, 1988; Kolata et al., 2001).

As the Sebree Trough developed during the latest Turinian and earliest Chatfieldian, southwestward sweeping surface currents across the Midcontinent met with northward moving cool subpolar currents in a subtropical convergence zone that was optimally

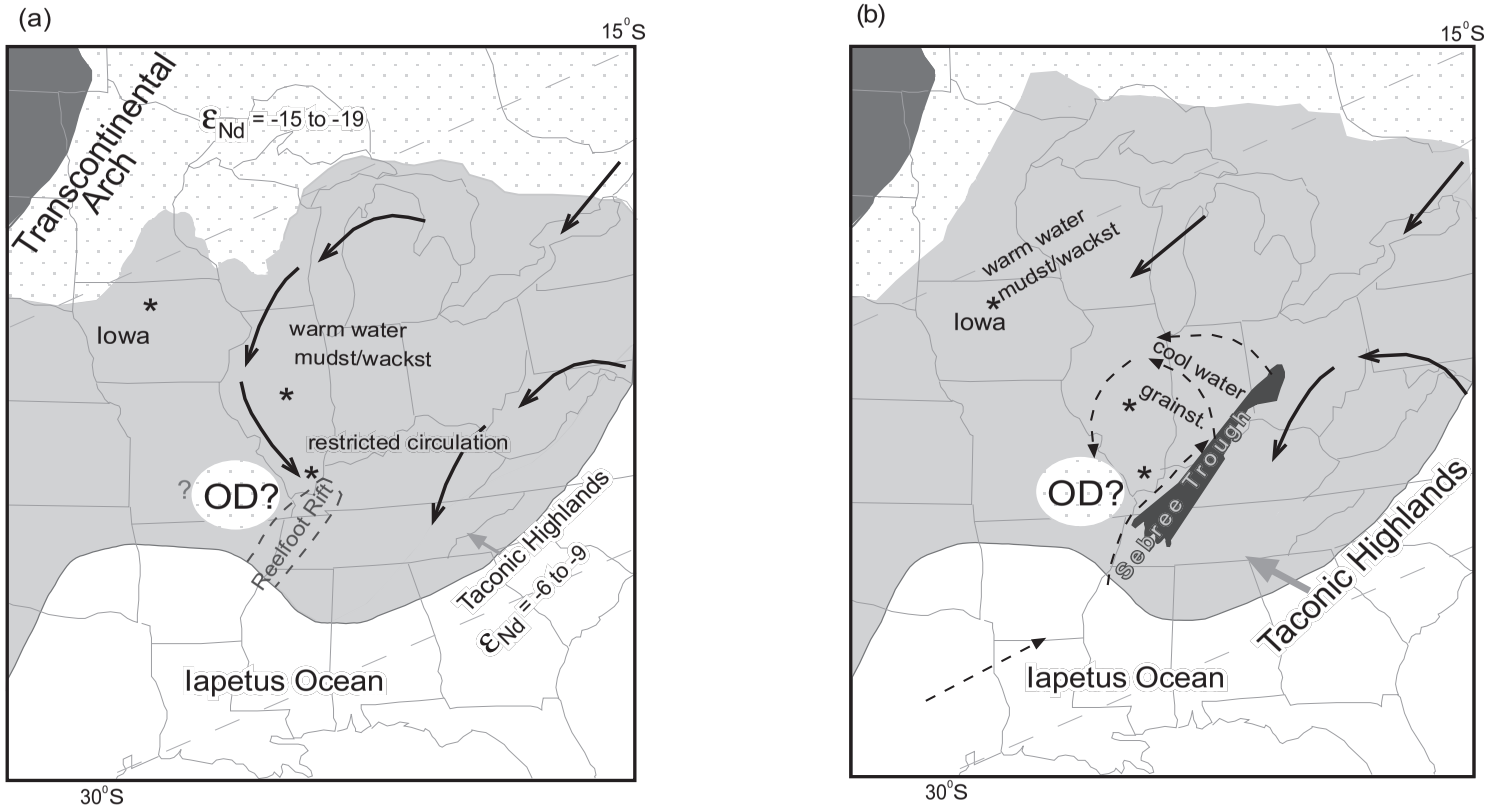

Figure 4.2 Paleocirculation patterns of the Middle and Late Ordovician Midcontinent. Dashed black arrows indicate deep water and solid black arrows indicate surface waters. Light gray arrows indicate prevailing wind direction. (a) Displays a restricted lagoonal type circulation. (b) Portrays quasi-estuarine type circulation, with a stratified water column. Stars indicate position of Iowa and Illinois cores. Stippled area indicates exposed Precambrian basement. Gray areas indicate epeiric seawater. 0.D. = possible location of the Ozark Dome

positioned along the southern margin of North America (Wilde, 1991). Eustatic sea level rise, coupled with freshwater runoff from the Taconic Highlands and wind induced surface currents caused a net shift in surface waters off the craton, allowing deep cool waters to be drawn further onto the craton (Fig. 4.2b) (Witzke, 1980; Witzke, 1987b; Ludvigson et al., 1996; Raatz and Ludvigson, 1996; Holland and Patzkowsky, 1996; Kolata et al., 2001). Kolata and Nelson (1997) identified the Sebree Trough as the conduit for the spread of these deep cool waters across the craton. The new circulation pattern, termed quasi-estuarine type circulation (Witzke, 1987b), caused much of the Midcontinent to develop a density stratified water column with deeper, oxygen poor, phosphate rich waters that were overlain by warm, oxygen rich, lower salinity surface waters that resulted from increased freshwater runoff from the Taconic Orogen and Transcontinental Arch (Ludvigson et al., 1996, Kolata et al., 2001).

The transition from lagoonal type circulation during deposition of the Platteville Group to quasi-estuarine type circulation is marked by the prominent phosphatic hardground DS2 and the transition to the grainstone temperate type lithology and faunas of the Galena Group of Illinois (Fig. 4.1) (Holland and Patzkowsky, 1996; Kolata et al., 2001). In Iowa, Galena Group strata is still dominated by the lime mudstones of a tropical-like facies, delineating the waning influence of cool, phosphate, rich, oxygen poor waters (Fig. 4.1) (Kolata et al., 2001). The occasional influx of cool waters into the Iowa area is recorded only by phosphatic hardgrounds and rare grainstone beds (Ludvigson et al., 1996; Kolata et al., 1998). Phosphatic hardgrounds in the upper Platteville and Galena Groups are believed to be drowning unconformities that record periods of nondeposition during sea level highstand and the spread of cool, phosphate rich, oxygen poor waters brought onto the

craton through the Sebree Trough (Holland and Patzkowsky, 1997; Kolata et al., 1998; Kolata et al., 2001). Longer periods of nondeposition in Illinois, closer to the Sebree Trough, are reflected in thinning of Galena Group strata from Iowa to Illinois. The prominent DS2 hardground of Illinois records a condensed period of time that is equivalent to deposition of the Spechts Ferry and Guttenberg members of the Decorah Formation, the oldest Formation of the Galena Group, in Iowa (Fig. 4.1) (Kolata et al., 1998). Phosphatic hardground surfaces, labeled DS3 and DS4, at the base and top of the Guttenberg Member in Iowa, respectively, are extensions of the DS2 surface into the Iowa area as sea level rise and the spread of cool, phosphate rich waters halted carbonate deposition (Fig. 4.1) (Kolata et al., 2001). The Galena Group across Illinois and Iowa is capped by a final, highly diachronous hardground surface labeled DS5 (Raatz and Ludvigson, 1996; Witzke and Bunker, 1996; Kolata et al., 2001). Conodont and graptolite data from the Galena Group and the overlying Utica shale indicate that the top of the Galena Group in Illinois is late Chatfieldian to Edenian in age, while in Iowa it is early Richmondian in age (Fig. 4.1) (Bergström and Mitchell, 1992; Bergström and Mitchell, 1994; Kolata et al., 2001).

The two subsurface cores sampled from Illinois, identified as the White and Sangamon county cores, display the major trend changes from the mudstone dominated upper Platteville Group to the primarily grainstone lithology of the overlying Galena Group. Part of the Spechts Ferry Member of the Decorah Formation has been previously identified in the Sangamon core (Ludvigson et al., 2004) but has not been identified in the White County core. This small portion of the Spechts Ferry Member in the Sangamon County core will be considered as part of the upper Platteville Group for the purposes of this study. The prominent phosphatic hardground surface at the base of the Galena Group in each

section has been identified as the DS2 surface identified in Kolata et al. (2001) based on core descriptions by Kolata et al. (1998). The Deicke K-bentonite has also been identified in both core sections but the Millbrig K-bentonite is absent (Kolata per comm, Kolata et al., 1998; Ludvigson et al., 2004). Description of the Peterson #1 core from central Iowa can be found in chapter 2 of this thesis (Fig. 2.2). The Platteville Group of the Iowa core was missing as a result of local faulting and therefore was not sampled.

4.3 Sampling and Methods

This study utilized two subsurface drill cores, one from Sangamon County in central Illinois (Illinois State Geological Survey site C#28; sec. 11 T15N R3W) and one from White County in southern Illinois (Fig. 4.1) (Illinois State Geological Survey site C#2740; sec. 27 T4S R14W). Ten gram samples were taken from each core at approximately 5 feet intervals, starting in the upper Platteville Group and spanning the entire Galena Group. Two to three grams of each sample were processed according to Fanton et al. (2002) in order to obtain $\varepsilon_{Nd}(450)$ and Sm/Nd data for each subsurface core. External reproducibility of $^{143}Nd/^{144}Nd$ is $\pm$ 0.000017 (2σ), based on replicate analyses of our internal Nd Ames standard. Over the course of this work the La Jolla standard yielded $^{143}Nd/^{144}Nd = 0.511841$. Epsilon Nd values presented in the text are back-corrected using the measured $^{147}Sm/^{144}Nd$ ratios to the time of deposition at 450 Ma. Although the stratigraphic age of the sampled cores span approximately 15 Ma, the maximum error introduced by using a single age for all samples is less than 0.2 epsilon units. Another 15 mg from each sample was processed following McCrea (1950) and analyzed using a Finnigan MAT Delta E dual inlet GIRMS to obtain $\delta^{13}C_{carb}$ data for each subsurface core. External precision of $\delta^{13}C_{carb}$ is better than $\pm$

0.2‰ using NBS19, which yielded 1.95 ± 0.10‰ (2σ).

Excursions in the ε_{Nd}, $\delta^{13}C$ and Sm/Nd data in this chapter were defined as being variations in values that were clearly defined against background noise, which includes closely spaced fluctuations in values with a sawtooth pattern. As a result, ε_{Nd} excursions have magnitudes greater than 3.5 units and $\delta^{13}C$ excursions have magnitudes greater than 1‰. The magnitude of the Sm/Nd excursions are as small as 0.005 units, but it has not yet been determined if such a small variation is truly significant enough to be termed an excursion. When comparing ε_{Nd}, $\delta^{13}C$ and Sm/Nd profiles between the Sangamon and White County cores the Deicke K-bentonite is used as a marker horizon for correlating the two core sections.

4.4 Results

4.4.1 The ε_{Nd} profiles from the White and Sangamon cores

The ε_{Nd} profiles of the White and Sangamon county cores differ greatly from the Platteville to the Galena Group. The average ε_{Nd} values of the Platteville Group in the White and Sangamon cores are -9.4 and -10.2, respectively (Fig. 4.3, Fig. 4.4, Table 4.1, Table 4.2). The Platteville Group profile is punctuated by three positive ε_{Nd} excursions in the White County core, labelled E2, E3a and E3b, with magnitudes of 4.2, 7.5 and 3.6 epsilon units, respectively (Fig. 4.4, Table 4.2). Four positive ε_{Nd} excursions can be identified in the Platteville Group of the Sangamon County core, labeled E1, E2, E3a and E3b, magnitudes are 7.8, 4,4, 3.7 and 5.3 epsilon units, respectively (Fig. 4.3, Table 4.1). Both cores display a positive shift in ε_{Nd} at the base of the Galena Group, labelled E4, coincident with the DS2 surface. The E4 shift in ε_{Nd} has a larger magnitude in the White section (11.7

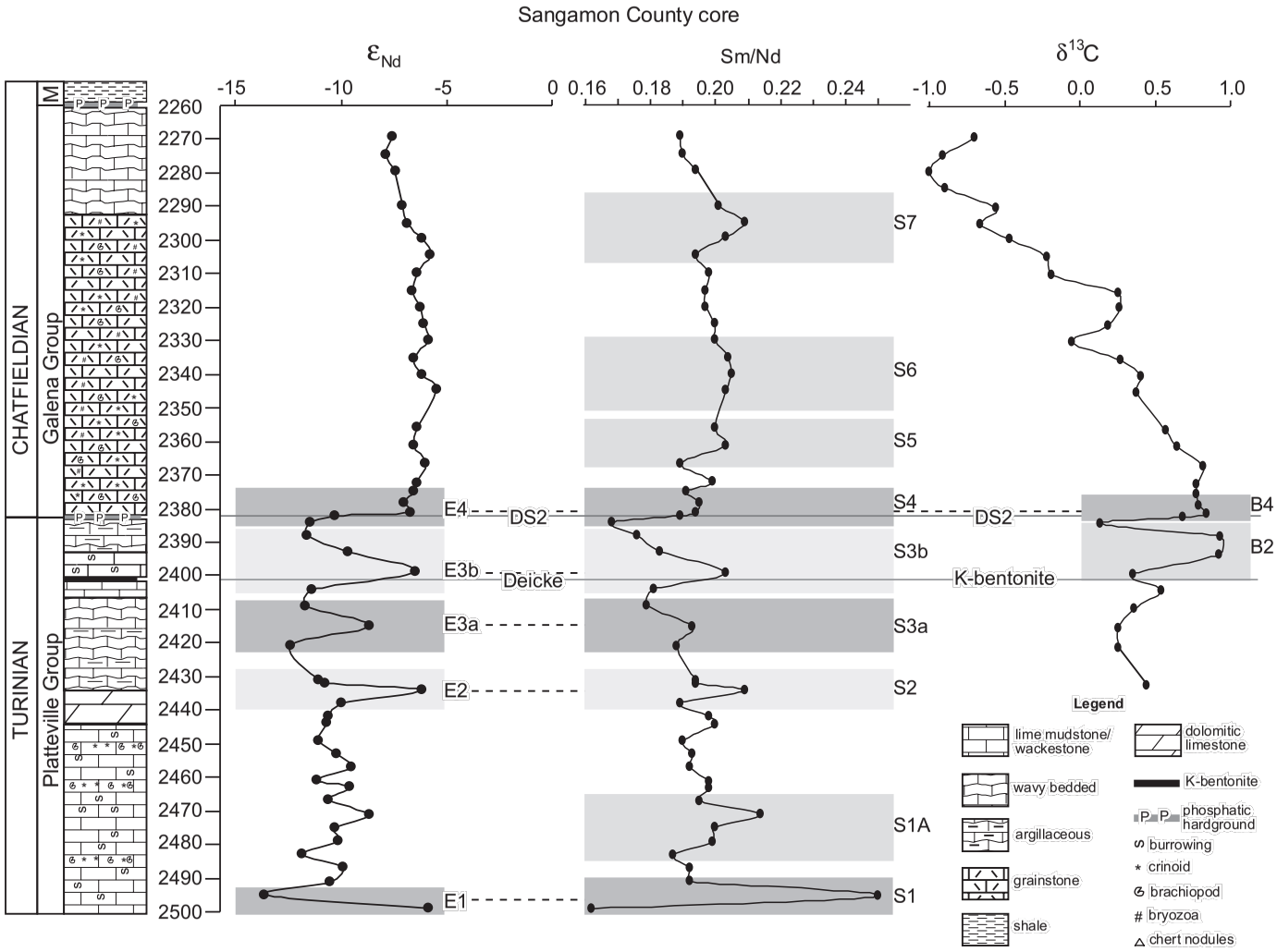

Figure 4.3 ε_{Nd}, Sm/Nd and $\delta^{13}C$ profiles plotted against stratigraphic section, in feet, for the Sangamon County core. Shaded areas delineate excursions and dashed lines connect correlative events. M = Maquoketa Formation.

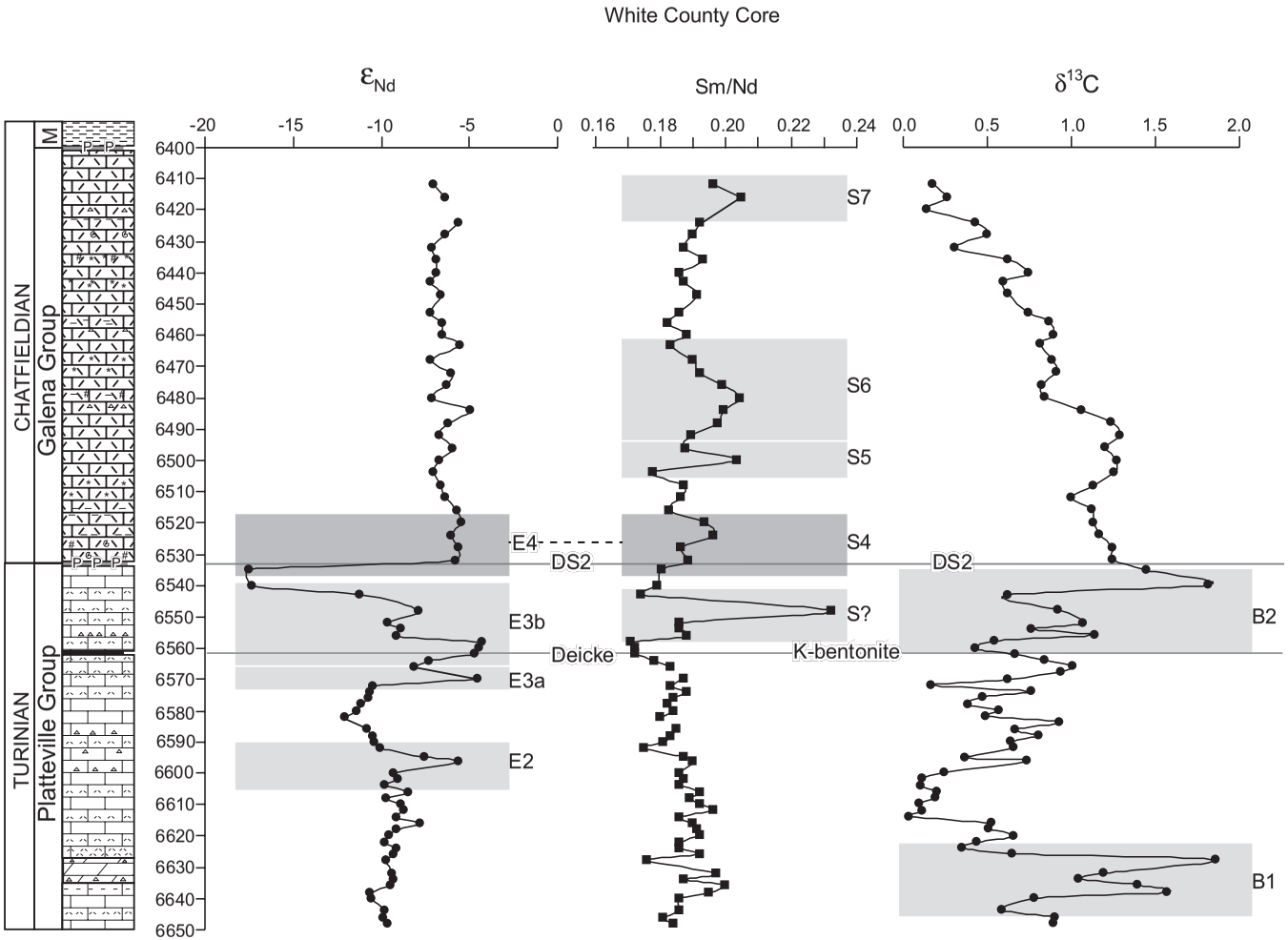

Figure 4.4 ε_{Nd}, Sm/Nd and $\delta^{13}C$ profiles plotted against stratigraphic section, in feet, for the White County core, Illinois. Shaded areas delineate excursions and dashed lines connect correlative events. Lithologic symbols are the same as in Figure 4.3. M = Maquoketa Formation.

Table 4.1 Concentration and isotope data for the Sangamon County core, Illinois

Subsurface depth (ft.)	Grp[a]	Insoluble residue (wt %)	$\delta^{13}C_{(carb)}$[b]	Nd (ppm)[c]	Sm (ppm)[c]	Sm/Nd[c]	$^{147}Sm/^{144}Nd$[c]	$^{143}Nd/^{144}Nd$[c]	$\varepsilon_{Nd}(450)$[c,e]
2269.1	G	4.7	-0.7	1.90	0.37	0.189	0.1199	0.512025	-7.5
2274.5	G	4.0	-0.9	2.99	0.60	0.190	0.1207	0.512011	-7.9
2279.6	G	3.3	-1.0	2.28	0.46	0.194	0.1233	0.512042	-7.4
2284.5	G	2.1	-0.9	N.D.	N.D.	N.D.	N.D.	N.D.	N.D.
2290.0	G	0.8	-0.6	1.41	0.30	0.201	0.1277	0.512070	-7.1
2295.0	G	1.7	-0.7	2.11	0.46	0.209	0.1327	0.512100	-6.8
2299.5	G	2.6	-0.5	1.29	0.27	0.203	0.1286	0.512122	-6.2
2304.5	G	1.0	-0.2	1.65	0.33	0.194	0.1233	0.512129	-5.7
2310.0	G	2.3	-0.2	2.67	0.55	0.198	0.1257	0.512102	-6.4
2315.2	G	3.6	0.3	1.01	0.20	0.197	0.1248	0.512087	-6.6
2320.0	G	1.0	0.3	1.43	0.29	0.197	0.1247	0.512107	-6.2
2325.0	G	0.7	0.2	2.15	0.45	0.200	0.1268	0.512121	-6.1
2330.0	G	1.3	-0.1	2.16	0.45	0.200	0.1270	0.512135	-5.8
2335.1	G	6.7	0.3	1.17	0.25	0.204	0.1294	0.512104	-6.6
2340.0	G	1.9	0.4	1.47	0.31	0.205	0.1301	0.512127	-6.2
2344.8	G	2.0	0.4	1.34	0.28	0.203	0.1286	0.512160	-5.4
2356.0	G	3.5	0.6	2.15	0.45	0.200	0.1282	0.512108	-6.4
2361.1	G	1.9	0.6	3.84	0.81	0.203	0.1285	0.512104	-6.5
2366.8	G	6.9	0.8	0.79	0.15	0.189	0.1198	0.512103	-6.0
2372.2	G	3.4	0.8	1.27	0.26	0.199	0.1264	0.512103	-6.4
2375.0	G	7.9	0.8	1.11	0.22	0.191	0.1215	0.512081	-6.6
2378.5	G	3.8	0.8	1.65	0.33	0.195	0.1236	0.512063	-7.0
2381.0	G	5.1	0.8	1.31	0.26	0.194	0.1230	0.512080	-6.7
2382.0	P	4.4	0.7	1.68	0.33	0.189	0.1198	0.511886	-10.3
2384.0	P	5.7	0.1	1.30	0.23	0.168	0.1069	0.511789	-11.4
2388.0	P	3.9	0.9	0.66	0.12	0.176	0.1119	0.511795	-11.6
2393.0	P	4.9	0.9	0.70	0.13	0.183	0.1161	0.511908	-9.6
2399.0	P	5.0	0.4	1.43	0.30	0.203	0.1288	0.512108	-6.4
2404.0	P	6.4	0.5	0.60	0.11	0.181	0.1150	0.511814	-11.4
2409.0	P	3.1	0.4	0.61	0.11	0.179	0.1138	0.511794	-11.7
2415.0	P	4.8	0.3	1.18	0.24	0.193	0.1226	0.511977	-8.6
2421.0	P	33.0	0.3	0.99	0.19	0.188	0.1194	0.511777	-12.4
2431.0	P	7.9	N.D.	0.94	0.19	0.194	0.1228	0.511851	-11.1
2432.0	P	10.3	0.4	0.87	0.17	0.194	0.1231	0.511872	-10.7
2434.0	P	7.9	N.D.	1.26	0.28	0.209	0.1329	0.512132	-6.2

(continued)

Table 4.1 (Continued)

Subsurface depth (ft.)	Grp[a]	Insoluble residue (wt %)	$\delta^{13}C_{(carb)}$ [b]	Nd (ppm)[c]	Sm (ppm)[c]	Sm/Nd[c]	$^{147}Sm/^{144}Nd$[c]	$^{143}Nd/^{144}Nd$[c]	$\varepsilon_{Nd}(450)$[c,e]
2438.0	P	2.2	N.D.	0.27	0.05	0.189	0.1202	0.511898	-10.0
2442.0	P	5.2	N.D.	0.29	0.06	0.198	0.1255	0.511886	-10.6
2444.0	P	2.8	N.D.	0.31	0.07	0.200	0.1271	0.511883	-10.7
2449.0	P	5.1	N.D.	0.43	0.09	0.190	0.1207	0.511847	-11.0
2453.0	P	4.3	N.D.	0.48	0.10	0.193	0.1225	0.511893	-10.2
2457.0	P	3.6	N.D.	0.51	0.10	0.192	0.1219	0.511930	-9.5
2461.0	P	5.7	N.D.	0.56	0.12	0.198	0.1256	0.511856	-11.2
2463.0	P	7.4	N.D.	0.57	0.12	0.198	0.1254	0.511937	-9.6
2467.0	P	3.3	N.D.	0.30	0.06	0.195	0.1238	0.511879	-10.6
2471.0	P	2.8	N.D.	0.59	0.13	0.214	0.1359	0.512016	-8.6
2475.0	P	3.7	N.D.	0.41	0.09	0.200	0.1266	0.511905	-10.3
2479.0	P	3.5	N.D.	0.47	0.10	0.199	0.1261	0.511910	-10.1
2483.0	P	2.2	N.D.	0.48	0.09	0.187	0.1188	0.511800	-11.8
2487.0	P	4.3	N.D.	1.03	0.21	0.192	0.1218	0.511907	-9.9
2491.0	P	3.3	N.D.	0.56	0.11	0.192	0.1218	0.511878	-10.5
2495.0	P	20.0	N.D.	1.37	0.36	0.250	0.1587	0.511828	-13.6
2499.0	P	5.2	N.D.	1.65	0.28	0.162	0.1030	0.512062	-5.8

[a] Name of the Group samples were collected from: G = Galena; P = Platteville

[b] $\delta^{13}C$ value of the carbonate measured in per mil

[c] Measured from the acid soluble fraction of carbonates

[e] ε_{Nd} values calculated at 450Ma. $\varepsilon_{Nd}(450) = \{(((^{143}Nd/^{144}Nd_{sample(0)} - (^{147}Sm/^{144}Nd_{sample(0)} (e^{\lambda(450Ma)} - 1)))/(^{143}Nd/^{144}Nd_{CHUR(0)} - (^{147}Sm/^{144}Nd_{CHUR(0)} (e\lambda^{(450Ma} - 1))))-1\} \times 10^{4.}$ Present day = (0)

N.D. = not determined

Table 4.2 Concentration and isotope data for the White County Core, Illinois

Subsurface depth (ft)	Grp[a]	insoluble residue (wt. %)	$\delta^{13}C_{(carb)}$[b]	Nd (ppm)[c]	Sm (ppm)[c]	Sm/Nd[c]	$^{147}Sm/^{144}Nd$[c]	$^{143}Nd/^{144}Nd$[c]	$\varepsilon_{Nd}(450)$[c,e]
6412	G	4.3	0.2	4.77	0.98	0.196	0.1245	0.512066	-7.0
6416	G	1.5	0.3	7.44	1.60	0.205	0.1300	0.512116	-6.4
6420	G	1.8	0.1	N.D.	N.D.	N.D.	N.D.	N.D.	N.D.
6424	G	2.0	0.4	3.64	0.73	0.192	0.1217	0.512130	-5.6
6428	G	2.0	0.5	2.92	0.58	0.190	0.1203	0.512085	-6.4
6432	G	1.4	0.3	3.52	0.69	0.187	0.1185	0.512046	-7.1
6436	G	1.2	0.6	4.42	0.89	0.193	0.1225	0.512067	-6.9
6440	G	2.0	0.7	1.72	0.33	0.186	0.1181	0.512053	-6.9
6443	G	1.7	0.6	2.18	0.42	0.187	0.1189	0.512038	-7.2
6447	G	2.7	0.6	3.19	0.64	0.191	0.1212	0.512076	-6.6
6453	G	0.8	0.7	1.65	0.32	0.186	0.1182	0.512039	-7.2
6456	G	1.6	0.9	1.48	0.28	0.182	0.1152	0.512064	-6.5
6460	G	2.6	0.9	3.18	0.63	0.188	0.1190	0.512074	-6.5
6463	G	0.5	0.8	2.17	0.41	0.183	0.1162	0.512121	-5.5
6468	G	1.6	0.9	3.02	0.60	0.190	0.1203	0.512045	-7.2
6472	G	0.8	0.9	2.67	0.53	0.192	0.1220	0.512111	-6.0
6476	G	0.7	0.8	2.74	0.57	0.199	0.1261	0.512105	-6.3
6480	G	1.4	0.8	3.08	0.66	0.204	0.1296	0.512074	-7.1
6484	G	2.4	1.1	2.53	0.53	0.199	0.1265	0.512180	-4.9
6488	G	1.2	1.2	2.78	0.57	0.198	0.1254	0.512110	-6.2
6492	G	1.2	1.3	2.28	0.45	0.190	0.1202	0.512070	-6.7
6496	G	1.7	1.2	1.86	0.36	0.187	0.1189	0.512106	-5.9
6500	G	4.7	1.3	7.11	1.51	0.204	0.1292	0.512098	-6.7
6504	G	3.3	1.3	0.77	0.14	0.178	0.1128	0.512032	-7.0
6508	G	4.8	1.1	2.11	0.41	0.187	0.1187	0.512071	-6.6
6512	G	6.0	1.0	2.18	0.42	0.186	0.1183	0.512079	-6.4
6516	G	5.7	1.1	5.99	1.14	0.183	0.1158	0.512106	-5.7
6520	G	3.0	1.1	4.97	1.00	0.193	0.1227	0.512142	-5.4
6524	G	2.0	1.2	2.99	0.61	0.196	0.1243	0.512118	-6.0
6528	G	2.0	1.2	1.92	0.37	0.186	0.1181	0.512118	-5.6
6532	G	2.5	1.2	2.53	0.50	0.189	0.1197	0.512111	-5.8
6535	P	16.7	1.4	3.79	0.71	0.180	0.1143	0.511499	-17.5
6540	P	13.3	1.8	4.04	0.76	0.179	0.1136	0.511505	-17.3
6543	P	3.9	0.6	0.76	0.14	0.174	0.1105	0.511810	-11.2
6548	P	7.0	0.9	1.42	0.34	0.232	0.1475	0.512087	-7.9
6552	P	1.3	1.1	0.63	0.12	0.186	0.1179	0.511916	-9.6
6554	P	5.6	0.8	0.98	0.19	0.186	0.1178	0.511967	-8.9

(continued)

Table 4.2 (continued)

Subsurface depth (ft)	Grp[a]	insoluble residue (wt. %)	$\delta^{13}C_{(carb)}$[b]	Nd (ppm)[c]	Sm (ppm)[c]	Sm/Nd[c]	$^{147}Sm/^{144}Nd$[c]	$^{143}Nd/^{144}Nd$[c]	$\varepsilon_{Nd}(450)$[c,e]
6556	P	5.4	1.1	0.78	0.15	0.188	0.1192	0.511941	-9.1
6558	P	3.8	0.5	1.40	0.25	0.171	0.1085	0.512223	-4.3
6560	P	3.9	0.4	1.36	0.25	0.172	0.1090	0.512197	-4.5
6562	P	2.8	0.7	1.93	0.34	0.172	0.1089	0.512158	-4.7
6564	P	9.2	0.8	2.14	0.40	0.178	0.1129	0.512081	-7.3
6566	P	1.9	1.0	1.28	0.24	0.183	0.1159	0.511985	-8.1
6568	P	2.3	0.9	N.D.	N.D.	N.D.	N.D.	N.D.	N.D.
6570	P	0.7	0.6	0.65	0.12	0.187	0.1185	0.512178	-4.5
6572	P	3.8	0.2	0.99	0.19	0.183	0.1159	0.511865	-10.5
6574	P	5.5	0.8	0.64	0.12	0.188	0.1194	0.511867	-10.6
6576	P	44.0	0.5	0.46	0.08	0.184	0.1165	0.511855	-10.7
6578	P	6.5	0.4	0.79	0.15	0.182	0.1155	0.511842	-11.2
6580	P	2.2	0.6	0.80	0.15	0.184	0.1168	0.511819	-11.4
6582	P	3.1	0.5	0.97	0.18	0.180	0.1141	0.511815	-12.0
6584	P	N.D.	0.9	N.D.	N.D.	N.D.	N.D.	N.D.	N.D.
6586	P	5.4	0.7	0.74	0.14	0.185	0.1175	0.511850	-10.8
6588	P	4.6	0.8	0.76	0.15	0.183	0.1160	0.511863	-10.5
6590	P	3.8	0.6	0.44	0.08	0.181	0.1147	0.511865	-10.4
6592	P	4.4	0.7	0.25	0.05	0.175	0.1113	0.511870	-10.1
6595	P	7.8	0.4	1.32	0.26	0.187	0.1187	0.512021	-7.6
6596	P	7.3	0.7	1.68	0.34	0.190	0.1208	0.512128	-5.6
6600	P	7.8	0.2	0.62	0.12	0.186	0.1178	0.511928	-9.3
6602	P	3.5	0.1	0.82	0.06	0.187	0.1184	0.511946	-9.0
6604	P	5.7	0.1	0.56	0.11	0.186	0.1179	0.511902	-9.8
6606	P	10.1	0.2	1.14	0.23	0.192	0.1215	0.511984	-8.4
6608	P	7.8	0.2	0.91	0.18	0.189	0.1201	0.511915	-9.7
6610	P	5.0	0.1	0.82	0.16	0.192	0.1216	0.511962	-8.9
6612	P	8.8	0.1	0.96	0.20	0.196	0.1243	0.511978	-8.7
6614	P	2.7	0.0	0.26	0.05	0.186	0.1178	0.511937	-9.2
6616	P	3.6	0.5	0.36	0.07	0.190	0.1204	0.512160	-7.8
6618	P	9.8	0.5	0.60	0.12	0.191	0.1211	0.511947	-9.2
6620	P	6.6	0.7	0.60	0.12	0.192	0.1209	0.511927	-9.6
6622	P	4.5	0.4	0.38	0.07	0.186	0.1183	0.511906	-9.8
6624	P	2.0	0.3	0.17	0.03	0.186	0.1183	0.511941	-9.1
6626	P	2.1	0.7	0.16	0.03	0.192	0.1221	0.511942	-9.3
6628	P	52.6	1.9	0.27	0.05	0.176	0.1114	0.511891	-9.7

(continued)

Table 4.2 (continued)

Subsurface depth (ft)	Grp[a]	insoluble residue (wt. %)	$\delta^{13}C_{(carb)}$[b]	Nd (ppm)[c]	Sm (ppm)[c]	Sm/Nd[c]	$^{147}Sm/^{144}Nd$[c]	$^{143}Nd/^{144}Nd$[c]	$\varepsilon_{Nd}(450)$[c,e]
6632	P	5.8	1.2	0.41	0.08	0.197	0.1247	0.511947	-9.4
6634	P	4.8	1.0	0.38	0.08	0.187	0.1183	0.511933	-9.3
6636	P	8.3	1.4	0.34	0.07	0.200	0.1271	0.511950	-9.4
6638	P	47.9	1.6	0.26	0.05	0.195	0.1239	0.511880	-10.6
6640	P	4.6	0.8	0.60	0.12	0.186	0.1179	0.511866	-10.5
6644	P	10.0	0.6	0.33	0.06	0.186	0.1178	0.511906	-9.8
6646	P	34.2	0.9	0.46	0.09	0.181	0.1151	0.511892	-9.9
6648	P	4.5	0.9	0.46	0.09	0.184	0.1169	0.511911	-9.6

[a] Name of the Group samples were collected from: G = Galena; P = Platteville

[b] $\delta^{13}C$ value of the carbonate measured in per mil

[c] Measured from the acid soluble fraction of carbonates

N.D. = not determined

[e] ε_{Nd} values calculated at 450Ma. $\varepsilon_{Nd}(450) = \{((^{143}Nd/^{144}Nd_{sample(0)} - (^{147}Sm/^{144}Nd_{sample(0)} (e^{\lambda(450Ma)} - 1)))/(^{143}Nd/^{144}Nd_{CHUR(0)} - (^{147}Sm/^{144}Nd_{CHUR(0)} (e\lambda^{(450Ma} - 1))))-1\} \times 10^{4.}$ Present day = (0)

epsilon units) when compared to the Sangamon core (5 epsilon units). In contrast to the Platteville Group, the Galena Group of the White and Sangamon cores have higher average ε_{Nd} values of -6.4 and -7.1 respectively, and the profiles display only small variations of less than 2 epsilon units (Fig. 4.3, Fig. 4.4).

The Deicke K-bentonite bed in the upper Platteville Group can be used to definitively correlate the E3b excursion between the White and Sangamon cores because the K-bentonite is an isochronous rock unit. Correlation of the E3b event leads to the deduction that the remaining E3a and E2 excursions are also correlative events (Fig. 4.5). Justification for this conclusion can be found in the similar magnitude and shape of excursion E2 between the White and Sangamon cores. However, event E3, including E3a and E3b, is substantially different in magnitude and shape between the two cores, appearing as one broad excursion with two peaks, E3a and E3b in the White core, and as two separate excursions, E3a and E3b, in the Sangamon core (Fig. 4.5). Excursion E1 is found only in the Sangamon core (Fig. 4.5) and without stratigraphic control between the basal strata of each sampled section it is difficult to determine if this is due to a sampling artifact, such as the base of the sampled Sangamon core is older than that of the White core, or if indeed the Sangamon core records an event that did not influence the White County core area.

4.4.2 The Sm/Nd profiles from the White and Sangamon cores

The Sm/Nd profiles of the White and Sangamon cores display a pronounced change from the Platteville to the Galena Group (Fig. 4.3, Fig. 4.4). The profiles of Sm/Nd ratios in both Illinois cores are defined by an overall decline in Sm/Nd values through the Platteville Group (Fig. 4.3, Fig. 4.4, Table 4.1, Table 4.2). However, while the upper Platteville Group

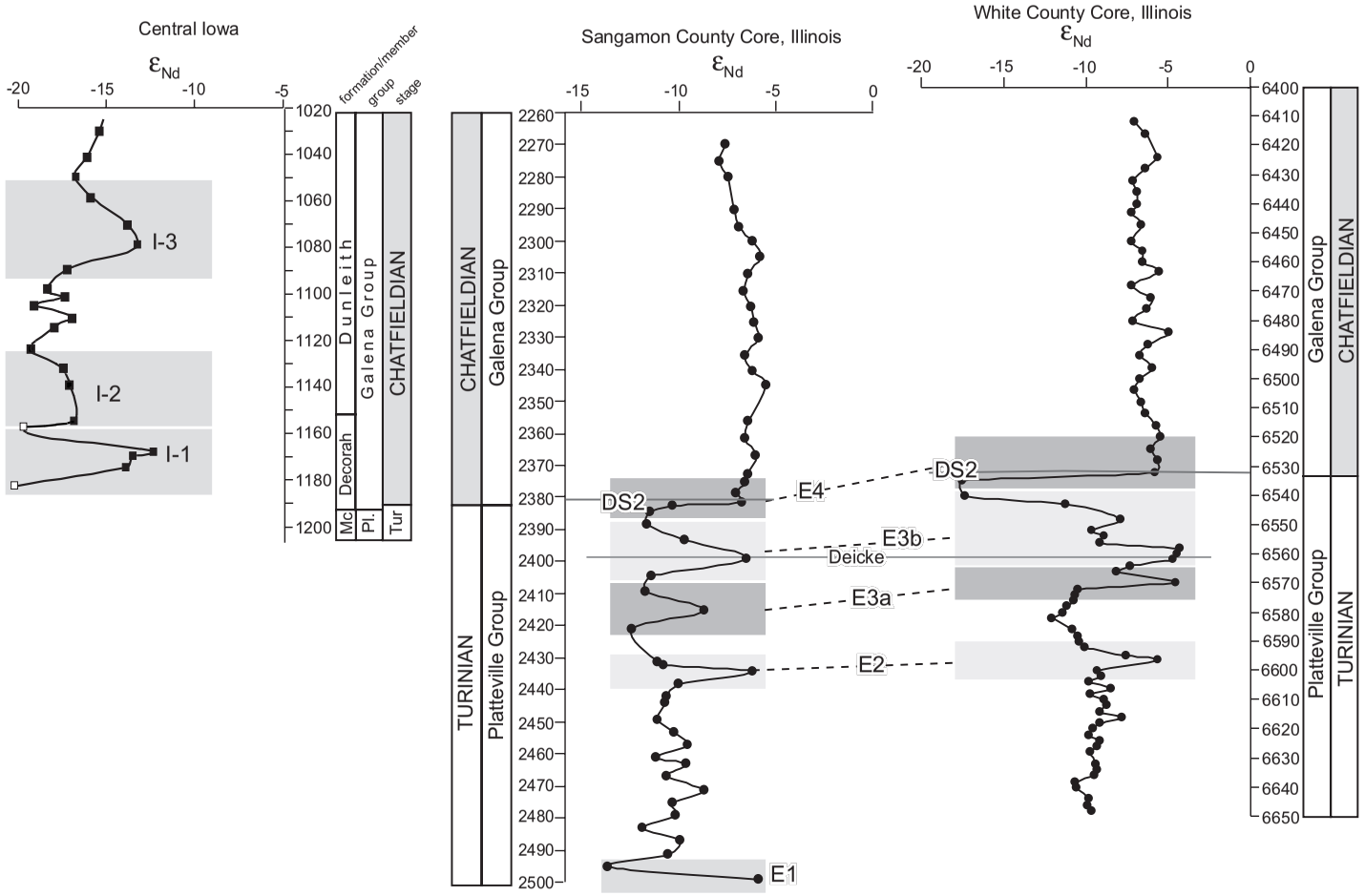

Figure 4.5 Comparison of ε_{Nd} profiles between Illinois sections and between Illinois and Iowa. Shaded regions mark excursions and dashed lines connect correlative excursions. Shaded Chatfieldian stages emphasize that while ε_{Nd} values continue to fluctuate in Iowa during this stage they are mostly unvariable in both Illinois sections. Mc. = McGregor Formation; Pl. = Platteville Group; Tur. = Turinian. Stratigraphic sections are measured in feet.

of the Sangamon core is punctuated by five positive Sm/Nd excursions (S1, S1A, S2, S3a and S3b) (Fig. 4.3), four of which are coeval with ε_{Nd} excursions (Fig. 4.3), the White core displays only one large positive Sm/Nd excursion (labelled S?) that does not correspond to an ε_{Nd} excursion (Fig. 4.4). A positive Sm/Nd excursion, coeval with the positive shift in ε_{Nd}, is present across the DS2 surface at the base of the Galena Group in each core and is labeled S4 (Fig. 4.3, Fig. 4.4). Sm/Nd ratios continue to vary into the Galena Group and three positive Sm/Nd excursions have been identified in each core as S5, S6, and S7. These three Sm/Nd excursions have a greater magnitude in the White core (Fig. 4.4) than in the Sangamon core (Fig. 4.3).

Correlation of the Sm/Nd profiles from the White core to the Sangamon core is hindered by obvious differences in the profiles from core to core (Fig. 4.6). The Sm/Nd profiles through the upper Platteville Group in the Illinois cores vary independently of each other and display no points of correlation. In fact the only point of clear correlation between the Sm/Nd profiles of the White and Sangamon cores is the S4 excursion, across the DS2 surface (Fig. 4.6). However, in the Galena Group, the S5, S6 and S7 excursions are tentatively correlated between the White and Sangamon cores (Fig. 4.6). Although the magnitudes of the S5, S6 and S7 excursions are always greater in the White profile than in the Sangamon profile, the relative magnitudes of the events are consistent within each core, with S5 being the largest excursion and S6 being the smallest excursion.

4.4.3 The $\delta^{13}C$ profiles from the White and Sangamon cores

The $\delta^{13}C$ profile through the upper Platteville Group of the White County core is marked by a 1.3‰ positive excursion at the base, labeled B1, followed by a series of small

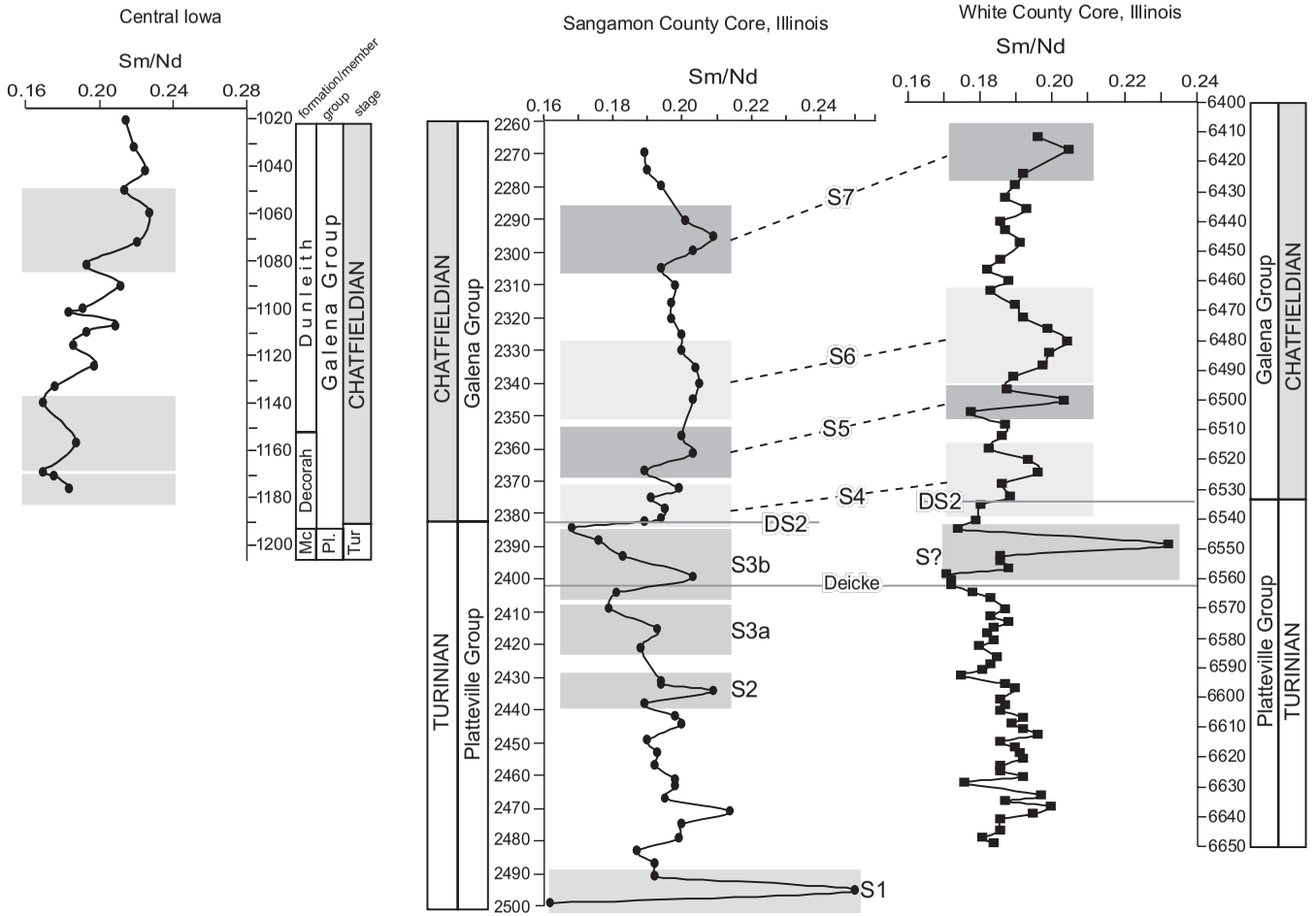

Figure 4.6 Comparison of Sm/Nd profiles between Illinois sections and between Illinois and Iowa. Shaded regions mark excursions and dashed lines connect correlative excursions. Shaded Chatfieldian stages emphasize the inability to correlate Sm/Nd excursions from the Galena Group of Iowa to the Galena Group of Illinois. Abbreviations are the same as in Figure 4.5. Stratigraphic sections are measured in feet.

variations in values that culminate in a 1.4‰ positive excursion, labeled B2, that begins at the Deicke K-bentonite and peaks below the DS2 surface (Fig. 4.4, Table 4.2). In the Sangamon County core the $\delta^{13}C$ profile, which includes only the very top of the upper Platteville Group, has a similar positive 1‰ excursion, labeled B2, that begins at the Deicke K-bentonite, peaks below the DS2 surface and in this case is followed by an abrupt drop in $\delta^{13}C$ values immediately below the DS2 surface. Unlike the White core, this 1‰ excursion is followed immediately by an additional 1‰ positive excursion, B4, right at the DS2 surface (Fig. 4.3).

Ludvigson et al. (2004) identified four $\delta^{13}C$ excursions in the upper Platteville Group of Iowa and Illinois, which they labeled the Spechts Ferry, Quimby's Mill, Grand Detour and Mifflin excursions. It is unknown how these excursions relate to the B1 and B2 excursions in these cores. However, the Spechts Ferry excursion of Ludvigson et al. (2004) begins just at the Deicke K-bentonite, suggesting it may be correlative to the B2 excursion of this study.

The $\delta^{13}C$ profiles of the White and Sangamon county cores both display an overall 2‰ decline in values through the Galena Group, values in the White core are offset by +1‰ relative to the Sangamon core (Fig. 4.3, Fig. 4.4). Comparison of both cores through the upper Platteville Group reveals an overall trend of higher $\delta^{13}C$ values corresponding to lower ε_{Nd} values. This is most striking just below the DS2 surface where minimum ε_{Nd} values correlate with peak $\delta^{13}C$ excursion values of event B2.

Despite the incomplete Sangamon $\delta^{13}C$ profile in the upper Platteville Group it is still possible to tentatively correlate the B2 excursion from the Sangamon core to the White core (Fig. 4.7). Peak B2 $\delta^{13}C$ values in both profiles occur below the DS2 surface and

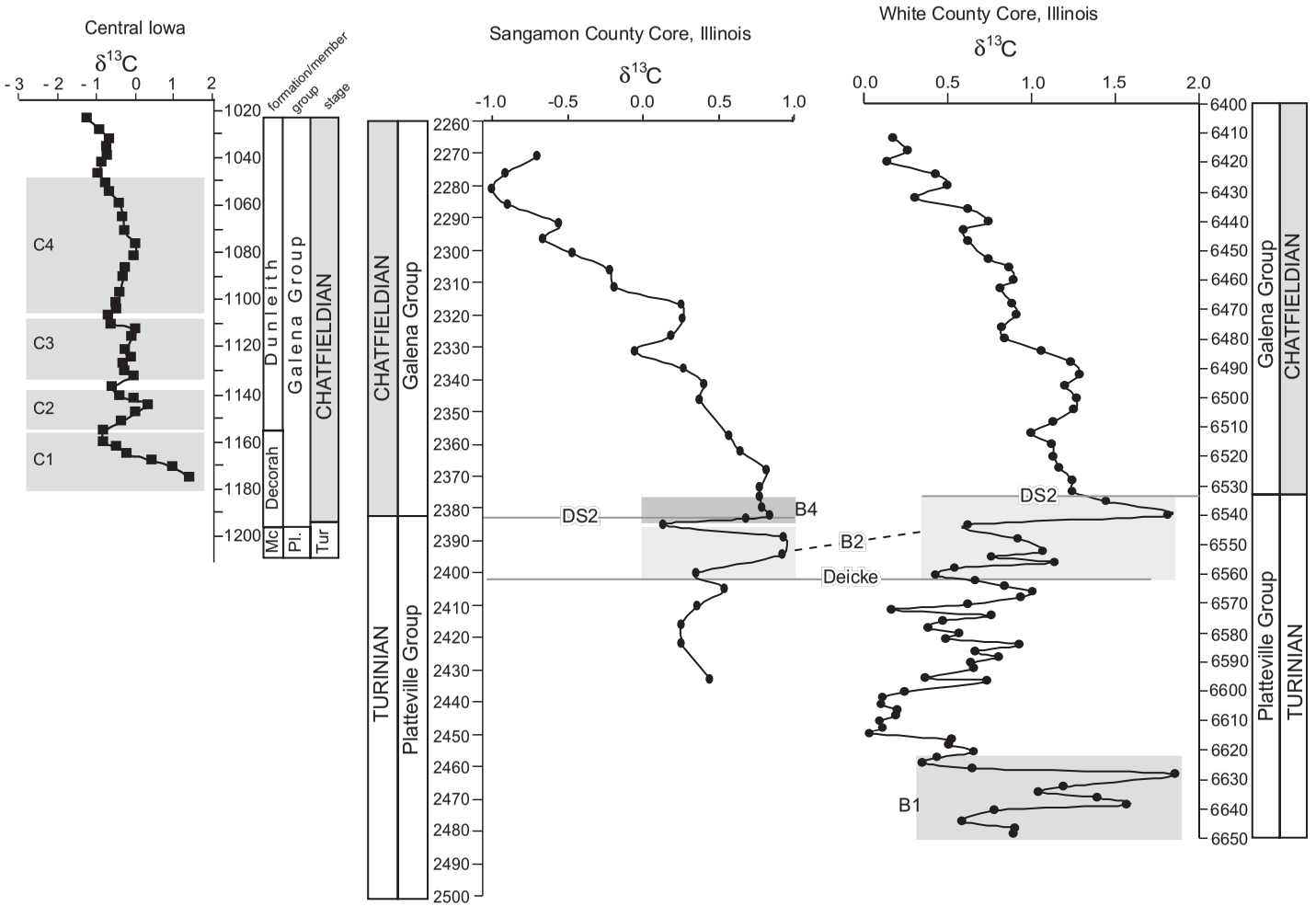

Figure 4.7 Comparison of $\delta^{13}C$ profiles between theIllinois sections and between Illinois and Iowa. Shaded regions indicate excursions and the dashed lines delineate correlative excursions. The shaded Chatfieldian stages highlight the difference in the $\delta^{13}C$ profiles of the Galena Group of Iowa to Illinois. Abbreviations are the same as in figure 4.5.

correlate with the minimum ε_{Nd} values below the DS2 surface. This suggests that the peak B2 values in the White core are not correlative to the B4 excursion, which occurs across the DS2 surface and is coincident with the peak values of the E4 excursion. The B2 $\delta^{13}C$ excursions from both cores also demonstrate an initial shift towards positive $\delta^{13}C$ values at the Deicke K-bentonite (Fig. 4.7). In the Sangamon core $\delta^{13}C$ values of the B2 excursion rise abruptly from the Deicke K-bentonite, culminating in peak values just above the bentonite. In contrast, the majority of the positive shift for the B2 excursion in the White core occurs well above the Deicke K-bentonite. The smaller stratigraphic interval between the Deicke K-bentonite and the DS2 surface in the Sangamon core suggests that this more abrupt positive excursion may be a factor of a more condensed section, or a section with a greater portion of missing strata in the Sangamon core. Further correlation of the two cores using the $\delta^{13}C$ profiles is hampered by the lack of other prominent $\delta^{13}C$ excursions (Fig. 4.7).

4.4.4 The Nd concentration versus stratigraphic depth for the White and Sangamon cores

Plots of Nd concentration against stratigraphic section reveal a marked change in concentration at or near the Platteville-Galena boundary. The average Nd concentration of the Platteville Group in both sections is 0.7 ppm, and variations in concentrations are less than 1 ppm (Fig. 4.8, Table 4.1, Table 4.2). The average Nd concentration in the Galena Group is 1.5 ppm for the Sangamon core (Fig. 4.8, Table 4.1) and 2.8 ppm for the White core (Fig. 4.8, Table 4.2). Variations in concentrations are much greater and more pronounced in the Galena Group than through the Platteville Group (Fig. 4.8).

Although these profiles are not used for correlating strata this change in concentration

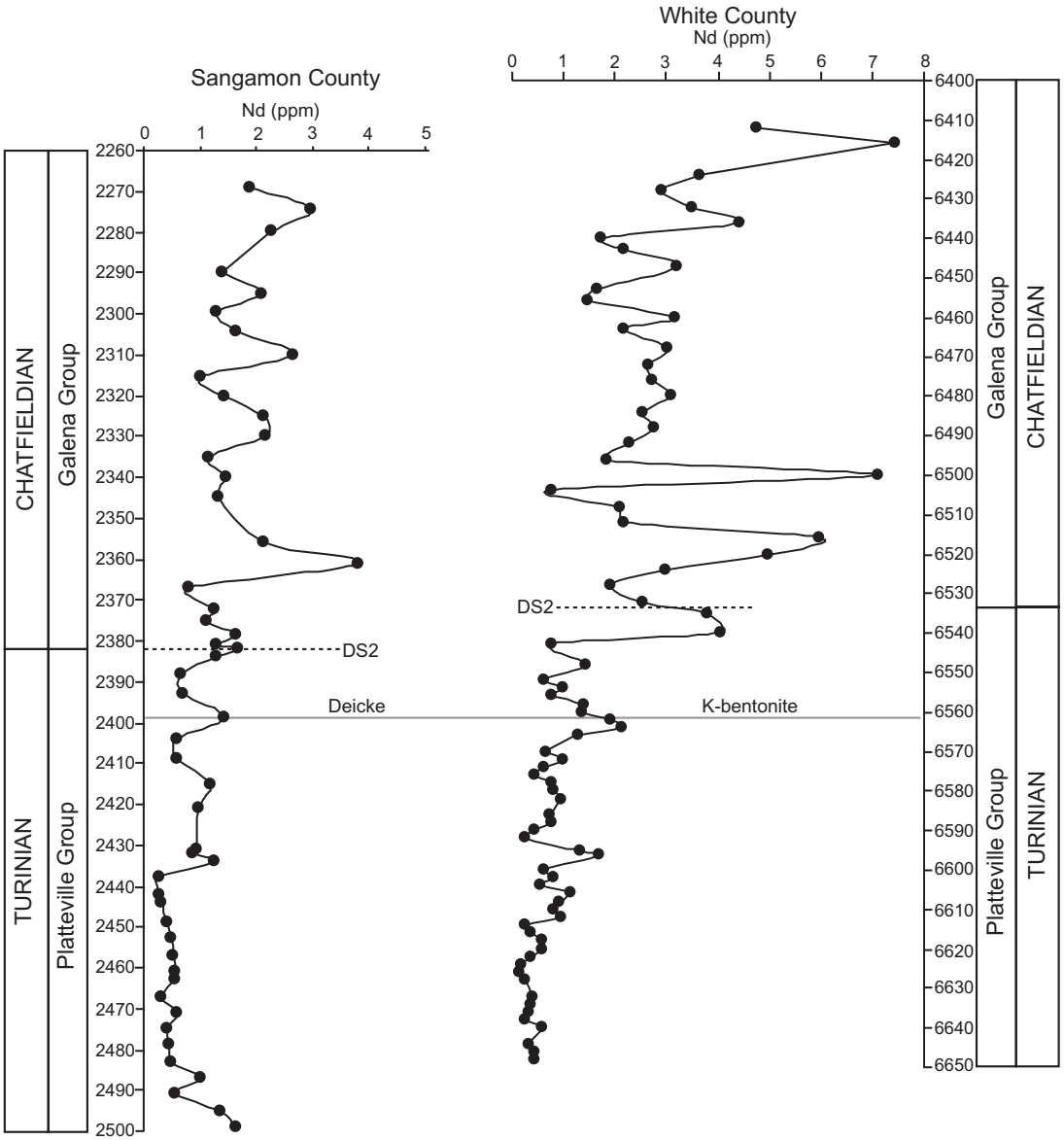

Figure 4.8 Nd concentration, in ppm, of the acid soluble fraction of the Illinois carbonates plotted against stratigraphic section, in feet. Note the greater average Nd concentration in the Galena Group compared to the Platteville Group. Greater variations in Nd concentration also occur in the Galena Group compared to the Platteville Group.

may record a change in depositional environment. No correlation is apparent between the Nd concentration of the AS fraction and the insoluble residue of the carbonates (Fig. 4.9). Therefore, variations in the Nd concentration of the AS fraction should not be a result of leaching Nd or Sm from the lattice of clay minerals or from dissolution of Fe-Mn coatings on detrital grains. Instead, the Nd concentration of the AS fraction should reflect variations in the concentration of Nd found in the carbonate lattice, in phosphate grains and in the Fe-Mn coatings on carbonate grains. These sources of Nd are all phases that incorporate Nd from seawater. It is possible then that changes in depositional environment may effect the amount of Nd these phases can acquire from seawater. Alternatively, changes in Nd concentration could reflect changes in the amount of one particular phase that provides Nd in the AS fraction. For example, stratigraphic variations in Nd concentrations could reflect changes in the amount of detrital phosphate present in each sample. The occurrence of phosphate in the samples may in turn be linked to changes in the depositional environment.

4.5 The influence of sea level and depositional environment on the ε_{Nd}, $\delta^{13}C$ and Sm/Nd profiles of Illinois

4.5.1 The ε_{Nd} profiles

Variations in the ε_{Nd} profiles of Iowa and Saskatchewan carbonates were attributed to sea level driven changes in the weathering flux of dissolved Nd to the Midcontinent epeiric sea from the Precambrian basement (ε_{Nd} = -22 to -15) and Taconic Highlands (ε_{Nd} = -6 to -9) (Fig 4.2). Sea level rise, submergence of the Precambrian Arch and Shield and influx of Taconic derived Nd drove positive shifts in the Nd isotope balance of Midcontinent seawater, while sea level fall and emergence of the Precambrian basement led to negative

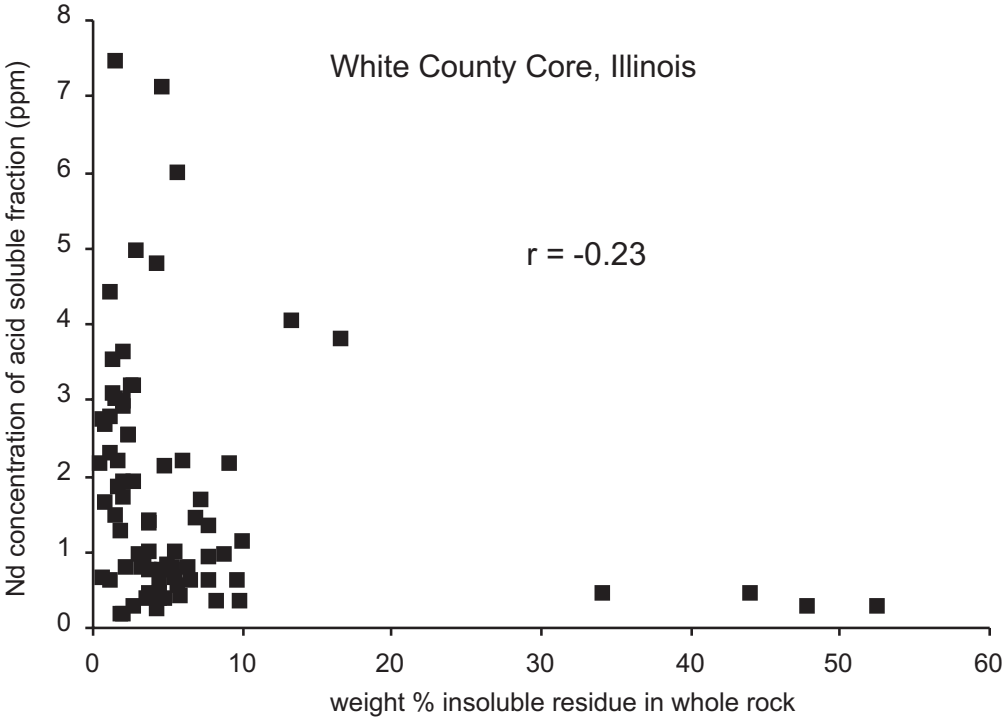

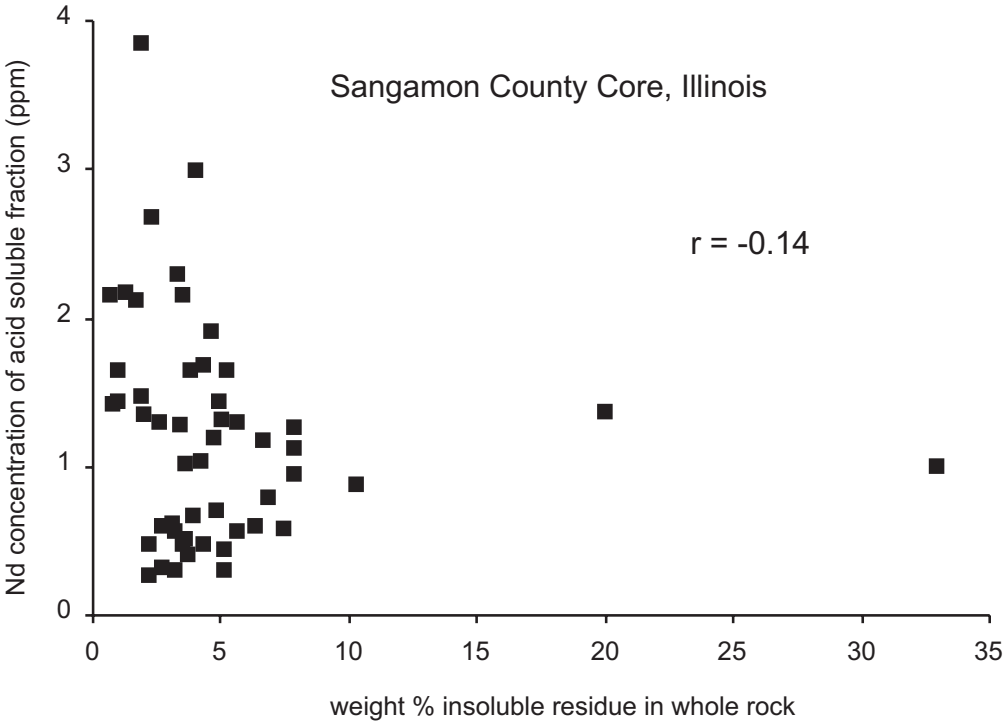

Figure 4.9 Plots of the weight percent insoluble residue against Nd concentration for the White and Sangamon County cores, Illinois. The lack of correlation between the weight percent insoluble residue and Nd concentration, shown by the low correlation coefficients, r, suggests that Nd in the samples is not primarily derived from Fe-Mn coatings on detrital grains.

shifts in the Nd isotope balance of Midcontinent seawater. The weathering flux of dissolved Nd from the Precambrian basement to Midcontinent seawater can be clearly seen in the -12 to -17 ε_{Nd} values of the White and Sangamon profiles (Fig. 4.3, Fig. 4.4). Likewise, it could be assumed that the -6 to -9 ε_{Nd} values in the Illinois profiles reflect a Taconic source of dissolved Nd to the epeiric sea. However, the striking positive shift in the ε_{Nd} values across the DS2 surface (E4), a boundary that records sea level rise, the expansion of cool Iapetus-derived waters onto the craton and the transition from tropical to temperate type facies, introduces Iapetus ocean water as a third possible source of dissolved Nd to the Midcontinent epeiric sea. Holmden et al. (1998) and Hooker et al. (1981), using conodonts in slope-rise deposits, and metalliferous crusts from pillow basalts, all from Scotland, estimate that Ordovician Iapetus ocean water had an ε_{Nd} signature of -0.6 to -5, probably as a result of dissolved Nd weathered from the Taconic Orogen and additional inputs from volcanic arcs. Therefore, the connection between the abrupt positive shift in the ε_{Nd} profiles and the DS2 surface suggests that sea level rise and the expansion of cool Iapetus-derived waters onto the craton through the Sebree Trough, coupled with partial submergence of the Precambrian basement, are responsible for the positive ε_{Nd} shifts recorded in the Illinois carbonates (Fig. 4.10). It follows that a decline in ε_{Nd} values would record sea level fall, exposure of the Precambrian basement and withdrawal of cool Iapetus waters from the craton (Fig. 4.10).

The multiple ε_{Nd} excursions in the upper Platteville Group of both the White and Sangamon cores (Fig. 4.3, Fig. 4.4) suggests that the expansion of cool Iapetus derived-waters onto the craton was not a singular event. Rather, the multiple ε_{Nd} excursions in the Platteville Group point to a series of temporary incursions of cool water onto the craton

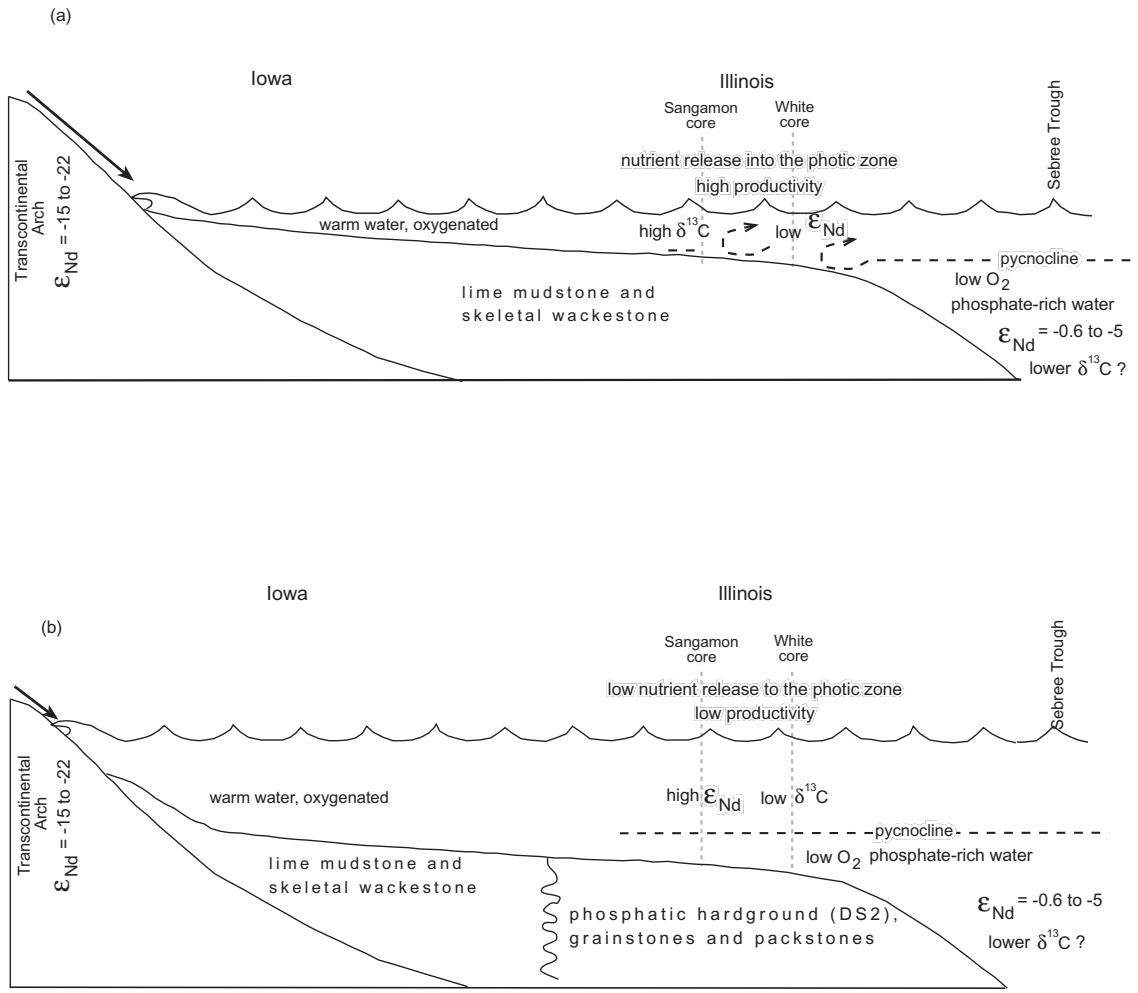

Figure 4.10 Schematic cross section from Iowa to Illinois. (a) Illustrates low sea level with low ε_{Nd} values in the Illinois area and high $\delta^{13}C$ values as stratification is disrupted and nutrients are supplied to the photic zone. (b) Shows sea level rise and an increase in ε_{Nd} values in Illinois seawater because of the influx of cool waters onto the craton with a more positive ε_{Nd} signature. A decrease in $\delta^{13}C$ values occurs at the same time because productivity declines as nutrients are trapped in bottom waters under a stratified water column. Note ε_{Nd} values of the Transcontinental Arch range from -15 to -22 and Iapetus waters have an ε_{Nd} signature of -0.6 to -5.

that predated the final E4 shift in ε_{Nd} at the Platteville-Galena boundary. The DS1 hardground surface in the upper Platteville Group (Fig. 4.1), although not present in the White and Sangamon cores, verifies that at least one cool water incursion episode occurred before the DS2 surface at the Platteville-Galena boundary (Kolata et al., 2001). Correlation of the E2, E3a and E3b ε_{Nd} excursions suggests that there were at least three incursions of cool water during deposition of the upper Platteville Group (Fig. 4.5).

Differences in the shape and magnitude of the E3a and E3b excursions between the White and Sangamon cores may be explained through a source of dissolved Nd being channeled onto the craton from the Iapetus ocean through the Sebree Trough. The positive limb of the E3a event in both sections reflects sea level rise and the influx of cool waters onto the craton at least as far as the Sangamon area (Fig. 4.10). During the proceeding sea level fall withdrawal of cool Iapetus waters from the craton may have driven the Nd isotope balance in the Sangamon area back to initial pre-excursion values. In the White area, closer to the trough, the cool waters may have maintained enough of a presence on the craton to prevent the Nd isotope balance from returning entirely to pre-excursion values. The ensuing sea level rise, recorded by the positive limb of the E3b event, drives another positive adjustment in the Nd isotope balance, one that is recorded as a smaller change in magnitude in the White area compared to the Sangamon area. Unexpectedly, the negative limb of the E3b excursion in the White core closer to the Trough, displays a much greater drop in ε_{Nd} values than does the correlative event in the Sangamon core (Fig. 4.5). Perhaps this is a sampling problem and the point of maximum sea level fall and the lowest ε_{Nd} value was not sampled in the Sangamon core, or perhaps the point of lowest sea level is not recorded in Sangamon strata. Alternatively, the difference may reflect exposure of older basement

rocks closer to the White core during this episode of sea level fall. One possible source for this Precambrian derived Nd may have been the Ozark Dome, a structural high of Precambrian basement that may or may not have been covered with sediment (Fig. 4.2) (Leslie and Bergström, 1997; Kolata et al., 1998; Kolata et al., 2001).

The grainstone, temperate type facies of the Galena Group indicates that the DS2 surface heralded a prolonged sustainable expansion of cool water, temperate type conditions across much of the Midcontinent epeiric sea (Holland and Patzkowsky, 1996; Kolata et al., 1998; Kolata et al., 2001). The almost unvaryingly high ε_{Nd} values of the Galena Group would attest to the dominance of the Nd isotope balance by dissolved Nd from the Iapetus ocean and probably the Taconic Highlands. The greater average ε_{Nd} value of the Galena Group of the White core compared to the Sangamon core (Fig. 4.5) is consistent with the White core being closer to the Sebree Trough, the source of a more positive ε_{Nd} signature (Fig. 4.10).

4.5.2 $\delta^{13}C$ profiles

The $\delta^{13}C$ profiles in the Illinois cores record changes, based on the Iowa example, in local, rather than global, C-cycling in the epeiric sea. The positive $\delta^{13}C$ excursions in the Galena Group of Iowa are each attributed to sea level rise and an increase in organic carbon burial. Sea level rise may have caused an expansion of cool, oxygen poor, phosphate rich waters into the Iowa area. A combination of nutrient rich waters upwelling along the Transcontinental Arch and lowered oxygen content in bottom waters would promote increased organic productivity and increased organic carbon burial in the Iowa area.

Sea level rise and the expansion of cool, phosphate rich, oxygen poor bottom waters

onto the craton during upper Platteville deposition in Illinois could also be expected to drive positive $\delta^{13}C$ excursions. However, using the ε_{Nd} profiles as chemostratigraphic sea level curves, positive excursions and trends in the $\delta^{13}C$ profiles consistently correspond to lower ε_{Nd} values, indicating lower sea level. The most striking example is the correlation of peak $\delta^{13}C$ excursion values of the B2 event, below the DS2 surface, with minimum ε_{Nd} values of the E4 event (Fig. 4.3, Fig. 4.4). The peak $\delta^{13}C$ excursion values of the B2 event also occur stratigraphically below the sea level rise indicated by the DS2 surface, in an interval interpreted by Witzke and Kolata (1996) to represent low sea level (Fig. 4.3, Fig. 4.4).

Sea level rise and expansion of cool waters onto the craton in the Illinois area established quasi-estuarine circulation and a stratified water column with saline, cool bottom waters, and low salinity, warm, oxygenated surface waters (Witzke, 1987b; Ludvigson et al., 1996). Unlike the Iowa area, stratification in the Illinois area, closer to the trough, would have been far from upwelling currents along the Transcontinental Arch. Without nearby upwelling currents, stratification may have trapped nutrients in bottom waters, limiting organic productivity and therefore burial of organic carbon. The reduction in nutrient supply, and a decline in organic productivity with increasing sea level and increasing stratification has also been observed by Brasier et al., (1992) and Glumac and Walker (1998). During sea level fall and withdrawal of cool waters, recorded by a drop in ε_{Nd} values, temperature and salinity differences between surface and bottom layers would diminish, ending stratification. A breakdown in salinity stratification could release nutrients to the overlying water column, increasing productivity and thereby organic carbon burial, driving positive $\delta^{13}C$ excursions (Fig. 4.10). Eventually the supply of nutrients initially

trapped in eutrophic bottom waters will be depleted, productivity will decline and sea level rise and expansion of cool waters onto the craton will re-establish stratification, resulting in lowered $\delta^{13}C$ values. The decline in $\delta^{13}C$ values throughout the Galena Group would correspond with an overall steady decline in productivity and organic carbon burial as quasi-estuarine circulation and the ensuing influx of deep cool, oxygen poor, phosphate rich bottom waters and salinity stratification became well established on the craton in the Illinois area (Fig. 4.10).

An additional factor to consider in the Illinois area, close to the Sebree Trough, is the impact of Iapetus waters on local C-cycling through simple mixing. The $\delta^{13}C$ values of intermediate to deep waters in the oceans are often believed to be 1‰ to 2‰ lower than $\delta^{13}C$ values of the surface ocean because of organic matter oxidation as particles settle through the water column (Perfetta et al., 1999; Kroopnick, 1985). By analogy, deeper Iapetus waters may have been depleted in ^{13}C relative to the shallower epeiric sea. Therefore, sea level rise and the addition of cool Iapetus-derived waters from the oxygen minimum zone may have lowered the $\delta^{13}C$ value of epeiric seawater in the Illinois area, close to the Sebree Trough. Sea level fall and a withdrawal of cool bottom waters would allow C-cycling in the epeiric sea to return to pre-mixing conditions, re-establishing higher $\delta^{13}C$ values. The steady decline in $\delta^{13}C$ values through the Galena Group may record the steadily increasing influence of cool Iapetus waters, with a low $\delta^{13}C$ value, on C-cycling in the Illinois area. It is likely that changes in the $\delta^{13}C$ value were driven by a combination of both sea level induced changes in C-cycling on the craton and from simple mixing of Iapetus and epeiric seawater.

The B4 positive $\delta^{13}C$ excursion, across the DS2 surface in the Sangamon core, and

the B1 positive $\delta^{13}C$ excursion at the base of the White core do not correspond with any sea level fall recorded by the ε_{Nd} profiles (Fig. 4.3, Fig. 4.4). In fact, the B4 excursion corresponds with sea level rise indicated by the DS2 surface and the ε_{Nd} profile and may reflect the temporary influence of conditions observed closer to the Arch in the Galena Group of Iowa. Small changes in depositional environment may also cause very localized changes in organic carbon burial that could result in $\delta^{13}C$ excursions not recorded in other sections and possibly not related to sea level change, such as the B1 excursion.

4.5.3 Sm/Nd profiles

Interpreting the Sm/Nd profiles of Illinois is problematic, in part because a mechanism explaining REE fractionation in epeiric seas is as yet undetermined. This is not surprising given that establishing controls on REE-processing in modern aqueous environments is still ongoing (Johannesson et al., 1997; Amakawa et al., 2000; Sholkovitz and Szymczak, 2000; Hannigan and Sholkovitz, 2001; Haley et al., 2004). Nonetheless, similar trends in increasing Sm/Nd ratios and interpreted increases in water depth in Ordovician cores through epeiric sea carbonates of Iowa and Saskatchewan support Sm/Nd profiles in carbonates recording REE fractionation driven by changing water depth in epeiric seas (Fanton et al., 2002). Positive Sm/Nd excursions in the Illinois cores could then be expected to coincide with expansion of cool water across the craton because these events coincide with sea level rise and, it is assumed, a deepening of the water column. This interpretation of the Sm/Nd profiles is consistent with the S1 through S4 positive Sm/Nd excursions in the Sangamon core (Fig. 4.3), which correspond with sea level rise suggested by the positive ε_{Nd} excursions E1, E2, E3a and E3b and E4. Of course, Sm/Nd

excursions in the Galena Group, such as S5 through S7 (Fig. 4.3), would continue to reflect changes in water depth even after expansion of cool waters across the craton resulted in an unchanging ε_{Nd} profile (Fig. 4.3, Fig. 4.4). The larger scale trends of the Sm/Nd profiles in both the White and Sangamon cores also mirror changes in water depth, as predicted by Witzke and Kolata (1989) and Witzke and Bunker (1996) (Fig. 4.3, Fig. 4.4). An overall decline in Sm/Nd ratios is consistent with the overall drop in water depth predicted for the upper Platteville Group, while the overall increase in Sm/Nd ratios into the Galena Group is consistent with the overall sea level rise and the flooding of the craton with cool waters from the Sebree Trough (Fig. 4.3, Fig. 4.4).

A difference between Sm/Nd excursions and water depth occurs in the upper Platteville Group of the White core where the ε_{Nd} profile and the Sm/Nd profiles are not correlative (Fig. 4.4). Despite the three ε_{Nd} excursions (E2, E3a and E3b) in this interval, there is only one positive Sm/Nd excursion, labeled (S?), which peaks above the ε_{Nd} excursion labeled 3b. One possible explanation for this discrepancy is that not all incidences of sea level rise and incursions of cool waters onto the craton result in a change in water depth. Subsidence rates and depositional rates in the White area, close to the Sebree Trough, may have kept up with sea level change, until the largest episode of sea level rise and expansion of cool waters at the DS2 surface. As well, not all changes in water depth must result from sea level rise and the incursion of cool waters onto the craton. Instead, changing subsidence rates or carbonate production rates may be responsible for the large positive Sm/Nd excursion (S?) in the upper Platteville Group of the White section.

An additional consideration when interpreting the Sm/Nd profiles in Illinois carbonates is that the REE-profile of Iapetus waters brought onto the craton through the

Sebree Trough may be a result of REE fractionation in the ocean and therefore may be distinct from, and independent of, REE-processing in the epeiric sea. For example, the HREE enrichment evident between the modern deep ocean and rivers and estuaries (Elderfield et al., 1990) could imply that Iapetus ocean water was HREE enriched relative to the epeiric sea. Therefore, we could expect that Sm/Nd ratios of Iapetus water would be greater than those in the epeiric sea because Sm is a heavier REE than Nd. Expansion of cool waters could then impart a higher Sm/Nd ratio to epeiric seawater in the Illinois area through simple mixing, it also could introduce a plethora of other, as yet, undefined parameters that could impact REE fractionation on the craton. Ultimately, Sm/Nd excursions in the Illinois cores could result from the interplay between REE fractionation in the epeiric sea and the REE concentrations introduced by the expansion of cool waters onto the craton, rather than from changes in water depth. For example, it is possible that the differences in the Sm/Nd profiles between the White and Sangamon cores reflects the difference in REE fractionation between a section further onto the craton dominated by epeiric sea processes and a section close to the Sebree Trough and Iapetus waters. Expansion of cool waters onto the craton, independent of changing water depth, is unlikely to be the sole mechanism driving changes in Sm/Nd ratios since the Sm/Nd profiles continue to fluctuate throughout the Galena Group, after the ε_{Nd} profiles, lithology and fauna indicate that cool waters and a temperate type environment had spread across the craton.

4.5.4 Nd concentrations versus stratigraphic depth - Illinois

It has been suggested that REE concentrations in modern marine sediments are a reflection of depositional rates (Bernat, 1975). REEs in carbonates are largely acquired by

sequestration of REEs at the sediment-water interface. Therefore slow accumulation of sediment gives particles at the sediment-seawater interface, such as phosphate and Fe-Mn hydroxides, a longer time to sequester REEs, hence slow depositional rates should result in carbonates with high REE concentrations. Fast sedimentation rates allow little time for REE-sequestration at the seawater-sediment interface and therefore fast depositional rates will result in carbonates with low REE concentrations. Lower average Nd concentrations in the upper Platteville Group of both sections compared to average Galena Group concentrations suggests that overall, Platteville Group carbonates were deposited more quickly than Galena Group carbonates in the Illinois area (Fig. 4.8). These projected depositional rates would correspond with changing structural trends between the Platteville and Galena Groups, which illustrate that in Illinois the upper Platteville Group is thicker than the Galena Group (Witzke and Kolata, 1989; Kolata et al., 1998; Kolata et al., 2001). High subsidence rates in Illinois near the failed Reelfoot Rift are responsible for thicker Platteville strata in Illinois, a condition that would not surprisingly lead to higher net sedimentation rates. In contrast, thinner Galena Group strata in Illinois may reflect declining subsidence rates and the high abundance of phosphatic hardground surfaces found in the Galena Group throughout the Midcontinent indicate interrupted periods of carbonate deposition (Kolata et al., 1998; Kolata et al., 2001). Therefore it is likely that Galena strata in the Illinois area do represent a period of slower sedimentation. Large positive fluctuations in the Nd concentrations of Galena Group strata may reflect periods of very slow carbonate deposition, possibly in response to the influx of cool waters with high phosphate contents temporarily retarding carbonate deposition.

4.6 Correlation of Midcontinent Ordovician strata using ε_{Nd}, $\delta^{13}C$ and Sm/Nd chemostratigraphy

4.6.1 ε_{Nd} profiles Illinois to Iowa

Comparison of the ε_{Nd} profiles between the White and Sangamon cores emphasizes that changes in the depositional environment, such as proximity to the Sebree Trough or the Precambrian basement, causes differences in the shape and magnitude of the ε_{Nd} excursions, even over the 220 km that separate these cores. At the same time the presence of the Deicke K-bentonite and the DS2 surface, which act as marker horizons between the cores, establish that these differences do not diminish the ability to recognize and correlate events between these sections (Fig. 4.5). However, it should be noted that unlike the isochronous K-bentonite the DS2 surface reflects a sea level event and period of non-deposition that may be diachronous from the Sangamon County core to the White County core (Kolata et al., 2001).

Correlation of coeval ε_{Nd} excursions cannot be made between the Iowa and Illinois ε_{Nd} profiles (Fig. 4.5). The Iowa and both Illinois profiles consist of multiple positive ε_{Nd} excursions that reflect sea level rise, submergence of the Arch and Shield and an influx of dissolved Nd from Taconic or Iapetus sources, followed by sea level fall, re-emergence of the Arch and Shield and withdrawal of dissolved Nd from Taconic or Iapetus sources. Both Iowa and Illinois profiles also exhibit a final positive shift in ε_{Nd} that is followed by unvarying positive ε_{Nd} values (Fig. 2.2, Fig. 4.5). In Illinois this occurs at the base of the Galena Group, while in Iowa this event does not occur until the top of the Galena Group. Therefore, the major difference between the Illinois and Iowa profiles is in the timing of these events. During Galena deposition, at the beginning of the Chatfieldian, the Illinois area was already

flooded with cool waters from the Sebree Trough, and Galena Group strata records an almost unvarying ε_{Nd} profile (Fig. 4.5). Further fluctuations in sea level, submergence of the Arch and Shield and encroachment of cool waters or Taconic sources during Galena deposition were then only recorded by the positive ε_{Nd} excursions of the Iowa profile (Fig. 2.2, Fig. 4.5). Further sampling of the upper Platteville Group of Iowa will reveal if the positive ε_{Nd} excursions in the upper Platteville Group of Illinois may be correlated to similar excursions in Iowa.

4.6.2 $\delta^{13}C$ profiles, Illinois to Iowa

Comparison of the $\delta^{13}C$ profiles between the White and Sangamon cores and the Iowa core highlights the importance of understanding local controls on C-cycling before trying to correlate the $\delta^{13}C$ profiles over any substantial distance (Fig. 4.7). Between the White and Sangamon cores sea level fluctuations drive similar changes in local C-cycling. As a result, the profiles exhibit a similar shape and it is possible to correlate the B2 positive $\delta^{13}C$ excursions (Fig. 4.7). Further correlation of the two sections using the $\delta^{13}C$ profiles is hampered by the lack of other prominent $\delta^{13}C$ excursions. Both sections demonstrate a 2‰ decline through the Galena Group but the other minor variations within this decline do not offer the option of a more refined correlation. Even though they cannot be used to correlate the sampled Illinois cores, the B1 excursion in the White section and the B4 excursion in the Sangamon core may prove useful in correlating other $\delta^{13}C$ profiles across Illinois.

Sea level fluctuations appear to drive different changes in local C-cycling between the Illinois and Iowa cores because of differences in local depositional environments. Sea level fall in the Illinois area results in a ^{13}C enrichment of the water column, while in the

Iowa area the depositional environment dictates that the same sea level fall may result in a ^{13}C depletion in the water column. Consequently, positive $\delta^{13}C$ excursions in the Illinois profiles may be found to correlate with a negative $\delta^{13}C$ excursion in the Iowa area. When local controls on C-cycling are not taken into consideration, one positive $\delta^{13}C$ excursion could be mistakenly correlated with another positive $\delta^{13}C$ excursion rather than a coeval negative $\delta^{13}C$ excursion. The differences in local C-cycling are also plainly apparent in the steady 2‰ decline in $\delta^{13}C$ values through the Galena Group of Illinois in comparison to the multiple positive $\delta^{13}C$ excursions observed in the Galena Group of Iowa. These differences in the $\delta^{13}C$ profiles of the Galena Group make it very difficult to correlate the Illinois and Iowa sections (Fig. 4.7). The differences in C-cycling and the resulting differences in the $\delta^{13}C$ profiles from Illinois to Iowa are a prime example of how caution should be exercised when correlating $\delta^{13}C$ profiles. If changes can be observed over such a relatively short distance in one epeiric sea, then trying to correlate $\delta^{13}C$ profiles between different cratons without understanding possible local controls on C-cycling could prove even more difficult.

4.6.3 Sm/Nd profiles, Illinois to Iowa

In the upper Platteville Group the presence of only one clear point of correlation between the Sm/Nd profiles of the White and Sangamon cores illustrates the complexity of determining REE-processing in epeiric seas. In the Galena Group, tentative correlations of Sm/Nd excursions, S5, S6 and S7, between the White and Sangamon cores offer the only chemostratigraphic method of correlating Galena Group strata between the two sections.

Comparison of the Illinois and Iowa cores reveals no obvious points of correlation.

It is possible that events S5, S6 and S7 may be correlative to any of the Sm/Nd excursions found in the Dunleith Formation of the Iowa section. Uncertainty regarding mechanisms that control REE fractionation in the water column, as recorded by the Sm/Nd ratios in carbonates, renders it difficult to use Sm/Nd ratios for regional correlation across the Midcontinent. If changing water depth is driving variations in Sm/Nd ratios, then Sm/Nd profiles may prove to be ineffective tools for correlation of coeval events. Comparison of the White and Sangamon cores already suggests correlation may be limited. Variations in water depth are often locally influenced by rates of subsidence and rates of deposition, and are not entirely a function of regional eustatic sea level change. Moreover, it is possible that water depth changes are not the primary mechanism driving changes in REE-cycling, which limits the use of Sm/Nd profiles for correlation.

4.7 Implications and Conclusions

Interpretation of the ε_{Nd}, $\delta^{13}C$ and Sm/Nd profiles through the Ordovician Illinois carbonates emphasizes that sea level fluctuations continue to play a dominant role in driving local changes in the Nd isotope balance, C-cycling and, to a lesser extent, REE-cycling of Midcontinent epeiric seawater. Positive excursions in the ε_{Nd} and Sm/Nd profiles can be related to sea level rise and the influx of cool, oxygen poor, phosphate rich bottom waters onto the craton through the Sebree Trough. This influx of cool waters, derived from the oxygen minimum zone of the Iapetus ocean, imparts a more positive ε_{Nd} signature and may impart a more positive Sm/Nd ratio to Midcontinent Ordovician seawater. As well, stratification of the water column in the Illinois area as a result of sea level rise and the influx of cool bottom waters is related to a decrease in $\delta^{13}C$ values of the Illinois profiles.

Stratification of the water column in the Illinois area, far from upwelling nutrient rich waters along the Transcontinental Arch, is thought to trap nutrients in bottom waters causing a decline in organic matter productivity and therefore a decline in organic carbon burial.

The relationship between changes in the ε_{Nd}, $\delta^{13}C$ and Sm/Nd profiles and sea level fluctuations indicates that these profiles may be used to correlate Ordovician Midcontinent strata between the White and Sangamon county cores in Illinois and possibly to Ordovician strata from Iowa. Comparison of the ε_{Nd}, $\delta^{13}C$ and Sm/Nd profiles from the White County core to the Sangamon County core reveals that chemostratigraphic correlation of strata over distances of less than 220 km is possible. However, even over this relatively short distance the shape and magnitude of excursions may be modified by the proximity of the strata to the Sebree Trough and the source of cool Iapetus derived waters. In the $\delta^{13}C$ and Sm/Nd profiles several excursions can be identified in only one Illinois core, possibly because of variations in local C-cycling or REE composition that result from differences in depositional environment from central to southern Illinois.

Comparison of the ε_{Nd}, $\delta^{13}C$ and Sm/Nd profiles between the Illinois cores and the Iowa core reveals that it may not be viable to use chemostratigraphy for regional correlations of Midcontinent Ordovician strata over larger distances. The ε_{Nd} and $\delta^{13}C$ values and Sm/Nd ratios of Midcontinent epeiric seawater appear to be strongly influenced by the local depositional environment, especially distance from major geographic features such as the Transcontinental Arch and Sebree Trough. By the early Chatfieldian sea level rise had established a stratified water column with cool, oxygen poor, phosphate rich bottom waters that were drawn onto the craton through the Sebree Trough. As a result, the chemostratigraphic profiles through the Galena Group of the Illinois cores record primarily

unvarying ε_{Nd} values, steadily declining $\delta^{13}C$ values and only small fluctuations in Sm/Nd ratios. In contrast, the chemostratigraphic profiles through the Galena Group of the Iowa core, further from the Sebree Trough, are highly variable recording multiple excursions that correspond to continued sea level rise, the temporary influx of cool waters and submergence of the Transcontinental Arch. Construction of ε_{Nd}, $\delta^{13}C$ and Sm/Nd profiles through the upper Platteville Group of Iowa will demonstrate whether the temporary incursions of cool waters onto the craton recorded in the chemostratigraphic profiles of the upper Platteville Group of Illinois can also be identified and correlated in the Iowa area further from the Sebree Trough.

Chemostratigraphic correlation of Ordovician Midcontinent strata using ε_{Nd}, $\delta^{13}C$ and Sm/Nd profiles demonstrates that these profiles may be best employed for correlation over smaller areas. Changes in facies between stratigraphic sections may indicate that correlation with these profiles may be difficult as local depositional conditions may influence the ε_{Nd} and $\delta^{13}C$ values and Sm/Nd ratios of epeiric seawater. This finding is most important when using $\delta^{13}C$ profiles from epeiric sea strata, which have been widely used to correlate across cratons, between cratons, and to make assumptions about the C-cycle of the global oceans (Joachimski and Buggisch, 1993; Ripperdan et al., 1992; Salztman et al., 1995; Patzkowsky et al., 1997; Saltzman et al., 1998; Saltzman, 2003). This study dictates that such widespread correlation and interpretation of epeiric sea strata using ε_{Nd}, $\delta^{13}C$ and Sm/Nd chemostratigraphy should be made only after evaluating the influence that the local depositional environment had on the shape, magnitude and timing of any excursion.

CHAPTER 5. SUMMARY

The ocean centered view of ε_{Nd} and $\delta^{13}C$ profiles in epeiric sea strata dictates that these profiles can be used as proxies for recording changes in the Nd isotope balance and C-cycling of adjacent oceans. A growing number of studies utilizing modern seawater sediments and ancient epeiric sea strata have alternatively suggested that ε_{Nd} and $\delta^{13}C$ values preserved in epeiric sea strata record only the ε_{Nd} and $\delta^{13}C$ composition of the epeiric sea and may or may not reflect the oceanic composition. This shift to a local, epeiric sea centered view of ε_{Nd} and $\delta^{13}C$ values in epeiric sea strata requires a new view and interpretation of ε_{Nd} and $\delta^{13}C$ profiles constructed from epeiric sea sequences.

Ordovician carbonates from the Midcontinent of North America were selected as a case study to determine what drives local changes in the Nd isotope balance and C-cycling within an epeiric sea. First, it was verified that changes in the ε_{Nd} and $\delta^{13}C$ composition of the limestones, dolomitic limestones and calcareous dolomites of each sample location preserved changes in the Nd and C isotope composition of the ancient overlying epeiric seawater. The ε_{Nd} profiles from the Ordovician carbonates of Iowa and Saskatchewan reveal that the Nd isotope balance of Midcontinent epeiric seawater was established by the relative contributions of dissolved Nd derived from the Precambrian basement and the Taconic Highlands. Additional ε_{Nd} profiles through Ordovician carbonates of Illinois suggest that Iapetus Ocean water, funneled onto the craton through the Sebree Trough, may be another source of dissolved Nd to the Midcontinent epeiric sea. Correlation between sea level

curves and the ε_{Nd} profiles of Iowa and Saskatchewan indicate that changes in the Nd isotope balance of epeiric seawater are driven by sea level fluctuations. Sea level rise and fall variously submerged and exposed the low relief Precambrian basement of the Transcontinental Arch and Canadian Shield, altering the Nd isotope balance of the adjacent epeiric sea. Therefore, the ε_{Nd} profiles from the Ordovician carbonates of Iowa and Saskatchewan prove to be an effective chemostratigraphic method for monitoring the submergence history of the Transcontinental Arch. Changes in the ε_{Nd} profiles from Illinois carbonates are also tied to changes in sea level. However, the Nd isotope balance of Midcontinent seawater in the Illinois area appears to be more strongly linked with proximity to the Sebree Trough and a source of Iapetus Ocean water, than with a source of Nd from the Arch and Shield. Therefore ε_{Nd} profiles from Illinois strata are a better indicator of environmental changes related to sea level rise and the influx of cool waters from the Sebree Trough than they are as a tool to monitor the submergence history of the Transcontinental Arch.

The study of Ordovician carbonates from Iowa and Saskatchewan also revealed smooth stratigraphic variations in Sm/Nd ratios. Comparison of Sm/Nd profiles to a known sea level curve for the Iowa and Saskatchewan sections, conodont paleoecology data, and the ε_{Nd} profiles suggests that these variations in Sm/Nd ratios are responding to changes in water depth. If Sm/Nd variations in carbonates are related to changes in water depth, then Sm/Nd profiles could become powerful tools for monitoring changes in ancient water depth, especially where other methods of determining water depth are absent or obscured by dolomitization. However, a mechanism relating water depth variations to changes in rare earth element cycling is, as yet, undetermined and much is still unknown about the behavior

of rare earth elements in epeiric seas. Additional Sm/Nd profiles from Ordovician carbonates of Illinois verify that not all fluctuations in Sm/Nd ratios can be attributed to known changes in water depth, suggesting that other factors in the depositional environment may influence rare earth element cycling in epeiric seawater.

Correlation of $\delta^{13}C$ profiles from the Iowa section with the ε_{Nd} curve, Sm/Nd profile and sea level curve indicate that changes in the C isotope composition of Midcontinent epeiric seawater are also driven by fluctuations in sea level. Sea level rise, submergence of the Transcontinental Arch and the influx of cool, phosphate rich, oxygen poor waters from the Sebree Trough increased productivity and burial of organic carbon. This resulted in a positive shift in the $\delta^{13}C$ composition of epeiric seawater. Sea level fall, exposure of the Arch, and regression of cool, phosphate rich, oxygen poor waters across the craton decreased productivity and organic carbon burial, causing a decrease in the $\delta^{13}C$ composition of epeiric seawater.

Additional $\delta^{13}C$ profiles from Ordovician carbonates of Illinois demonstrate that fluctuations in sea level appear to drive opposite changes in the $\delta^{13}C$ values of Midcontinent epeiric seawater closer to the Sebree Trough. In the Illinois area sea level rise appears to cause a *decrease* in the $\delta^{13}C$ composition of Midcontinent epeiric seawater while sea level fall drives an increase in the $\delta^{13}C$ composition of epeiric seawater. These opposite responses of the $\delta^{13}C$ composition of epeiric seawater to similar fluctuations in sea level requires that caution be used when correlating $\delta^{13}C$ profiles across a single craton and especially between separate cratons. Even similar $\delta^{13}C$ excursions that can be globally correlated should not necessarily be taken as evidence for ocean centered changes in the global C-cycle. Because changes in the $\delta^{13}C$ composition of an epeiric sea can be a result of sea level driven changes

in local C-cycling, global sea level change could produce synchronous changes in the C-isotope composition of epeiric seawater from around the world without actually producing a noticeable change in the $\delta^{13}C$ value of the intervening oceans.

The connection between sea level fluctuations and changes in the ε_{Nd}, $\delta^{13}C$ and Sm/Nd profiles indicates that these profiles may be used to correlate epeiric sea strata across the Midcontinent of North America. Correlation of Ordovician carbonates from Iowa to Saskatchewan using the ε_{Nd} and Sm/Nd profiles confirms that correlation of epeiric sea strata is one possible use for these profiles. However, comparison of the Iowa profiles to additional ε_{Nd}, $\delta^{13}C$ and Sm/Nd profiles from Ordovician carbonates of Illinois indicates that the magnitude and timing of sea level driven ε_{Nd}, $\delta^{13}C$ and Sm/Nd excursions may differ across the craton with changes in depositional environment. The differences in the ε_{Nd}, $\delta^{13}C$ and Sm/Nd profiles from Iowa to Illinois illustrate that correlation of coeval strata across the Midcontinent epeiric sea may be hampered by the fact that sea level driven excursions may be dampened, magnified or non-existent as depositional environment changes across the craton. Proximity to major geographic features such as the Transcontinental Arch, Sebree Trough and Taconic Highlands had the greatest impact on shaping the ε_{Nd}, $\delta^{13}C$ and Sm/Nd composition of neighboring epeiric seawater.

Without an understanding of how local changes may impact the Nd isotope balance and C-cycling of an epeiric sea, ε_{Nd} and $\delta^{13}C$ profiles through epeiric sea strata may, in many cases, be used incorrectly to deduce large scale ocean centered changes in paleocirculation, basin configuration, productivity, oxygen levels and the overall global C-cycle. Instead, by understanding what mechanisms drive local changes in the ε_{Nd} and $\delta^{13}C$ values and Sm/Nd ratios of an epeiric sea these profiles can be used as new tools for

investigating ancient epeiric sea environments. The ε_{Nd}, $\delta^{13}C$ and Sm/Nd profiles may prove especially useful in investigating Paleozoic strata, where the primary record of marine deposition is recorded by epeiric sea sequences.

REFERENCES

Ainsaar, L., Meidla, T., and Martma, T., 1999, Evidence for a widespread carbon isotopic event associated with late Middle Ordovician sedimentological and faunal changes in Estonia: Geological Magazine, v. 136, p. 49-62.

Amakawa, H., Alibo, D.S., and Nozaki, Y., 2000, Nd isotopic composition and REE pattern in the surface waters of the eastern Indian Ocean and its adjacent seas: Geochimica et Cosmochimica Acta, v. 64, p. 1715-1727.

Arthur, M.A., Dean, W.E., and Pratt, L.M., 1988, Geochemical and climatic effects of increased marine organic carbon burial at the Cenomanian/Turonian boundary: Nature, v. 335, p. 714-717.

Arthur, M.A., Schlanger, S.O., and Jenkyns, H.C., 1987, The Cenomanian-Turonian oceanic anoxic event, II. Palaeoceanographic controls on organic-matter production and preservation, *in* Brooks, J., and Fleet, A.J., eds., Marine Petroleum Source Rocks: Geological Society Special Publication, no. 26, p. 401-420.

Awwiller, D.N., 1994, Geochronology and mass transfer in Gulf Coast mudrocks (south-central Texas, U.S.A.): Rb-Sr, Sm-Nd and REE systematics: Chemical Geology, v. 116, p. 61-84.

Azmy, K., Veizer, J., Bassett, M.G., and Copper, P., 1998, Oxygen and carbon isotopic composition of Silurian brachiopods: Implications for coeval seawater and glaciations: Geological Society of America Bulletin, v. 110, p. 1499-1512.

Banner, J.L., Hanson, G.N., and Meyers, W.J., 1988, Rare earth element and Nd isotopic variations in regionally extensive dolomites from the Burlington-Keokuk Formation (Mississippian): Implications for REE mobility during carbonate diagenesis: Journal of Sedimentary Petrology, v. 58, p. 415-432.

Barnes, C.R., and Fåhraeus, L.E., 1975, Provinces, communities and the proposed nektobenthic habitat of Ordovician conodontophorids: Lethaia, v. 8, p. 133-149.

Baum, J.S., Baum, G.R., Thompson, P.R., and Humphrey, J.D., 1994, Stable isotopic evidence for relative and eustatic sea-level changes in Eocene to Oligocene carbonates, Baldwin County, Alabama: Geological Society of America Bulletin, v. 106, p. 824-839.

Bellanca, A., Masetti, D., and Neri, R., 1997, Rare earth elements in limestone/marlstone couplets from the Albian-Cenomanian Cismon section (Venetian region, northern Italy): Assessing REE sensitivity to environmental changes: Chemical Geology, v. 141, p. 141-152.

Bergström, S.M., and Mitchell, C.E., 1992, The Ordovician Utica Shale in the eastern Midcontinent region: Age, lithofacies and regional relationships, *in* Chaplin, J.R., and Barrick, J.E., eds., Special Papers in Paleontology and Stratigraphy: A Tribute to Thomas W. Amsden: Oklahoma Geological Survey Bulletin, v. 145, p. 67-89.

Bergström, S.M., and Mitchell, C.E., 1994, Regional relationships between late Middle and early Late Ordovician standard successions in New York and Quebec and the Cincinnati region in Ohio, Indiana, and Kentucky, *in* Landing, E., ed., Studies in Stratigraphy and Paleontology in Honor of Donald W. Fisher: New York State Museum Bulletin, v. 481, p. 5-20.

Bergström, S.M., Saltzman, M.R., Huff, W.D., and Kolata, D.R., 2001, The Guttenberg (Chatfieldian, Ordovician) $\delta^{13}C$ excursion (GICE): Significance for North American and trans-Atlantic chronostratigraphic correlations and for assessment of the age relationships between the North American Millbrig and Baltoscandic Kinnekulle K-bentonites: Geological Society of America, Abstracts with Programs, v. 33, p. A77.

Bernat, M., 1975, Les Isotopes de l'uranium et du thorium et les terres rares dans l'environment marin: Coh. ORSTROM Ser. Geol., v. 7, p. 65-83.

Bertram, C.J., Elderfield, H., Aldridge, R.J., and Morris, S.C., 1992, Sr-87 Sr-86, Nd-143 Nd-144 and REEs in Silurian phosphatic fossils: Earth and Planetary Science Letters, v. 113, p. 239-249.

Bickert, T., Patzold, J., Samtleben, C., and Munnecke, A., 1997, Paleoenvironmental changes in the Silurian indicated by stable isotopes in brachiopod shells from Gotland, Sweden: Geochimica et Cosmochimica Acta, v. 61, p. 2717-2730.

Brand, U., and Bruckschen, P., 2002, Correlation of the Askyn River section, southern Urals, Russia, with the Mid-Carboniferous Boundary GSSP, Bird Spring Formation, Arrow Canyon, Nevada, USA: Implications for global paleoceanography: Palaeogeography, Palaeoclimatology, Palaeoecology, v. 184, p. 177-193.

Brasier, M.D., 1992, Nutrient-enriched waters and the early skeletal fossil record: Geological Society of London Journal, v. 149, p. 621-629.

Brenchley, P.J., Carden, G.A., Hints, L., Kaljo, D., Marshall, J.D., Martma, T., Meidla, T., and Nolvak, J., 2003, High-resolution stable isotope stratigraphy of Upper Ordovician sequences: Constraints on the timing of bioevents and environmental changes associated with mass extinction and glaciation: Geological Society of America Bulletin, v. 115, p. 89-104.

Brenchley, P.J., Marshall, J.D., Carden, C.A.F., Robertson, D.B.R., Long, D.G.F., Meidla, T., Hints, L., and Anderson, T.F., 1994, Bathymetric and isotopic evidence for a short-lived Late Ordovician glaciation in a greenhouse period: Geology, v. 22, p. 295-298.

Byrne, R.H., and Kim, K., 1990, Rare earth element scavenging in seawater: Geochimica et Cosmochimica Acta, v. 54, p. 2645-2656.

Canter, L.K., 1998, Facies, cyclostratigraphy and secondary diagenetic controls on reservoir distribution, Ordovician Red River Formation, Midale Field, southern Saskatchewan, 8th International Williston Basin Symposium Core Workshop Volume, p. 41-65.

Cook, T.D., and Bally, A.W., 1975, Stratigraphic atlas of North and Central America: Princeton, Princeton University Press, p. 38.

Edwards, R.L., Chen, J.H., and Wasserburg, G.J., 1987, ^{238}U-^{234}U-^{230}Th-^{232}Th systematics and the precise measurement of time over the past 500,000 years: Earth and Planetary Science Letters, v. 81, p. 175-192.

Elderfield, H., and Greaves, M.J., 1982, Rare earth elements in seawater: Nature, v. 296, p. 214-219.

Elderfield, H., and Pagett, R., 1986, Rare earth elements in ichthyoliths: Variations with redox conditions and depositional environment: The Science of the Total Environment, v. 49, p. 175-197.

Elderfield, H., and Sholkovitz, E.R., 1987, Rare earth elements in the pore waters of reducing nearshore sediments: Earth and Planetary Science Letters, v. 82, p. 280-288.

Elderfield, H., Upstill-Goddard, R., and Sholkovitz, E.R., 1990, The rare earth elements in rivers, estuaries, and coastal seas and their significance to the composition of ocean waters: Geochimica et Cosmochimica Acta, v. 54, p. 971-991.

Eugster, O., Tera, F., and Wasserburg, G.J., 1969, Isotopic analyses of barium in meteorites and in terrestrial samples: Journal of Geophysical Research, v. 74, p. 3897-3908.

Fanton, K.C., Holmden, C., Nowlan, G.S., and Haidl, F.M., 2002, $^{143}Nd/^{144}Nd$ and Sm/Nd stratigraphy of Upper Ordovician epeiric sea carbonates: Geochimica et Cosmochimica Acta, v. 66, p. 241-255.

Felitsyn, S., Sturesson, U., Popov, L., and Holmer, L., 1998, Nd isotope composition and

rare earth element distribution in early Paleozoic biogenic apatite from Baltoscandia: A signature of Iapetus Ocean water: Geology, v. 26, p. 1083-1086.

Fuller, J.G.C.M., 1961, Ordovician and contiguous formations in North Dakota, South Dakota, Montana, and adjoining areas of Canada and United States: Bulletin of the American Association of Petroleum Geologists, v. 45, p. 1334-1363.

German, C.R., and Elderfield, H., 1990, Rare earth elements in the NW Indian Ocean: Geochimica et Cosmochimica Acta, v. 54, p. 1929-1940.

Girard, C., and Albarède, F., 1996, Trace elements in conodont phosphates from the Frasnian/Famennian boundary: Palaeogeography, Palaeoclimatology, Palaeoecology, v. 126, p. 195-209.

Gleason, J.D., Patchett, P.J., Dickinson, W.R., and Ruiz, J., 1995, Nd isotopic constraints on sediment sources of the Ouachita-Marathon fold belt: Geological Society of America Bulletin, v. 107, p. 1192-1210.

Glumac, B., and Walker, K., 1998, A Late Cambrian positive carbon-isotope excursion in the southern Appalachians: Relation to biostratigraphy, sequence stratigraphy, environments of deposition and diagenesis: Journal of Sedimentary Research, v. 68, p. 1212-1222.

Goldstein, S.J., and Jacobsen, S.B., 1987, The Nd and Sr isotopic systematics of river-water dissolved material: Implications for the sources of Nd and Sr in seawater: Chemical Geology, v. 66, p. 245-272.

Goldstein, S.L., and O'Nions, R.K., 1981, Nd and Sr isotopic relationships in pelagic clays and ferromanganese deposits: Nature, v. 292, p. 324-327.

Grandjean, P., and Albarède, F., 1989, Ion probe measurement of rare earth elements in biogenic phosphates: Geochimica et Cosmochimica Acta, v. 53, p. 3179-3183.

Grandjean, P., Cappetta, H., and Albarède, F., 1988, The REE and e_{Nd} of 40-70 Ma old fish debris from the west-African platform: Geophysical Research Letters, v. 15, p. 389-392.

Grandjean, P., Cappetta, H., Michard, A., and Albarède, F., 1987, The assessment of REE patterns and $^{143}Nd/^{144}Nd$ ratios in fish remains: Earth and Planetary Science Letters, v. 84, p. 181-196.

Grandjean-Lécuyer, P., Feist, R., and Albarède, F., 1993, Rare-earth elements in old biogenic apatites: Geochimica et Cosmochimica Acta, v. 57, p. 2507-2514.

Haidl, F.M., Longman, M.W., Pratt, B.R., and Bernstein, L.M., 1997, Variations in

lithofacies in Upper Ordovician Herald and Yeoman Formations (Red River), North Dakota and southeastern Saskatchewan, *in* Wood, J., and Martindale, B., eds., CSPG-SEPM Core Conference Volume, Calgary, v. 5-39, Canadian Society of Petroleum Geologists.

Haley, B.A., Klinkhammer, G.P., and McManus, J., 2004, Rare earth elements in pore waters of marine sediments: Geochimica et Cosmochimica Acta, v. 68, p. 1265-1279.

Hannigan, R.E., and Sholkovitz, E.R., 2001, The development of middle rare earth element enrichments in freshwaters: weathering of phosphate minerals: Chemical Geology, v. 175, p. 495-508.

Hatch, J.R., Jacobson, S.R., Witzke, B.J., Risatti, B., Anders, D.E., Watney, W.L., Newell, K.D., and Vuletich, A.K., 1987, Possible late Middle Ordovician organic carbon isotope excursion: Evidence from Ordovician oils and hydrocarbon source rocks, Mid-Continent and east-central United States: American Association of Petroleum Geologists Bulletin, v. 71, p. 1342-1354.

Holland, S.M., and Patzkowsky, M.E., 1996, Sequence stratigraphy and long-term paleoceanographic change in the Middle and Upper Ordovician of the eastern United States, American Craton, *in* Witzke, B.J., Ludvigson, G.A., and Day, J., eds., Paleozoic Sequence Stratigraphy: Views from the North American Craton, Geological Society of America Special Paper, no. 306, p. 117-129.

Holland, S.M., and Patzkowsky, M.E., 1997, Distal orogenic effects on peripheral bulge sedimentation: Middle and Upper Ordovician of the Nashville Dome: Journal of Sedimentary Research, v. 67, p. 250-263.

Holmden, C., Creaser, R.A., Muehlenbachs, K., Bergström, S.M., and Leslie, S.A., 1996, Isotopic and elemental systematics of Sr and Nd in 454 Ma biogenic apatites: Implications for paleoseawater studies: Earth and Planetary Science Letters, v. 142, p. 425-437.

Holmden, C., Creaser, R.A., Muehlenbachs, K., Leslie, S.A., and Bergström, S.M., 1998, Isotopic evidence for geochemical decoupling between ancient epeiric seas and bordering oceans: Implications for secular curves: Geology, v. 26, p. 567-570.

Holser, W.T., 1997, Geochemical events documented in inorganic carbon isotopes: Palaeogeography, Palaeoclimatology, Palaeoecology, v. 132, p. 173-182.

Holser, W.T., Magaritz, M., and Ripperdan, R.L., 1996, Global isotopic events, *in* Walliser, O.H., ed., Global Events and Event Stratigraphy in the Phanerozoic: Berlin, Springer, p. 63-88.

Hooker, P.J., Hamilton, P.J., and O'Nions, R.K., 1981, An estimate of the Nd isotopic composition of Iapetus seawater from ca. 490 Ma metalliferous sediments: Earth and Planetary Science Letters, v. 56, p. 180-188.

Hoyle, J., Elderfield, H., Gledhill, A., and Greaves, M., 1984, The behavior of the rare earth elements during mixing of river and sea waters: Geochimica et Cosmochimica Acta, v. 48, p. 143-149.

Immenhauser, A., Kenter, J.A.M., Ganssen, G., Bahamonde, J.R., Vliet, V.A., and Saher, M.H., 2002, Origin and significance of isotope shifts in Pennsylvanian carbonates (Austrias, NW Spain): Journal of Sedimentary Research, v. 72, p. 82-94.

Immenhauser, A., Porta, G.D., Kenter, J.A.M., and Bahamonde, J.R., 2003, An alternative model for positive shifts in shallow-marine carbonate $\delta^{13}C$ and $\delta^{18}O$: Sedimentology, v. 50, p. 1-7.

Jacobson, S.R., Finney, S.C., Hatch, J.R., and Ludvigson, G.A., 1995, *Gloeocapsomorpha prisca*-driven organic carbon isotope excursion, late Middle Ordovician (Rocklandian), North American mid-continent: new data from Nevada and Iowa, *in* Cooper, J.D., Droser, M.L., and Finney, S.C., eds., Ordovician Odyssey: Short Papers for the Seventh International Symposium on the Ordovician System, Las Vegas, Nevada, U.S.A.: Fullerton, The Pacific Section Society for Sedimentary Geology, p. 305-308.

Jenkyns, H.C., 1996, Relative sea-level change and carbon isotopes: data from the Upper Jurassic (Oxfordian) of central and Southern Europe: Terra Nova, v. 8, p. 75-85.

Joachimski, M.M., and Buggisch, W., 1993, Anoxic events in the late Frasnian-Causes of the Frasnian-Famennian faunal crisis?: Geology, v. 21, p. 675-678.

Johannesson, K.H., Stetzenbach, K.J., and Hodge, V.F., 1997, Rare earth elements as geochemical tracers of regional groundwater mixing: Geochimica et Cosmochimica Acta, v. 61, p. 3605-3618.

Jones, C.E., Halliday, A.N., Rea, D.K., and Owen, R.M., 1994, Neodymium isotopic variations in North Pacific modern silicate sediment and the insignificance of detrital REE contributions to seawater: Earth and Planetary Science Letters, v. 127, p. 55-66.

Kaljo, D., Kiipli, T., and Martma, T., 1997, Carbon isotope event markers through the Wenlock-Pridoli sequence at Ohesaare (Estonia) and Priekule (Latvia): Palaeogeography, Palaeoclimatology, Palaeoecology, v. 132, p. 211-223.

Keith, B.D., 1988, Regional facies of the Upper Ordovician Series of eastern North America, *in* Keith, B.D., ed., The Trenton Group (Upper Ordovician Series) of eastern North America, American Association of Petroleum Geologists Studies in Geology, no. 29, p. 1-16.

Kendall, A.C., 1976, The Ordovician carbonate succession (Bighorn Group) of southeastern Saskatchewan: Department of Mineral Resources Saskatchewan Geological Survey, 186 p.

Keto, L.S., and Jacobsen, S.B., 1987, Nd and Sr isotopic variations of Early Paleozoic oceans: Earth and Planetary Science Letters, v. 84, p. 27-41.

Keto, L.S., and Jacobsen, S.B., 1988, Nd isotopic variations of Phanerozoic paleoceans: Earth and Planetary Science Letters, v. 90, p. 395-410.

Kimura, H., Matsumoto, R., Kakuwa, Y., Hamdi, B., and Zibaseresht, H., 1997, The Vendian-Cambrian $\delta^{13}C$ record, North Iran: evidence for overturning of the ocean before the Cambrian explosion: Earth and Planetary Science Letters, v. 147, p. 1-7.

Kolata, D.R., Frost, J.K., and Huff, W.D., 1987, Chemical correlation of K-bentonite beds in the Middle Ordovician Decorah subgroup, upper Mississippi Valley: Geology, v. 15, p. 208-211.

Kolata, D.R., Huff, W.D., and Bergström, S.M., 1998, Nature and regional significance of unconformities associated with the Middle Ordovician Hagan K-bentonite complex in the North American midcontinent: Geological Society of America Bulletin, v. 110, p. 723-739.

Kolata, D.R., Huff, W.D., and Bergström, S.M., 2001, The Ordovician Sebree Trough: An oceanic passage to the Midcontinent United States: Geological Society of America Bulletin, v. 113, p. 1067-1078.

Kolata, D.R., and Nelson, W.J., 1991, Tectonic history of the Illinois Basin, *in* Leighton M.W. et al., eds., Interior Cratonic Basins, American Association of Petroleum Geologists Memoir, no. 51, p. 263-285.

Kolata, D.R., and Nelson, W.J., 1997, Role of the Reelfoot Rift-Rough Creek graben in the evolution of the Illinois Basin, *in* Ojakangas, R.W., ed., Middle Proterozoic to Cambrian rifting, central North America, Geological Society of America Special Paper, no. 312, p. 287-298.

Kreis, L.K., and Kent, D.M., 2000, Basement controls on Red River sedimentation and hydrocarbon production in southeastern Saskatchewan, Summary of Investigations, 2000, Vol 1, Saskatchewan Energy and Mines Miscellaneous

Report 2000-4.1, p. 21-42.

Kroopnick, P.M., 1985, The distribution of ^{13}C of ΣCO_2 in the world oceans: Deep-Sea Research, v. 32, pp. 57-84.

Kump, L.R., 1999, Interpreting carbon-isotope excursions: carbonates and organic matter: Chemical Geology, v. 161, p. 181-198.

Kump, L.R., Arthur, M.A., Patzkowsky, M.E., Gibbs, M.T., Pinkus, D.S., and Sheehan, P.M., 1999, A weathering hypothesis for glaciation at high atmospheric pCO_2 during the Late Ordovician: Palaeogeography, Palaeoclimatology, Palaeoecology, v. 152, p. 173-187.

Laenen, B., Hertogen, J., and Vandenberghe, N., 1997, The variation of the trace-element content of fossil biogenic apatite through eustatic sea-level cycles: Palaeogeography, Palaeoclimatology, Palaeoecology, v. 132, p. 325-342.

Lécuyer, C., Grandjean, P., Barrat, J., Nolvak, J., Emig, C., Paris, F., and Robardet, M., 1998, $\delta^{18}O$ and REE contents of phosphatic brachiopods: A comparison between modern and lower Paleozoic populations: Geochimica et Cosmochimica Acta, v. 62, p. 2429-2436.

Leslie, S.A., and Bergström, S.M., 1997, Use of K-bentonite beds as time-planes for high-resolution lithofacies analysis and assessment of net rock accumulation rate: An example from the upper Middle Ordovician of eastern North America, *in* Klapper, G., Murphy, M.A., and Talent, J.A., eds., Paleozoic Sequence Stratigraphy, Biostratigraphy, and Biogeography: Studies in Honor of J. Granville ("Jess") Johnson, Geological Society of America Special Paper, no. 321, p. 11-21.

Longman, M.W., Fertal, T.G., and Glennie, J.S., 1983, Origin and geometry of Red River dolomite reservoirs, western Williston Basin: American Association of Petroleum Geologists Bulletin, v. 67, p. 744-771.

Ludvigson, G.A., Jacobsen, S.R., Witzke, B.J., and González, L., 1996, Carbonate component chemostratigraphy and depositional history of the Ordovician Decorah Formation, Upper Mississippi Valley, *in* Witzke, B.J., Ludvigson, G.A., and Day, J., eds., Paleozoic Sequence Stratigraphy: Views from the North American Craton, Geological Society of America Special Paper, no. 306, p. 307-330.

Ludvigson, G.A., Witzke, B.J., González, L.A., Carpenter, S.J., and Hasiuk, F.J., 2001, New complexities in the expression of Late Ordovician carbon isotope excursions straddling the Turinian-Chatfieldian boundary interval: Geological Society of America Abstracts with Programs, v. 33, p. 214.

Ludvigson, G.A., Witzke, B.J., González, L.A., Carpenter, S.J., Schneider, C.L., and Hasiuk, F., 2004, Late Ordovician (Turinian-Chatfieldian) carbon isotope excursions and their stratigraphic and paleoceanographic significance: Palaeogeography, Palaeoclimatology, Palaeoecology, v. 210, p. 187-214.

Ludvigson, G.A., Witzke, B.J., Schneider, C.L., Smith, E.A., Emerson, N.R., Carpenter, S.J., and González, L.A., 2000, A profile of the mid-Caradoc (Ordovician) carbon isotope excursion at the McGregor Quarry, Clayton County, Iowa: Geological Society of Iowa Guidebook, v. 70, p. 25-31.

Magaritz, M., and Holser, W., 1990, Carbon isotope shifts in Pennsylvanian seas: American Journal of Science, v. 290, p. 977-994.

Magaritz, M., Krishnamurthy, R.V., and Holser, W.T., 1992, Parallel trends in organic and inorganic carbon isotopes across the Permian/Triassic boundary: American Journal of Science, v. 292, p. 727-739.

Magaritz, M., and Stemmerik, L., 1989, Oscillation of carbon and oxygen isotope compositions of carbonate rocks between evaporite and open marine environments, Upper Permian of East Greenland: Earth and Planetary Science Letters, v. 93, p. 233-240.

Martin, E.E., and Haley, B.A., 2000, Fossil fish teeth as proxies for seawater Sr and Nd isotopes: Geochimica et Cosmochimica Acta, v. 64, p. 835-847.

McCrea, J.M., 1950, On the isotopic chemistry of carbonates and a paleotemperature scale: Journal of Chemical Physics, v. 18, p. 849-857.

Meidla, T., Ainsaar, L., Hints, L., Hints, O., Martma, T., and Nolvak, J., 1999, The mid-Caradocian biotic and isotopic event in the Ordovician of the East Baltic: Acta Universitatis Carolinae-Geologica, v. 43, p. 503-506.

Norford, B.S., Haidl, F.M., Bezys, R.K., Cecile, M.P., McCabe, H.R., and Paterson, D.F., 1994, Middle Ordovician to Lower Devonian strata of the Western Canada Sedimentary Basin, *in* Mossop, G., and Shetson, I., eds., Geological Atlas of the Western Canada Sedimentary Basin: Calgary, Canadian Society of Petroleum Geologists and Alberta Research Council, p. 109-127.

Nowlan, G.S., and Barnes, C.R., 1981, Late Ordovician conodonts from the Vaureal Formation, Anticosti Island, Quebec: Geological Survey of Canada Bulletin, v. 329, p. 1-49.

Ohr, M., Alexander, N.H., and Peacor, D.R., 1994, Mobility and fractionation of rare earth elements in argillaceous sediments: Implications for dating diagenesis and

low-grade metamorphism: Geochimica et Cosmochimica Acta, v. 58, p. 289-312.

Ohr, M., Halliday, A.N., and Peacor, D.R., 1991, Sr and Nd isotopic evidence for punctuated clay diagenesis, Texas Gulf Coast: Earth and Planetary Science Letters, v. 105, p. 110-126.

Osadetz, K.G., and Haidl, F.M., 1989, Tippecanoe Sequence: Middle Ordovician to Lowest Devonian - vestiges of a great epeiric sea, *in* Ricketts, B.D., ed., Western Canada Sedimentary Basin: A Case History, Canadian Society of Petroleum Geologists, p. 121-137.

Palmer, M.R., 1985, Rare earth elements in foraminifera tests: Earth and Planetary Science Letters, v. 73, p. 285-298.

Palmer, M.R., and Elderfield, H., 1985, Variations in the Nd isotopic composition of foraminifera from Atlantic Ocean sediments: Earth and Planetary Science Letters, v. 73, p. 299-305.

Palmer, M.R., and Elderfield, H., 1986, Rare earth elements and neodymium isotopes in ferromanganese oxide coatings of Cenozoic foraminifera from the Atlantic Ocean: Geochimica et Cosmochimica Acta, v. 50, p. 409-417.

Panchuk, K., 2002, Epeiric sea carbon cycling from analytical and numerical perspectives [M.Sc. thesis]: Saskatoon, University of Saskatchewan, 79p.

Pancost, R.D., Freeman, K.H., and Patzkowsky, M.E., 1999, Organic-matter source variation and the expression of a late Middle Ordovician carbon isotope excursion: Geology, v. 27, p. 1015-1018.

Pancost, R.D., Freeman, K.H., Patzkowsky, M.E., Wavrek, D.A., and Collister, J.W., 1998, Molecular indicators of redox and marine photoautotroph composition in the late Middle Ordovician in Iowa, U.S.A.: Organic Geochemistry, v. 29, p. 1649-1662.

Patchett, P.J., Ross, G.M., and Gleason, J.D., 1999a, Continental drainage in North America during the Phanerozoic from Nd isotopes: Science, v. 283, p. 671-673.

Patchett, P.J., Roth, M.A., Canale, B.S., de Freitas, T.A., Harrison, J.C., Embry, A.F., and Ross, G.M., 1999b, Nd isotopes, geochemistry and constraints on sources of sediments in the Franklinian mobile belt, Arctic Canada: Geological Society of America Bulletin, v. 111, p. 578-589.

Patterson, W.P., and Walter, L.M., 1994, Depletion of ^{13}C in seawater ΣCO_2 on modern carbonate platforms: Significance for the carbon isotopic record of carbonates: Geology, v. 22, p. 885-888.

Patzkowsky, M.E., Slupik, L.M., Arthur, M.A., Pancost, R.D., and Freeman, K.H., 1997, Late Middle Ordovician environmental change and extinction, harbinger of the Late Ordovician or continuation of Cambrian patterns: Geology, v. 25, p. 911-914.

Patzkowsky, M.E., and Holland, S.M., 1993, Biotic response to a Middle Ordovician paleoceanographic event in eastern North America: Geology, v. 21, p. 619-622.

Perfetta, P.J., Shelton, K.L., and Stitt, J.H., 1999, Carbon isotope evidence for deep-water invasion at the Marjumiid-Pterocephaliid biomere boundary, Black Hills, USA: A common origin for biotic crises on Late Cambrian shelves: Geology, v. 27, p. 403-406.

Picard, S., Lécuyer, C., Barrat, J., Garcia, J., Dromart, G., and Sheppard, S.M.F., 2002, Rare earth element contents of Jurassic fish and reptile teeth and their potential relation to seawater composition (Anglo-Paris Basin, France and England): Chemical Geology, v. 186, p. 1-16.

Piepgras, D.J., and Jacobsen, S.B., 1992, The behavior of rare earth elements in seawater: Precise determination of variations in the North Pacific water column: Geochimica et Cosmochimica Acta, v. 56, p. 1851-1862.

Piepgras, D.J., and Wasserburg, G.J., 1980, Neodymium isotopic variations in seawater: Earth and Planetary Science Letters, v. 50, p. 128-138.

Piepgras, D.J., Wasserburg, G.J., and Dasch, E.J., 1979, The isotopic composition of Nd in different ocean masses: Earth and Planetary Science Letters, v. 45, p. 223-236.

Pope, M.C., and Steffen, J.B., 2003, Widespread, prolonged late Middle to Late Ordovician upwelling in North America: A proxy record of glaciation: Geology, v. 31, p. 63-66.

Pratt, B.R., Bernstein, L.M., Kendall, A.C., and Haidl, F.M., 1996, Occurrence of reefal facies in Red River strata (Upper Ordovician) subsurface of Saskatchewan, Summary of Investigations, 1996, Miscellaneous Report, Volume 96-4, Saskatchewan Energy and Mines, p. 147-152.

Raatz, W.D., and Ludvigson, G.A., 1996, Depositional environments and sequence stratigraphy of Upper Ordovician epicontinental deep water deposits, eastern Iowa and Minnesota, *in* Witzke, B.J., Ludvigson, G.A., and Day, J., eds., Paleozoic Sequence Stratigraphy: Views from the North American Craton, Geological Society of America Special Paper, no. 306, p. 143-159.

Reynard, B., Lécuyer, C., and Grandjean, P., 1999, Crystal-chemical controls on rare-

earth element concentrations in fossil biogenic apatites and implications for paleoenvironmental reconstructions: Chemical Geology, v. 155, p. 233-241.

Ripperdan, R.L., Magaritz, M., Nicoll, R.S., and Shergold, J.H., 1992, Simultaneous changes in carbon isotopes, sea level, and conodont biozones within the - Cambrian-Ordovician boundary interval at Black Mountain, Australia: Geology, v. 20, p. 1039-1042.

Saltzman, M.R., 2002, Carbon isotope excursion ($\delta^{13}C$) stratigraphy across the Silurian-Devonian transition in North America: Evidence for a perturbation of the global carbon cycle: Palaeogeography, Palaeoclimatology, Palaeoecology, v. 187, p. 83-100.

Saltzman, M.R., 2003, Late Paleozoic ice age: Oceanic gateway or pCO_2?: Geology, v. 31, p. 151-154.

Saltzman, M.R., Bergström, S.M., Kolata, D.R., and Huff, W.D., 2001, The Ordovician (Chatfieldian) Guttenberg carbon isotope excursion. 1. New data from the eastern North American mid-continent and Baltoscandia: Geological Society of America, Abstracts with Programs, v. 33, (4) p. A41.

Saltzman, M.R., Davidson, J.P., Holden, P., Runnegar, B., and Lohmann, K.C., 1995, Sea-level-driven changes in ocean chemistry at an Upper Cambrian extinction horizon: Geology, v. 23, p. 893-896.

Saltzman, M.R., Runnegar, B., and Lohmann, K.C., 1998, Carbon isotope stratigraphy of Upper Cambrian (Steptoean Stage) sequences of the eastern Great Basin: Record of a global oceanographic event: Geological Society of America Bulletin, v. 110, p. 285-297.

Schaltegger, U., Stille, P., Rais, N., Pique, A., and Clauer, N., 1994, Neodymium and strontium isotopic dating of diagenesis and low-grade metamorphism of argillaceous sediments: Geochimica et Cosmochimica Acta, v. 58, p. 1471-1481.

Scholle, P.A., and Arthur, M.A., 1980, Carbon isotope fluctuations in Cretaceous pelagic limestones: potential stratigraphic and petroleum exploration tool: American Association of Petroleum Geologists Bulletin, v. 64, p. 67-87.

Scotese, C.R., and McKerrow, W.S., 1990, Revised world maps and introduction, *in* McKerrow, W.S., and Scotese, C.R., eds., Palaeozoic Palaeogeography and Biogeography: Geological Society Memoir, no. 12, p. 1-21.

Shaw, H.F., and Wasserburg, G.J., 1985, Sm-Nd in marine carbonates and phosphates: Implications for Nd isotopes in seawater and crustal ages: Geochimica et Cosmochimica Acta, v. 49, p. 503-518.

Sholkovitz, E., and Szymczak, R., 2000, The estuarine chemistry of rare earth elements: comparison of the Amazon, Fly, Sepik and the Gulf of Papua systems: Earth and Planetary Science Letters, v. 179, p. 299-309.

Sholkovitz, E.R., and Schneider, D.L., 1991, Cerium redox cycles and rare earth elements in the Sargasso Sea: Geochimica et Cosmochimica Acta, v. 55, p. 2737-2743.

Simo, J.A., Emerson, N.R., Byers, C.W., and Ludvigson, G.A., 2003, Anatomy of an embayment in an Ordovician epeiric sea, Upper Mississippi Valley, USA: Geology, v. 31, p. 545-548.

Singer, A.J., and Shemesh, A., 1995, Climatically linked carbon isotope variation during the past 430,000 years in Southern Ocean sediments: Paleoceanography, v. 10, p. 171-177.

Sloan, R.E., 1987, Tectonics, biostratigraphy and lithostratigraphy of the Middle and Late Ordovician of the Upper Mississippi Valley, *in* Sloan, R.E., ed., Middle and Upper Ordovician Lithostratigrahy and Biostratigraphy of the Upper Mississippi Valley, Minnesota Geological Survey Report of Investigations, 35, p. 7-20.

Staudigel, H., P., D., and A., Z., 1985, Sr and Nd isotope systematics in fish teeth: Earth and Planetary Science Letters, v. 76, p. 45-56.

Stille, P., 1992, Nd-Sr isotope evidence for dramatic changes of paleocurrents in the Atlantic Ocean during the past 80 my: Geology, v. 20, p. 387-390.

Stille, P., Steinmann, M., and Riggs, S.R., 1996, Nd isotope evidence for the evolution of the paleocurrents in the Atlantic and Tethys Oceans during the past 180 Ma: Earth and Planetary Science Letters, v. 144, p. 9-19.

Sweet, W.C., 1979, Late Ordovician conodonts of the western midcontinent province: Brigham Young University Geol. Studies, v. 26, p. 45-85.

Sweet, W.C., 1984, Graphic correlation of upper Middle and Upper Ordovician rocks, North American Midcontinent Province, U.S.A., *in* Bruton, D.L., ed., Aspects of the Ordovician System: University of Oslo Paleontological Contribution, no. 295, p. 23-35.

Sweet, W.C., and Bergström, S.M., 1976, Conodont biostratigraphy of the Middle and Upper Ordovician of the United States Midcontinent, *in* Bassett, M.G., ed., The Ordovician System: Proceedings of a Paleontological Association Symposium, University of Wales Press and National Museum of Wales, p. 121-151.

Sweet, W.C., and Bergström, S.M., 1984, Conodont provinces and biofacies of the Late Ordovician, *in* Clark, D.L., ed., Conodont Biofacies and Provincialism: Geological Society of America Special Paper, no. 196, p. 69-87.

Telmer, K., and Viezer, J., 1999, Carbon fluxes, pCO_2 and substrate weathering in a large northern river basin, Canada: carbon isotope perspectives: Chemical Geology, v. 159, p. 61-86.

Turekian, K.K., Katz, A., and Chan, L., 1973, Trace element trapping in pteropod tests: Limnology and Oceanography, v. 18, p. 240-249.

Vance, D., and Burton, K., 1999, Neodymium isotopes in planktonic foraminifera: A record of the response of continental weathering and ocean circulation rates to climate change: Earth and Planetary Science Letters, v. 173, p. 365-379.

Veizer, J., Ala, D., Azmy, K., Bruckschen, P., Buhl, D., Bruhn, F., Carden, G.A.F., Diener, A., Ebneth, S., Godderis, Y., Jasper, T., Korte, C., Pawellek, F., Podlaha, O.G., and Strass, H., 1999, $^{87}Sr/^{86}Sr$, $\delta^{13}C$, and $\delta^{18}O$ evolution of Phanerozoic seawater: Chemical Geology, v. 161, p. 59-88.

Veizer, J., Fritz, P., and Jones, B., 1986, Geochemistry of brachiopods: Oxygen and carbon isotopic records of Paleozoic oceans: Geochimica et Cosmochimica Acta, v. 50, p. 1679-1696.

Veizer, J., Holser, W.T., and Wilgus, C.K., 1980, Correlation of $^{13}C/^{12}C$ and $^{34}S/^{32}S$ secular variations: Geochimica et Cosmochimica Acta, v. 44, p. 579-587.

Wenzell, B., and Joachimski, M.M., 1996, Carbon and oxygen isotopic composition of Silurian brachiopods (Gotland/Sweden): Palaeoceanographic implications: Palaeogeography, Palaeoclimatology, Palaeoecology, v. 122, p. 143-166.

Whittaker, S.G., and Kyser, T.K., 1993, Variations in the neodymium and strontium isotopic composition and REE content of molluscan shells from the Cretaceous Western Interior seaway: Geochimica et Cosmochimica Acta, v. 57, p. 4003-4014.

Wilde, P., 1991, Oceanography in the Ordovician, *in* Barnes, C.R., and Williams, S., eds., Advances in Ordovician Geology: Geological Survey of Canada Special Paper, no. 90-9, p. 283-298.

Witzke, B.J., 1980, Middle and Upper Ordovician paleogeography of the region bordering the Transcontinental Arch, *in* Fouch, T.D., and Magathan, E.R., eds., Rocky Mountain Paleogeography Symposium 1, Paleozoic Paleogeography of the West Central United States, p. 1-18.

Witzke, B.J., 1987a, Middle and Upper Ordovician stratigraphy in the Iowa subsurface, *in* Sloan, R.E., ed., Middle and Late Ordovician lithostratigraphy and biostratigraphy of the Upper Mississippi Valley, Report of Investigations, Volume 35: St. Paul, Minnesota Geological Survey, p. 40-43.

Witzke, B.J., 1987b, Models for circulation patterns in epicontinental seas applied to Paleozoic facies of North America: Paleoceanography, v. 2, p. 229-248.

Witzke, B.J., 1990, Paleoclimatic constraints for Palaeozoic Palaeolatitudes of Laurentia and Euroamerica, *in* McKerrow, W.s. and Scotese, C.R., eds., Palaeozoic, Palaeogeography and Biogeography, Geological Society Memoir, no. 12, pp. 57-73

Witzke, B.J., and Bunker, B.J., 1996, Relative sea-level changes during Middle Ordovician though Mississippian deposition in the Iowa area, North American craton, *in* Witzke, B.J., Ludvigson, G.A., and Day, J., eds., Paleozoic Sequence Stratigraphy: Views from the North American Craton, Geological Society of America Special Paper, no. 306, p. 307-330.

Witzke, B.J., and Kolata, D.R., 1989, Changing structural and depositional patterns, Ordovician Champlanian and Cincinnatian series of Iowa-Illinois, *in* Ludvigson, G.A., and Bunker, B.J., eds., New perspective on the Paleozoic history of the Upper Mississippi Valley; an examination of the Plum River fault zone, Iowa Department of Natural Resources, p. 55-77.

Woodruff, F., and Savin, S.M., 1985, $\delta^{13}C$ values of Miocene Pacific foraminifera: correlations with sea level and biological productivity: Geology, v. 13, p. 119-122.

Wright, J., Seymour, R.S., and Shaw, H.F., 1984, REE and Nd isotopes in conodont apatite: Variations with geological age and depositional environment, *in* Clark, D.L., ed., Conodont Biofacies and Provincialism, Geological Society of America Special Paper, no. 196, p. 325-340.

Yapp, C.J., and Poths, H., 1993, The carbon isotope geochemistry of goethite (α-FeOOH) in ironstone of the Upper Ordovician Neda Formation, Wisconsin, USA: Implications for early Paleozoic continental environments: Geochimica et Cosmochimica Acta, v. 57, p. 2599-2611.